Genomic and Physiological Characterization of the Mutant *time for coffee* within the *Arabidopsis thaliana* Circadian Clock

Inaugural-Dissertation

zur

Erlangung des Doktorgrades
der Mathematisch-Naturwissenschaftlichen Fakultät
der Universität zu Köln

vorgelegt von

Alfredo Sánchez Villarreal

aus Ciudad de México, Distrito Federal

México

Köln 2010

Die vorliegende Arbeit wurde am Max-Planck-Institut für Züchtungsforschung Köln, in der Arbeitsgruppe von Dr. Seth J. Davis, Abteilung für Entwicklungsbiologie der Pflanzen (Direktor Prof. Dr. George Coupland) angefertigt.

Berichterstatter:
Prof. Dr. George Coupland
Prof. Dr. Ulf-Ingo Flügge

Prüfungsvorsitzender:
Prof. Dr. Ute Höcker

Besitzer: Dr. Imre Somssich

Tag der mündlichen Prüfung: 29 Juni 2010

Fuí en pos de un sueño,

un sueño tal vez vago, pero claro en que tenía que llevarse a cabo;

sin embargo no encontré lo que esperaba

y perdí mucho en el camino

Caí y me perdí y hube de andar entre las más terribles tinieblas,

y enfrentado conmigo mismo ahondé los rincones más obscuros

Luz y amor iluminaron el camino,

levanto mis vasijas rotas y las reconstruyo buscándome en ellas

el camino a uno mismo es difícil de andar

Hoy que un viaje termina, otro sigue en curso

y sé que al final de su recorrido veré con claridad que haber perseguido ese sueño ha valido la pena.

I left pursuing a dream,

perhaps a vague dream, but clear in the knowledge that it had to be followed;

however I did not find what I was looking for

and I lost almost everything in the way

Fallen and lost, I had to walk through the shadows,

and faced with myself lured the darkest insides

Light and love enlightened the way,

pick up the broken pieces for looking into myself

the way to oneself is hard to follow

Now that the voyage ends, another is still in course

and I now that in its end, I will see that pursuing that dream has been worth it.

A mis padres, Elena y Víctor

por todo su amor, comprensión y dedicación

por su esfuerzo en darme a mí y mis hermanos las herramientas más importantes en esta vida

quien soy y nada de lo que he hecho y tengo hubiera sido posible sin lo que me han dado

A mi hermano, Víctor

por abrir un mundo en mi vida

por su guía en la vida y las riquezas que obtuve y aprendí de él

esas me iluminaron y calmaron el alma cuando más lo necesité

A mi hermana, Citlalli

quien a través de los años me ha puesto contacto con el mundo de una y mil maneras

a través de ello he podido compartir cosas con las personas de "nuestra generación"

A Aída

por todo su amor, amistad, comprensión y paciencia

quien me ayudó cuando más lo necesitaba,

no hay forma en que pueda agradecértelo.

por ser una guía profesional, sin tus palabras no hubiera encontrado un camino que seguir en mi doctorado

Abstract

Circadian clocks are internal timekeepers that provide organisms with a sense of time. These oscillators, which are entrained by external stimuli, predict the daily day/night transitions and have a periodicity of about 24 hours. The *Arabidopsis thaliana* circadian clock is composed of interconnected transcriptional-translational feedback loops. The morning expressed elements *CCA1* and *LHY*, which are clock controlled and light inducible, repress the transcription of the evening element *TOC1*. At dusk, *TOC1* repression is relieved as CCA1 and LHY protein diminish. Then TOC1 stimulates the expression of the morning components closing the loop. Still, how the light signal at dawn entrains this clock has remained elusive. *time for coffee* (*tic*) was originally reported as a circadian-clock mutant based on its early phase and a short period. It was found that *tic* is defective in sensing dawn because its clock incorrectly resets before morning light. Because *TIC* mRNA and protein were found to be constant through a diurnal cycle, an activation event could trigger TIC time-specific function within the oscillator. Therefore TIC action takes place before the expression of *CCA1* and *LHY* and coincides in time with clock entrainment by light.

In this thesis, I report the results from a microarray study that led to a detailed phenotypic analysis of *tic* in an effort to uncover the mechanism to clock entrainment. I could confirm and expand the defective clock-gene expression profile of *tic*. Interestingly *tic* showed increased transcriptional changes in response to the environment compared to wild type. Global transcriptomic analysis indicated that *tic* has altered redox homeostasis and defects in ABA signalling pathways. Furthermore GO enrichment analysis highlighted that stress and environmental responses were among the most abundant categories misexpressed in *tic*. In conclusion, *TIC* was found to be an essential component for global transcriptome reprogramming to a dawn light signal.

The results obtained through the microarray analysis directed me to demonstrate that *tic* resulted in an array of pleiotropic phenotypes. Besides its clock defects, *tic* presented hypersensitivity to oxidative stress, altered ABA-related signalling and responses, such as drought tolerance, defects in iron homeostasis, alterations in starch metabolism and disrupted stress responses. Furthermore it is suggested that *tic* has a role in nucleotide and secondary metabolism. All together, I concluded that *TIC* functions in maintaining metabolic homeostasis through modulation of stress responses.

To start to understand TIC biochemical function, a yeast two hybrid screen was performed. Through this screen for TIC interactors, the SNF1 stress-related kinase AKIN10, a proposed master metabolic sensor, was isolated. It was shown through *in vitro* studies that TIC could be phosphorylated by AKIN10. The physiological relevance of the interaction between TIC and AKIN10 toward the circadian clock was genetically tested. I found that AKIN10 had an effect on clock period that was TIC dependent. Thus, this physical and genetic interaction could define the basis for a metabolic input to the oscillator.

In the *A. thaliana* genome *TIC* has a single homolog sequence termed *TKL*. To examine a plausible role of *TKL* in the circadian clock, a T-DNA mutant, termed *tkl-1*, was characterized. I found that *tkl-1* had no observable defects of circadian rhythms. This finding was supported by phylogenetic analyses of TIC-like encoded proteins that suggested an evolutionary divergence between TIC and TKL. From these results it was concluded that *TKL* is not part of the circadian clock.

In summary from the data presented here, I hypothesize that clock entrainment occurs through metabolic signals, probably derived from photosynthesis and cellular energy homeostasis. These signals would be integrated to the oscillator by TIC. In this way, TIC would promote the anticipation of the oncoming new day.

Zusammenfassung

Zirkadiane Uhren sind interne Zeitmesser, die Lebewesen mit einer Wahrnehmung für Zeit ausstatten. Diese Oszillatoren werden durch externe Stimuli eingestellt und ermöglichen den Organismen die Einregelung auf den 24-stündigen Tag/Nachtrhythmus. Die zirkadiane Uhr von *Arabidopsis thaliana* besteht aus einem Netzwerk von transkriptionellen und translationellen Rückkopplungen. Die am Morgen exprimierten Gene *CCA1* und *LHY* sind durch Licht induzierbar und uhrenkontrolliert und können die Transkription des Abend-Gens *TOC* unterdrücken. Am Abend nimmt die Protein-Konzentration von CCA1 und LHY ab und die Repression von *TOC* wird somit aufgehoben. TOC1 stimuliert daraufhin die Expression der Morgen-Gene und schließt so den Tag/Nachtrhythmus. Welchen Einfluß das Licht am Morgen auf die Einstellung der Uhr hat, ist bisher unbekannt. Die zirkadiane Uhr Mutante *time for coffee (tic)* weist eine frühe Phase und kurze Periode auf. Es wurde gezeigt, dass *tic* einen Defekt in der Wahrnehmung der Morgendämmerung besitzt, da die zirkadiane Uhr vor dem Lichtsignal am Morgen zurückgestellt wird. Protein- und mRNA-Konzentration von TIC sind während des täglichen Tag/Nachtrhythmus konstant sodass eine Aktivierung von TIC für seine Funktion innerhalb des Oszillators verantwortlich sein muss. Die Funktion von TIC findet vor der Expression von *CCA1* und *LHY* statt und stimmt somit zeitlich mit der Uhr-Einstellung durch Licht überein.

In dieser Arbeit berichte ich die Ergebnisse einer Microarray-Analyse sowie einer detaillierten phänotypischen Analyse der Mutante *tic*. Interessanterweise zeigt *tic* eine verstärkte transkriptionelle Antwort auf Umwelteinflüsse und Stress im Vergleich zum Wildtyp. Desweiteren besitzt *tic* einen Defekt in der ABA-Signaltransduktion sowie in der Redox-Homöostase. TIC ist somit essentiell für die globale Transkriptregulation als Antwort auf das Lichtsignal in der Morgendämmerung.

Die Ergebnisse der Microarray-Analyse deuteten desweiteren auf eine Vielzahl von pleiotrophen Phänotypen hin. *tic* besitzt eine Hypersensitivität gegenüber oxidativem Stress, veränderte Toleranz für Trockenheit, Defekte in der Eisen-Homöostase, Veränderungen im Stärke-Metabolismus und eine gestörte Stress-Antwort. Außerdem scheint *tic* eine Rolle im Nukleotid- und sekundären Stoffwechsel zu spielen. Die Funktion von TIC scheint daher die Erhaltung der metabolischen Homöostase durch Modulation der Stress-Antwort zu sein.

Um die biochemische Funktion von TIC genauer zu untersuchen, wurde ein Hefe-2-Hybridscreen durchgeführt. Dadurch konnte AKIN10, eine SNF1-verwandte Kinase, als Interaktor von TIC identifiziert werden. Durch *in vitro* Studien konnte gezeigt werden, dass TIC durch AKIN10 phosphoryliert wird. Die Relevanz der Interaktion von TIC und AKIN10 für die zirkadiane Uhr wurde mittels genetischer Studien getestet. Ich konnte zeigen, dass AKIN10 einen Effekt auf die Periode der Uhr hat, welcher abhänging von TIC ist. Daher könnte diese physische und genetische Interaktion die Basis für den metabolischen Einfluß auf den Oszillator darstellen.

Im *A. thaliana* Genom findet sich ein Homolog zu *TIC, TKL*. Um eine mögliche Rolle von *TKL* in der zirkadianen Uhr zu untersuchen, wurde eine T-DNA Mutante, *tkl-1*, charakterisiert. Ich konnte zeigen, dass *tkl-1* keinen detektierbaren Defekt in der zirkadianen Rhythmik hat. Dieses Ergebnis wurde weiter durch phylogenetische Analysen von TIC-ähnlichen Proteinen unterstützt, die auf eine evolutionäre Divergenz von TIC und TKL hindeuten. Aufgrunddessen wurde geschlussfolgert, dass TKL keinen Teil der zirkadianen Uhr darstellt.

Aus den hier dargestellten Ergebnissen ziehe ich den Schluß, dass die Einstellung der zirkadianen Uhr durch metabolische Signale erfolgt, die möglicherweise aus der Photosynthese und der zellulären Energie-Homöostase stammen. Diese Signale könnten mithilfe von TIC in den Oszillator integriert werden. Dadurch würde TIC die Antizipation des neuen Tages vermitteln.

TABLE OF CONTENTS

LIST OF FIGURES

LIST OF TABLES

List of abbreviations

ABA	(+/-) Abscisic acid
aRNA	antisense RNA
ATH1	*A. thaliana* ATH1 genome array 22K
cDNA	complementary DNA
CFU	Colony Forming Units
Col-0	*A. thaliana* Columbia ecotype
DNA	deoxyribonucleic acid
DPI	diphenyleneiodonium chloride
FDR	False Discovery Rate
GC-RMA	Guanine-Cytosine Robust Multichip Array
GO	Gene Ontology
H_2O_2	hydrogen peroxide
KEGG	Kyoto Encyclopedia of Genes and Genomes
mRNA	messenger RNA
MV	methylviologen dichloride
LD	Light/Dark photoperiod
log2	logarithm base 2
PCA	Principal Component Analysis
PCR	Polymerase Chain Reaction
RNA	ribonucleic acid
ROS	Reactive Oxygen Species
SAR	Systemic Acquired Resistance
SHAM	salicylhydroxamic acid
SWC	Soil Water Capacity
TCA	tricarboxylic acid cycle
Y2H	yeast two hybrid
Ws-2	*A. thaliana* Wasilewska ecotype
wt	wild type

I. Introduction

I. Circadian clocks in a rotating world

Circadian clocks are a time-measuring machinery that provide organisms with the ability to anticipate daily changes. The term "circadian" derives from the latin words *circa* = almost, *dies* = day, as these clock have a ~24 hour pace. This ~24 hour rhythm is a consequence of the cyclic transitions between day and night due to Earth´s rotation. These light to dark transitions have been present since the origin of life and are the most dominant environmental cue most terrestrial organisms face. Therefore they evolved the circadian clocks as a mean to anticipate the light to dark transitions. Consequently, many organisms adapted their physiological and behavioural responses to predict these changes. These responses include leaf movement, flower bud opening and stomata aperture in plants, conidiation in fungi, behavioural conduct in flies and melatonin secretion and sleep cycles in mammals (Dunlap, 2003). Thus a circadian clock provides fitness to the organisms by predicting the changes of day and night (Wijnen, 2006; Bell-Pedersen, 2005).

In a world that never stops rotating, rhythmic patterns could simply be driven by the daily exposure to light/dark periods. Rhythms that are sustained by this transition are diurnal rhythms, which do not predict future environmental changes (Dunlap, 2003). Circadian-clock-driven rhythms provide an advantage to diurnal rhythms as the former anticipates to the light to dark transitions. These circadian rhythms are defined by three main characteristics (McClung, 2006). First, a circadian rhythm persists even in the absence of environmental time cues, such as occurs under constant light and temperature. The observed rhythmic oscillation that takes place under constant conditions is called the free-running period. Second, the periodicity of this rhythm, which is about 24 hours, is fairly constant over a wide range of physiologically relevant temperatures. This is known as temperature compensation. Finally the circadian driven rhythm can be entrained by strong environmental signals, such as light/dark and warm/cold cycles typical of a day. These signals reset the clock on a daily basis (Salomé, 2005). In conclusion, a circadian rhythm is self sustainable and is adjusted on a daily basis to its current environment.

The study of the circadian clocks includes the analysis of the observed oscillation during the free-running period. This oscillation acquires the shape of a sinusoidal wave, which can be explained by mathematical terms. As a wave, the parameters of period,

amplitude and phase describe properties of the circadian clocks under study (McClung, 2006). The period refers to the distance between to peaks or troughs, which is the length of one complete cycle. The amplitude is half the distance of the wave from its highest to the lowest point. The phase is commonly measured as the distance from the last entrained oscillation to the first peak under free-running conditions (figure I.1). All together, these parameters define oscillating patterns for a given rhythm.

The first observations of the existence of an internal rhythm come from the 4th century B.C., but these findings were forgotten for centuries. It was until 1729 that the knowledge of an internal pacemaker was reintroduced and experimentally proven (Dunlap, 2003). J.J. DeMarian made pioneering examinations in *Mimosa* describing a rhythm of leaf movement. In the same century, Carl Linnaeus observed that different plant species opened their floral buds on a daily basis at a specific time of the day. Later during the 19th century, Darwin also described the daily pattern of leaf movement in plants. Finally in the 20th century, Erwin Bünning proposed that circadian rhythms provided adaptive values to the organisms (Dunlap, 2003). Recently, the adaptive value of having a circadian system in resonance with its environment has been demonstrated (Ouyang, 1998; Dodd, 2005), confirming Bünning´s hypothesis.

The selective advantage provided by an internal pacemaker had been demonstrated in algae and plants. In a competition experiment, strains of cyanobacteria that had circadian clocks with a wild type, short, or long period, were subjected to T-cycles in three different batches. Each T-cycle consisted in equivalent light/dark periods for a total amount of 22 (11:11), 24 (12:12) or 30 (15:15) hours. After 27 days of incubation under these conditions, the strain that outgrew the others was the one with a clock that matched its environment (Ouyang, 1998). In the same fashion, Dodd *et al.* (2005) demonstrated that higher plants with a clock which resonates with the external LD cycle, had enhanced growth, higher carbon fixation and improved photosynthesis, leading to increased survival compared to plants with a clock that did not match the experimental T-cycle. These studies provided evidence for how a clock synchronized with the environment enhances fitness, in both lower and higher organisms.

Circadian clocks are present in organisms ranging from bacteria to eukaryotes. The study of the pacemakers of model organisms like *Synechococcus*, *Drosophila*, *Neurospora*, *Arabidopsis* and *Mus* have shown features in common. These include that each clock has positive and negative elements that comprise a transcriptional feedback loop (Bell-Pedersen, 2005). In general, the transcription of the positive elements induces the
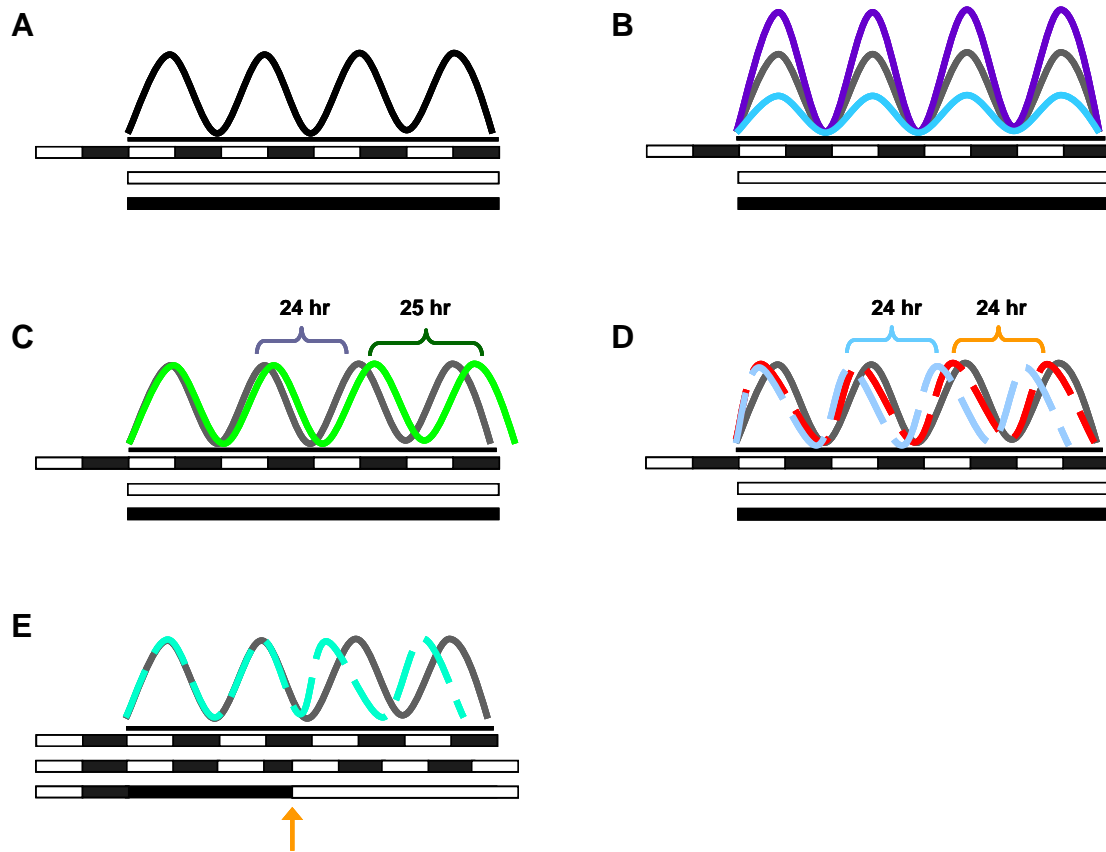
Figure I.1. Circadian rhythms persist even in the absence of environmental signals. The wave like output from the circadian clocks can be studied by mathematical parameters.
A) Circadian rhythms from organisms previously entrained by an environmental cue, in the example by 12 hr light/ 12 hr dark cycles, keep their pace under free running conditions, either under constant light or darkness (represented by white and black bars, respectively at the bottom of the figure).
B) Amplitude. The half the distance from the highest to the lowest point of a wave is the amplitude. The rhythms can be of high (purple) or low (blue) amplitude.
C) Period. The distance between two peaks or troughs of a wave is the period. In the absence of an entrainment signal the period of circadian clock mutants may be shorter or longer than 24 hrs. As an example of the later a long period is shown in green.
D) Phase. A point in the wave relative to the last entraining signal is called phase. The moment of a phase event can take place before or after the expected time under free running conditions (red and blue waves) without affecting the period. Under diurnal environmental stimuli the clock is entrained and the effect of a different phase relative to wild type is masked (red wave). However under free running conditions a shorter or longer phase would cause a shift of the wave relative to a normal or wild-type phase (blue wave).
E) Re-entrainment. A circadian rhythm can be entrained by a strong environmental signal, in the example light (orange arrow). Re-entrainment shifts the rhythm, but does not affect period, nor other circadian parameters (cyan wave). The clock is more susceptible to re-entrainment at the verge of the expected light/dark transitions. Note that the arrow indicates a shift to light conditions during the second half of the dark period.
In figures B to E the wild type or normal rhythm (A, black wave) is shown in gray for aiding in the comparisons.

expression of the negative elements, which in turn repress the expression of the formers, thus closing the loop. Therefore in many organisms, the circadian clock consists of a transcriptional-translational feedback loop. Interestingly, though the all these clocks share an analogous mechanism, their components are not conserved between them, suggesting that the circadian clocks must have appeared several times throughout evolution.

The clock transcriptional-translational feedback loop cannot sustain a ~24 hour rhythm by itself. To keep such a pace, this loop requires posttranslational processes that govern the activity and stability of both the positive and negative elements (Gallego, 2007). Reversible phosphorylation is emerging as an essential mechanism that drives the timing of the loop by activating, inactivating or providing a targeting signal for protein degradation. Several examples of changing the protein phosphorylation status by kinases and phosphatases have been described in *Neurospora crassa, Drosophila melanogaster* and *Mus musculus* clocks (Gallego, 2007). From all these studies emerges a view in which phosphorylation is essential to fine tune the function of the circadian clocks (Merrow, 2006; Gallego, 2007).

II. The *Arabidopsis thaliana* circadian clock

A. Generalities

Physiological observations of the existence of an oscillator in plants existed, but the molecular and genetic processes behind those rhythms were unknown (Dunlap, 2003). Evidence of fluctuating plastid and nuclear mRNA through the length of the day in tomato fruits were originally thought to be consequence of the light-regulated expression (Piechulla, 1987). This and the lack of a model for studying clock rhythms, impaired the study of the circadian clock in plants. This situation dramatically changed when *Arabidopsis thaliana* was established as a model for plants to study the circadian clock, by describing that the expression of the *CHLOROPHYLL A/B BINDING PROTEIN* (*CAB*) followed a rhythm under constant conditions (Millar, 1991). Thus a tractable rhythm in a genetically amenable plant provided promise to decipher the clock mechanisms in angiosperms. A few years later, the field gained its most valuable tool by using the firefly luciferase gene as a reporter of clock-gene expression (Millar, 1995a), which allowed the identification and study of a plethora of mutants in the circadian clock (Millar, 1995a,b).

Through the molecular-genetic analysis of mutants, the first model of the plant circadian clock was proposed. The core of the *A. thaliana* oscillator was proposed to comprise of a loop between two morning components and one evening component. The formers are two Myb-related transcription factors, *CIRCADIAN CLOCK ASSOCIATED* (*CCA1*) and *LATE ELONGATED HYPOCOTYL* (*LHY*) (Wang, 1998; Schaffer, 1998; Mizoguchi, 2002), whose encoded proteins bind to the Evening Element (EE) in the promoter of *TIMING OF CAB EXPRESSION/ PSEUDORESPONSE REGULATOR1* (*TOC1/PRR1),* the evening component (Alabadí, 2001). This binding represses *TOC1* transcription, but at dusk the protein levels of CCA1 and LHY diminish and the repression of *TOC1* is relieved. As a consequence, *TOC1* mRNA reaches its maximum around dusk, and by an unknown mechanism, TOC1 protein activates the transcription of *CCA1* and *LHY* (Alabadí, 2001; Mizoguchi, 2002). Though these three elements have been considered the core of the plant clock (Dunlap, 2003), this model cannot fully explain all experimental data (Locke, 2006).

Additional mutants that affect circadian rhythms have been documented and those genes remain to be placed within the clockwork. Mutations in several genes, such as *GIGANTEA* (*GI*), *EARLY FLOWERING 3* (*ELF3*), *EARLY FLOWERING 4* (*ELF4*), *TIME FOR COFFEE* (*TIC*), *LUX ARRHYTMO* (*LUX*), *TEJ*, and *ZEITLUPE* (*ZTL*), among many others, alter clock rhythms (Harmer, 2009). Also the TOC1-related family of pseudoresponse regulators (*PPR9*, *PRR7*, *PRR5*, *PRR3*) work within the circadian clock framework, as mutations in these genes affect clock rhythms (Makino, 2002; Salomé, 2005; Harmer, 2009). The transcription of these genes was described to peak sequentially through the circadian cycle with partially overlapping functions (Matsushika, 2000; Salomé, 2005). The expression of some of above molecules is light induced. Thus it has been proposed that those light inducible genes could function as components of a light-input pathway to the clock. For this reason, more complex clock models have arisen aided by computational modelling (Locke, 2005 and 2006; Zeilinger 2006).

Mathematical models have been formalized to comprise a clock with three interconnected feedback loops, which harbour unknown components within them. In a three-loop model, besides their described role in the core oscillator, CCA1 and LHY also participate in a morning loop to induce the expression of *PRR7* and *PPR9*, which in turn bind and repress the transcription of the formers (Imaizumi, 2010; Nakamichi, 2010). A so-called evening loop places TOC1 as a repressor of an unidentified Y component, which feeds back by inducing *TOC1* expression. *GI* was proposed to be the Y component, but *GI*

only partially fulfils this role (Locke, 2006; Hubbard, 2009). Within this model, the identity of an X factor, which serves as the component between *TOC1* expression and *CCA1/LHY* was mathematically required. A gene with these characteristics has not yet been found (figure I.2). An element acting between *TOC1* and *CAA1/LHY* transcription was identified and termed *CCA1 HIKING EXPEDITION* (*CHE*) (Pruneda-Paz, 2009). This factor cannot be X, as its protein only binds the promoter of *CCA1* and not that of *LHY*. Furthermore CHE binding to *CCA1* promoter represses *CCA1* transcription. This is opposed to the expected X function of an activator (Imaizumi, 2010).

Transcription of several clock components, including *CCA1, LHY*, *PRR9, PRR7* and *GI* was reported as light inducible (Más, 2008). Therefore it was proposed that light signals at dawn and dusk could be integrated to the oscillator by the morning elements and *GI*, respectively. This notion of an oscillator with interconnected loops was the first rational model established for a ~24 hour clock in plants (Locke, 2006; Zeilinger, 2006). This model could be confirmed experimentally, for example the *cca1/lhy/toc1* triple mutant was shown to be arrhythmic (Ding, 2007b).

Most knowledge of *A. thaliana* clockwork has been transcriptional, as studies involving post-translation modifications have lagged in comparison to clocks of other model organisms. Nonetheless recent studies have shown that post-translational modifications are essential for the function of the plant circadian clock. For example it has been shown that ZTL, a light-sensitive protein, binds to TOC1 during the night, directing TOC1 to degradation by the proteasome (Más 2003). Furthermore ZTL was proposed as a circadian blue-light photoreceptor that is stabilized by GI only under blue light (Kim, 2007). Contrary to the action of ZTL on TOC1 stability, PRR3 protects TOC1 from degradation (Para, 2007). Protein targeted degradation also takes place in the morning phase of the oscillator. As an example, LHY protein turnover was shown to be regulated by de-etiolated 1 (DET1). There it was demonstrated that DET1 inhibited LHY degradation in a light-independent process (Song, 2005).

Besides protein targeted degradation, protein phosphorylation has been shown to be necessary for proper rhythms. For example, the above mentioned interaction between TOC1 and PRR3 is enhanced when the later is phosphorylated (Para, 2007). Also casein kinase 2 (CK2) was shown to phosphorylate CCA1. Upon phosphorylation, CCA1 binding to DNA was enhanced and consequently rhythms of output genes could be sustained (Sugano, 1999; Daniel, 2004). Recently a GTPase, termed *LIP1*, was implicated in light input to the oscillator (Kevei 2007). In summary, post-translational mechanisms have an
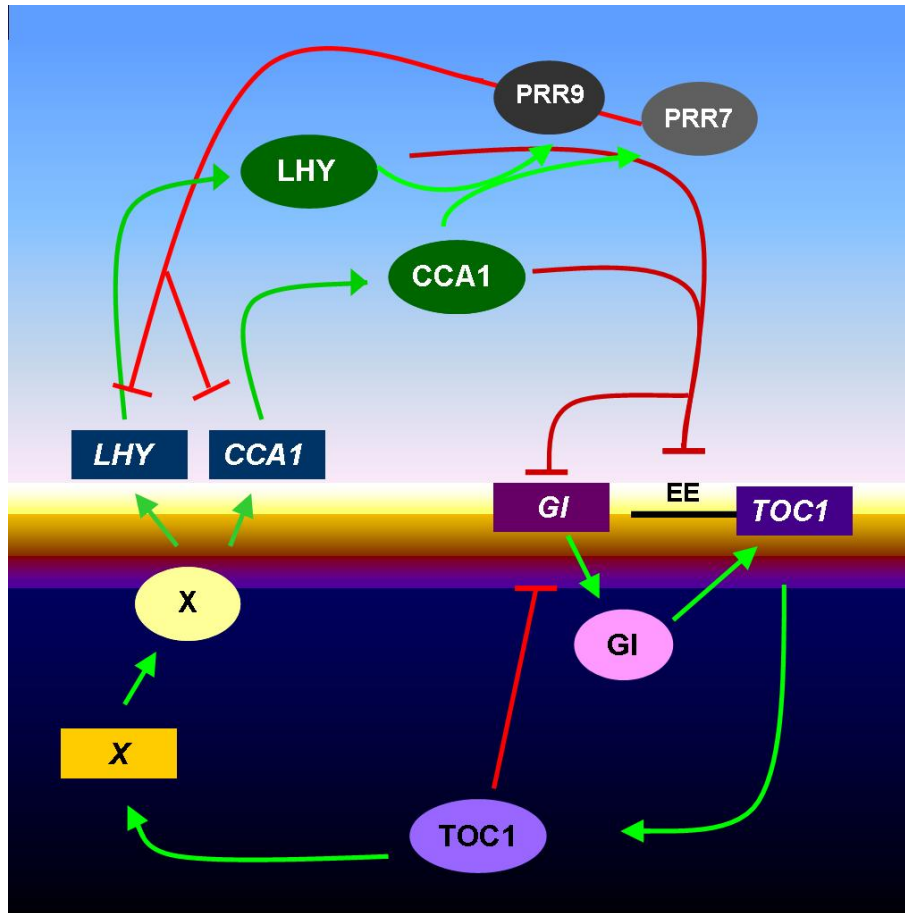
Figure I.2. Three loop model of *Arabidopsis thaliana* circadian clock.
The core of the oscillator is composed by two morning negative elements and one evening positive component (Alabadi, 2001). The two Myb like transcription factors *CCA1* and *LHY* are transcriptionally induced after dawn and their protein products bind to the Evening Element (EE) in the promoter of evening genes, such as *TOC1*, repressing their transcription. At dusk *TOC1* repression is relieved as CCA1 and LHY are degraded, leading to *TOC1* transcription. TOC1 closes the loop by inducing *CCA1* and *LHY* transcription by a yet unknown mechanism.
The three loop model of the clock incorporated one morning and one evening loop. During the day, CCA1 and LHY induce the transcription of the pseudoresponse regulators *PRR9* and *PRR7*, whose protein products bind to the promoters of the formers repressing their transcription. Within the evening loop, *GI* is transcriptionally induced as the repression from its promoter is relief before dusk and GI protein stimulates *TOC1* transcription. Then TOC1 feeds back by repressing the transcription of *GI*. In the three lop model (Locke, 2006), an unknown component named X, is the missing factor between TOC1 and *CCA1* and *LHY* transcription. The component X action would take place before dawn and may participate in clock entrainment.
Green arrows indicate induction and red bars represent repression. Day and night are indicated by clear pale blue and dark blue respectively. Dawn and dusk are indicated by graded color changes representing the sunrise/sunset (left and right side respectively).

important role in fine tuning the clock and now are starting to come into scene in the plant oscillator.

B. Light in clock entrainment and as an input signal to the oscillator

The circadian clock anticipates diurnal changes providing a competitive advantage compare to simply responding to the transitions of light to dark and dark to light. To keep track of the environment, the circadian clock is reset on a daily basis and in plants this resetting is driven by the dark to light transition at dawn. This resetting is called entrainment, which shifts the phase of gene expression to the changing photoperiod (Salomé, 2005). Thus entrainment is particularly required in locations away from the equator where day length changes dramatically on a daily basis, especially during mid-Spring and mid-Autumn. Clock entrainment occurs on a daily basis through "zeitgebers" (from the german word "time-givers") that consist predominantly as light and temperature changes (Salomé, 2005). My thesis work has focused on clock entrainment by light, because the dawn dark to light transition is the main environmental cue that entrains the clock (Salomé, 2005) and most clock controlled gene expression patterns follow light inputs (Michael, 2008).

Plants perceive light through different classes of photoreceptors. The phytochromes mainly sense red and far-red light, whereas the cryptochromes perceive preponderantly blue light (Fankhauser, 2002; van der Horst, 2004). These molecules are essential for plant development, as mutations in photoreceptor genes impair the de-etiolation process (Fankhauser, 2002). Interestingly photoreceptors transcription was reported to be under circadian control (Toth, 2001). Photoreceptor mutants were used to establish their role within the circadian clock. It was described that the photoreceptor function within the clock was wavelength specific: *phytochrome B* (*phyB*) was the main red light photoreceptor, *cryptochrome 1* (*cry1*) the blue light photoreceptor and *phytochrome A* (*phyA*) the low fluence light photoreceptor (Somers, 1998). It was shown that photoreceptors mutant displayed a light intensity dependent effect on clock periodicity. Only under low fluence rates these mutants exhibited a lengthened period (Somers, 1998). This effect obeys Aschoff rule, which states that the higher the light intensity, the shorter the period (Dunlap, 2003). Thus the light-signal input to the clock and the clock response to light were not affected in the photoreceptors mutants. Though photoreceptor mutants affected the clock period (Somers, 1998), it was found that *phyA* and *phyB* were not

necessary for circadian responses (Anderson, 1997). Furthermore it was described that even a quadruple photoreceptor mutant (*phyA/phyB/cry1/cry2*) displayed robust circadian rhythms (Yanovsky, 2000). Consequently though light input is essential for clock periodicity, photoentrainment still takes place without the main photoreceptors. This result suggested that other molecules may be responsible of transducing light signals to the oscillator.

If photoreceptors do not transduce light signals to the clock, other light perceiving molecules could act as circadian photoreceptors. As mentioned before, ZTL has been described as a blue-light photoreceptor. ZTL structure contains a Light-Oxygen-Voltage (LOV) domain that is essential for the light dependent binding of ZTL with GI (Kim, 2007). Two other proteins exist in the *A. thaliana* genome with a similar structure to ZTL. These are the LOV-KELCH PROTEIN 2 (LKP2) and FLAVIN BINDING KELCH REPEAT F-BOX 1 (FKF1), which both posses a LOV domain, though no clear role in light perception has yet been established for these products. *ztl* was described as a clock mutant that altered period in a fluence-dependent manner (Somers, 2000). *lkp2* and *fkf1* single mutants showed subtle effects on circadian rhythms, but a *ztl/lkp2/fkf1* triple mutant became essentially arrhythmic (Baudry, 2010). Thus *ZTL* had a major role in the circadian clock. Consequently *ZTL* remains a likely candidate for light transduction to the clock.

Several other mutants affect light input to the clock. *ELF3* has been described as arrhythtmic under continuous light, but rhythmic in darkness (Hicks, 1996). *ELF3* light input to the clock may take place at dusk as its clock stops at this time (McWatters, 2000). It has been described that *ELF3* together with *ELF4* negatively regulate light input to the clock (McWatters, 2007), while *SENSITIVITY TO RED LIGHT REDUCED* (*SRR1*) acts as a positive regulator of light input (Staiger, 2003). Other genes described with a dual role in light input as well as photomorphogenesis are *FAR RED ELONGATED HYPOCOTYL 3* (*FHY3*) (Allen, 2006), *LIGHT INSENSITIVE PERIOD 1* (*LIP1*) (Kevei, 2007) and *XAP5 CIRCADIAN TIMEKEEPER* (*XCT*) (Martin-Tyron, 2008). All together, light input to the clock, in particular to entrainment, is far from resolved and awaits to be clarified by finding the missing pieces as well by fully understanding the input function of known light signalling mutants.

C. *TIME FOR COFFEE* in the *A. thaliana* circadian clock

time for coffee (*tic*) was isolated from a mutagenized population for its short phase of *CAB:LUC* bioluminescent expression (Hall, 2003). The mutant exhibited a low amplitude rhythm that rapidly dampened *CAB* expression under constant conditions. Besides the low amplitude rhythms, the period length of *CAB2* and *COLD AND CIRCADIAN REGULATED 2* (*CCR2*, also known as *AtGRP7*) reporter genes were shorter in *tic* than in the wild type, under constant light and in dark conditions, respectively (Hall, 2003). Furthermore the robustness of the rhythms was weaker in *tic* than the wild type, because this mutant displayed higher variability in its rhythm, causing a higher mathematical error (Hall, 2003). Interestingly, when the periodicity of the mutant was scored by the movement of leaves, it was found that *tic* had a longer period than wild type (Hall, 2003). In that work, *tic* was described as being a fully recessive mutant.

tic growth displayed a phenotype consisting of a short hypocotyl and chlorotic leaves, which resembled that of *cca1/lhy* double mutant (Hall, 2003); *cca1/lhy* is defective in dawn circadian events (Mizoguchi, 2002). By release assays, which consisted in giving a 2 hour dark interval to plants previously shifted from cycling light-dark conditions to continuous light, it was shown that the clock in *tic* would restart between late night or early morning (Hall, 2003). This particular result gave birth to the name of "time for coffee," as the authors felt that at this time any human activity required a cup of coffee to "go on." All together, the data described a new circadian-clock mutant that functions between late night and dawn suggesting that *tic* participates in the clock light entrainment without altering downstream light signalling.

Further characterization of *TIC* included analyses of expression and rhythms of several clock genes. For this, the original mutant was introgressed to Ws-2 by backcrossing at least 4 times to this ecotype background. This was done as in the Ws-2 background many genetic resources were available to study epistatic relationships between *tic* and other clock mutants (Ding, 2007). The *CAB:LUC* gene expression was analysed in double mutants between *tic* and clock gene mutants. It was found that *tic* combined with any other evening clock mutant resulted in immediate lost of rhythms or just after one cycle (Ding, 2007). The authors also studied the diurnal and circadian gene expression of *tic*. The expression analysis of genes including *GI*, *TOC1*, *ELF3*, *CCA1* and *LHY* was found to have an advanced phase compared to the wild type. Luciferase reporter genes and gene expression analysis led to conclude that *tic* resulted in shorter periods and dampening of

rhythms (Ding 2007). Though the clock-gene expression in *tic* presented an early phase, the daily mean expression levels of these genes in *tic* and wild type was equal. The exception was *LHY,* whose mRNA abundance was found to be low and arrhythmic (Ding, 2007). Taken together, these results supported the hypothesis of TIC action within the clock and specifically participating in *LHY* expression, before dawn.

TIC was cloned and was found to correspond to the *A. thaliana* genomic sequence At3g22380 (Ding, 2007). The original *tic* mutation, referred as *tic-1,* had a cytosine to thymine transition in the fourth exon generating an encoded premature stop codon. It was reported that *TIC* genomic sequence has more than 4500 nucleotides that encode for a novel hypothetical protein sequence of 1500 amino acids with unknown functional domains, with exception of a theoretical ATP-GTP binding P-loop domain located in the last exon. Ding *et al.* (2007) demonstrated that the sequence At3g22380 was *TIC* by restoring the wild-type circadian responses in *tic-1* after complementation with the former. The authors also described the circadian defects in a transgenic line with a T-DNA insertion in the second exon termed *tic-2*, which is in the Col-0 background. *TIC* was found to be a single copy gene, though it has a paralog sequence in *A. thaliana* genome that was named TIC-like (*TKL* for the acronym of *TICKLE*). In conclusion TIC gene was identified and was demonstrated to be necessary for clock function with two different alleles.

Because many clock genes are circadian regulated, *TIC* mRNA expression was evaluated and was found that it did not cycle. Consequently TIC protein was analysed, it was observed that TIC was constitutively nuclear localised and that the protein levels were fairly constant through a circadian cycle (Ding, 2007). Collectively, it was proposed that TIC was a nuclear early-morning regulator of the circadian clock and that TIC function would be triggered via an as yet unknown mechanism.

III. Genome transcriptional control by the circadian clock

In the last years, it has been experimentally demonstrated that having a clock that matches and adjusts to its environment enhances fitness (Ouyang, 1998, Dodd, 2005). The oscillator generates a network with its environment by perceiving environmental signals, such as light and temperature, called the input pathways to the clock, and controlling responses as gene expression and metabolic reprogramming, which are termed the outputs

of the clock (Salomé, 2005; Wijnen, 2006). These clock-driven responses can also feedback to the clock. Consequently the oscillator can modulate the perception of these input signals (Harmer, 2009). At the end, the ultimate function of the circadian clock is to coordinate the physiological and metabolic processes to take place at the time when they are needed.

Microarray expression analysis demonstrated the pervasiveness of the circadian clock in the plant transcriptome (Harmer, 2000). Estimates of the percentage of genes under circadian control ranged between 6% up to 15%, but more recent views concluded that at least 30% of the transcriptome is under clock control (Covington, 2008; Hubbard, 2009). This percentage of genes is relatively similar to those found under clock control in the fly and mouse transcriptomes (Hubbard, 2009). These transcript profile analyses demonstrated how the circadian clock drives the expression of different biological processes in anticipation of physiological events.

Harmer *et al.* (2000) were the first to show that the clock governed the transcription of several metabolic pathways. The induction of gene expression in sets of photosynthetic genes and from the phenylpropanoid biosynthesis pathway took place early in the day and before dawn, respectively, whereas cold responsive genes were expressed before dusk. Furthermore the authors also established that the clock controlled the coordination of carbon, sulfur and nitrogen metabolism, as well as numerous developmental programmes. The clock exerted such a control on these diverse processes by driving the expression of key transcription factors or rate limiting enzymes (Harmer, 2000). Later, microarray studies analysed with improved algorithms described that pathways as the isoprenoid metabolism, key in carotenoid, tocopherol and phytohormones ABA and GA biosynthesis, were all under circadian control (Covington, 2008). In summary these data showed that the clock has a pervasive role in the physiology of plants and consequently is capable of adjusting most biological responses.

Other transcriptomic analysis took into consideration not only circadian microarray datasets, but also diurnal data and concluded that at least 89% of the transcribed genome is controlled by either the clock, diurnal cycles or thermocycles (Michael, 2008). This analysis suggested that such an extensive control was achieved by dispersed promoter sequences throughout the plant genome that provide a particular time frame of expression (Michael, 2008). These authors also found that at least in one of the conditions tested, more than 10,000 genes were under circadian control, while more than 16,000 were diurnally controlled. Interestingly an overlap of only 8,500 between both of them was found, giving

the possibility that a fraction of diurnal environmental stimuli are not under clock control. Furthermore most of the genes expression peaks tended to be toward either dawn or dusk. Thus, it seems that either clock or diurnal controlled, most of the responses to the environment are tightly time coordinated using the light/dark transitions as the main environmental signal.

As stated above, Covington *et al.* (2008) found a significant set of genes that were circadian regulated and responsive to hormone treatments, in particular to ABA, cytokinines, methyl jasmonate, salicylic acid and auxin. The exerted control by the circadian clock on the transcription of hormones is not a surprise as hormones are outputs of the clock. After all, hormones are involved in many physiological responses, from growth and stomata opening to many others that occur at a specific time of the day (Buchanan, 2000). It has been shown that hormones can feedback to the clock and are capable of affecting period length, amplitude or phase (Hanano, 2006). Furthermore the responses to hormones are gated by the circadian clock. For example stomata opening is dictate by the clock in well watered plants, opening in the dawn and closing before dusk (Dodd, 2005). ABA, which promotes stomatal closure, is less effective early in the day than at the end of it (Robertson, 2008). Similarly many auxin genes are clock regulated and the later gates the sensitivity to the hormone depending on the time of day (Covington, 2007; Rawat, 2009). The gated response to auxin explains the observed growth of plants around dawn in a LD cycle (Nozue, 2007). At this time of the day, auxin levels and plant responsiveness coincide with increased water turgor pressure and renewal of carbon supply, promoting growth. In resume, the plethora of genes under circadian control and the capacity the clock has on modulating multiple responses through a gating mechanism, highlights the importance of the circadian clock in adjusting the plant to its environment.

Interestingly from all the available microarray expression profiles, the circadian datasets were found to overlap with ABA (Mizuno, 2008, Matsui, 2008) and cADPR (Dodd, 2007) datasets. The relationship between the clock and ABA is extremely interesting because the later controls many environmental stress responses as water use and responses to drought, as well as to cold. Recently it was found that *TOC1* expression is induced by ABA (Legnaioli, 2009). Therefore the link between the circadian clock and ABA-related responses could define a link of how the clock prepares and deals with stress responses and enhances fitness.

The overlap between ABA and clock microarray datasets arise from the circadian control of many key genes involved in ABA biosynthesis or signal transduction.

Furthermore genes such as *EARLY RESPONSE TO DEHYDRATION 10 (ERD10)* and *7 (ERD7)*, *COLD REGULATED 15 B (COR15B)* and *A (COR15A)* and *RESPONSE TO DISSECATION (RD29A)* were found to be transcriptionally induced during the day (Mizuno, 2008). All of these genes are involved in the responses to drought and water deprivation or osmotic stress. A detailed examination by Covington *et al.* (2008), not only showed that ABA induced genes are expressed during the day, but that key enzymes in ABA precursors and biosynthesis are also clock controlled. These included *CLOROPLASTOS ALTERADOS 1 (CLA1)*, *PHYTOENO SYNTHASE (PSY)*, *9-CIS'EPOXYCAROTENOID DIOXYGENASE (NCED3)* and *ABA DEFICIENT 2 (ABA2)*, which participate in isoprenoid precursors synthesis, carotenoid synthesis and ABA biosynthesis, respectively. Recalling that carotenoids participate in the xantophyll cycle in chloroplast to avoid excess of solar energy absorption, as well as the circadian control of stomatal opening (Robertson, 2008), the circadian clock seems to link the light period of the day with stress and water loss, and consequently prepares in advance to them.

Given the relationship between the circadian clock and ABA, it is no surprise that microarray datasets from osmotic, salt and water deprivation stress also have a high number of genes circadian regulated (Covington, 2008). By means of a genome tilling arrays, it was shown that both annotated and unannotated regions responded to a diversity of abiotic stress. In the same report the similarity between salt and osmotic stress profiles was the highest between all the treatments. ABA treated samples showed certain similarity with the previous stresses, whereas cold and heat profiles shared less identity (Zeller, 2009). Unfortunately in this analysis plants were grown under continuous light and no data is available about the time of the treatments. However as seen from their principal component analysis, time was an important factor, as all the samples after 1 hour of treatment clustered together and apart from those that were sampled 12 hrs after their respective treatments (Zeller, 2009).

So far, I have focused on introducing pathways whose peak of expression is at dawn or early in the day, but dusk is also a signal for circadian control. At dusk genes involved in starch remobilization and lipid modification reach their higher expression (Harmer, 2000, Smith, 2007). The later has been interpreted as a correlation with the anticipation of cold nights and consequently freezing tolerance. In fact, the circadian clock controls the expression of cold responsive genes through the *C-REPEAT BINDING FACTOR 1/ DEHYDRATION RESPONSIVE ELEMENT BINDING 1 (CBF1/DREB1)* family of transcription factors. The expression of the more than 100 targets known as the

CBF/DREB regulon not only provides freezing tolerance but also resistance to salt and drought (Hotta, 2007). Though the later share the resistance profile with the ABA induced genes, the CBF/DREB transcription factors are totally independent of ABA (Urano, 2010). Interestingly Franklin *et al.* (2007) demonstrated that *CBF1*, *CBF2* and *CBF3* expression was increased under a low R/FR ratio and only after experiencing this condition plants acquired freezing tolerance. Because these conditions are mainly found at dawn and dusk, to a greater extent at higher latitudes, and the circadian clock gates cold responses (Fowler, 2005), the expression of these genes prepares the plant for the oncoming night. Thus the circadian clock, ABA and light signals coordinate the transcriptional cold response and interconnects the clock input and output pathways.

IV. The circadian clock and metabolism: a link toward homeostasis

A. Overview of metabolism in circadian systems

In recent years, the clock field has seen a change of perspective by several discoveries linking the traditional view of the transcriptional-translational feedback loop to cellular metabolism and homeostasis. Most of these breakthrough discoveries were obtained in the mammalian circadian clock, which I will briefly describe here. The mammal clock is comprised of the positive elements *CIRCADIAN LOCOMOTOR OUTPUT CYCLES KAPUT* (*CLOCK*) and *BRAIN AND MUSCLE ARYL HYDROCARBON RECEPTOR NUCLEAR TRANSLOCATOR (ARNT)-LIKE* (*BMAL1*), which induce the transcription of the negative elements *CRYPTOCHROME* (*CRY*) and *PERIOD* (*PER*). The formers are interconnected in a secondary loop with *REVERSE ERYTHROBLASTOSIS VIRUS α* (*REV-ERBα*) and *RETINOIC ACID RECEPTOR-RELATED ORPHAN RECEPTOR α* (*RORA*) (Wijnen, 2006). Within this system, a metabolic framework has been incorporated with an important role.

SIRTUIN1 (SIRT1), a NAD dependent enzyme, associates with CLK and this is required for CLK acetylation activity (Nakahata, 2008). Furthermore, NAD levels cycle within 24 hours and a NAD rate-limiting enzyme, nicotinamide phophoribosyltransferase (NAMPT), is circadian regulated, and consequently its inhibition affect clock rhythms (Nakahata, 2009). These findings could be related to those reported decades earlier in which pyridine nucleotides were found to cycle in *N. crassa* (Brody, 1973). Evidence of a

link between energy metabolism and the clock was provided by the discovery that adenosine monophosphate activated protein kinase (AMPK), an enzyme that responds to nutrient availability, phosphorylates CRY targeting it for degradation (Lamia, 2009). In a similar fashion, the circadian clock regulates heme metabolism by controlling some rate-limiting enzymes in heme biosynthesis. Heme affects the clock because it binds *REV-ERBα*, which then represses the expression of glucose catabolic genes and *BMAL1* (Yin, 2007). A couple of reports linked carbohydrate metabolism to the circadian clock. The inhibition of a glycogen synthase had effects on clock period regulation (Hirota, 2008) and also induced the degradation of *REV-ERBα* (Yin, 2006). These reports indicated that energy metabolism can feedback to the circadian clock by altering some of its components.

Transcriptomic studies suggested associations between the circadian clock and metabolism. Analysis of microarray data from mammals had shown that within the circadian transcriptome there is a high representation of genes that encode for enzymes involved in mitochondrial oxidative phosphorylation, glucose and lipid metabolism, (Kohsaka, 2006), all of them sources of energy. As mentioned above, NAD levels oscillate in a circadian fashion and at least NAMPT is also under circadian control (Nakahata 2009). NAD is coenzyme for many dehydrogenases that participate in oxidation reactions and the Krebs cycle. Also NAD is a substrate for ADP ribosylation (Eckel-Manhan, 2009), and it is required for the synthesis of cADPR through the action of ADP ribosyl cyclase (ADPR cyclase) (Lee, 1997). All together, the data highlighted that cellular energy control through pyridine nucleotides and/or through ATP could be linked to circadian control.

B. Links between the plant circadian clock and metabolism

In plants the first evidence of a link between the circadian clock and metabolism was provided Dodd *et al.* (2007). These authors found that cyclic adenosine diphosphate ribose (cADPR), which is synthethized from NAD by the ADP ribosyl cyclase, peaked early in the morning and affected the clock oscillation. A decrease in the concentration of cADPR lengthened the period of clock-controlled genes, whereas nicotinamide inhibited the ADP ribosyl cyclase and weakened circadian calcium oscillations (Dodd, 2007).

Previously it was demonstrated that ADPR cyclase activity was induced by ABA and that 30% of all ABA responsive genes were expressed in a similar pattern that those from cADPR (Sánchez, 2004). Recalling that circadian clock microarray datasets overlapped with ABA transcriptomic profiles (Mizuno, 2008), a link between the circadian

clock and metabolism in plants through cADPR could be suggested. Therefore a link between the transcriptional control of the circadian clock, ABA and cADPR in adjusting metabolism could exist.

What could lie as a common factor between the clock, ABA and energy is the status of carbon availability through the day. Previously several screens for altered sugar responses led to the description of *glucose insensitive* (*gin*), *sugar insensitive* (*sis*) and *sucrose uncoupled* (*sun*) mutants. Many of these mutants were ABA mutants, being allelic to *ABA insensitive 4* (*ABI4)* and *ABA2* (Rook, 2006). Therefore ABA and carbon are tightly linked. It has been reported that ABA and carbohydrates repress the expression of photosynthetic and plastocyanin genes (Rook, 2006) by binding to a minimal light-responsive promoter fragment of photosynthetic genes (Acevedo-Hernández, 2005). Therefore it seems that a relationship between ABA and carbohydrate exists and share similar roles in repressing photosynthesis.

Already has been mentioned the pervasiveness of the circadian clock and its relation with ABA gene expression profiles, but carbohydrates also influence the expression of clock responsive genes. Blasing *et al.* (2005) reported that half of the circadian controlled genes could respond to sugar. Similarly cellular sugar levels showed a major contribution in the establishment of diurnal gene expression patterns (Blasing, 2005). Interestingly these authors described that sugar-controlled gene expression was sensitive and responsive to low sugar levels, but not to high sugar. Through the study of a plastidial mutant in the *PHOSPHOGLUCOMUTASE* (*PGM*) gene, which impaired starch synthesis, they observed that when endogenous sugars levels diminished, sugar responsive genes were rapidly and highly expressed. In contrast, when high sugar levels were present during the light period gene expression did not change. Therefore in the wild-type strains the transcriptional reprogramming to declining levels of sugars occurs at the end of the night (Blasing, 2005). It seems that the circadian clock and the diurnal changes in carbon availability through photosynthesis are tightly linked and are responsible for most, if not all, the 24 hour cyclic gene expression patterns in natural diurnal cycles.

A link between ABA and sugar signalling could be provided by the *ARABIDOPSIS PROTEIN KINASE 10* (*AKIN10* or *SnRK1*). *AKIN10* belongs to a family of serine-threonine kinases that share high homology with the conserved *SUCROSE NON FERMENTING 1* (*SNF1*) yeast kinase (Polge, 2007). These kinases are multisubunit proteins that are essential for transcriptional metabolic reprogramming and consequently developmental control (Polge, 2007). As a pair of examples, in yeast, SNF1 controls the

transcriptional switch of a quarter of the genome in the transition from fermentative to oxidative metabolism in response to glucose deprivation. In mammals, when the AMP activated protein kinase (AMPK) senses a low ATP/AMP ratio, represses anabolic pathways and induces the catabolic ones (Polge, 2007). In a similar fashion, *AKIN10* and a kinase with high identity to it, *AKIN11*, were proposed to be a central component in the control of cellular energy signalling and homeostasis (Baena-Gonzalez, 2007, 2008). In the case of AKIN10, the kinase senses and responds to the cellular ATP/AMP ratio. When this ratio is high, the kinase is inactivated, but a low ratio triggers its activity (Baena-González, 2008).

The transcript profile of *AKIN10* activation showed that the expression of anabolic pathways was repressed, in particular protein and ribosomal protein synthesis. On the other hand, the transcription of catabolic pathways was induced including starch remobilization, hydrolysis of polysaccharides and cell wall, and β-oxidation of lipids (Baena-González, 2007, 2008). Genes that were expressed upon AKIN10 activation were repressed by the addition of sugars (Baena-González, 2007). Therefore it is plausible that over a diurnal cycle, AKIN10 senses a change in ATP/AMP ratio through the decreasing levels of available carbohydrates. Furthermore AKIN10 activity has been shown to decrease starch content while increases the levels of monosaccharides (Baena-González, 2007). Also it was observed that AKIN10 activity led to an ABA hypersensitive phenotype which was enhanced by addition of glucose (Jossier, 2009). All together, the data places cellular energy homeostasis at the hearth of transcriptional control of primary carbohydrate metabolism and ABA, between which a link with the circadian clock awaits to be clarified.

V. The circadian clock, light and environmental stimuli

A. Light as a source of ROS and energy

Photosynthesis is the primary and most important metabolic process plants commit to, because it is their source of energy. The ultimate step of the photosynthetic process is the generation of NADPH and ATP synthesis. The energy obtained is then used in the Calvin cycle (Nelson, 2000). Though photosynthesis is essential, the light absorption creates oxidative stress due to the formation of reactive oxygen species (ROS) such as singlet oxygen ($^1O_2$), superoxide ($O_2^{\bullet-}$) and hydrogen peroxide (H_2O_2). Furthermore under

stress conditions or high light irradiance, the electron flow through the photosynthethic chain overcomes the passage of electrons from the ferredoxin to several reductases causing an over-reduction of the plastoquinone and cytochrome b complex (Oelze, 2008).

To cope with ROS production plants have energy dissipating strategies and several ROS quenching systems. The first ones involve conformational changes in the photosystems, absorption of light by carotenoids and the non photochemical quenching by the xantophyll cycle. The quenching systems involve a series of enzymes including the ascorbate and glutathione pools, thioredoxins, peroxiredoxins, glutaredoxins, as well as the superoxide dismutases and catalases (Oelze, 2008, Wormuth, 2007).

Because plants are aerobic organisms, photosynthesis is not the only source of ROS production. Through respiration, plants consume carbohydrates and reducing equivalents as NADH and FADH to yield ATP, as well as substrates from the tricarboxylic cycle (TCA) for biosynthetic pathways through oxidative phosphorylation. Besides respiration, during the light period plants also make photorespiration, which is enhanced under high light or stressful conditions (Buchanan, 2000; Noguchi, 2007). To alleviate stress, the plant mitochondria dissipates excessive electron flow through the rotenone insensitive NAD(P)H oxidases and the cyanide resistant alternative oxidase (AOX). These processes enhance plant fitness by improving photosynthesis under stress conditions (Noguchi, 2007, Rhoads, 2007).

As ROS generation is concomitant to photosynthesis and respiration, it was surprising that ROS responsive genes were not found to be under clock control (Covington, 2008). This could be explained by three characteristics of ROS responsive genes. First, the transcription of these genes is induced upon stress. Secondly, many enzymes activity change due to their redox state (Oelze, 2008, Wormuth, 2007). Finally, their rate of transcription is environment dependent. It has been observed that the longer the photoperiod or the higher the light intensity, ROS antioxidant genes are higher expressed and the ascorbate pool increases (Becker, 2006 and Bartoli, 2006, respectively). In summary, plants have a complex network to cope with ROS generation and the role of the circadian clock in ROS transcriptional control still is unclear.

B. Stress and energy as a metabolic input to the clock

A link between energy metabolism, ROS production and environmental responses could be provided by the changes in NAD and poly-ADPribosylation in response to stress.

Though NAD synthesis has been shown to be rhythmic only in mammals (Nakahata, 2009, Ramsey, 2009), as photosynthesis is under circadian control, pyridine nucleotide levels could oscillate through the day. It has been reported that the degree of poly ADP ribose (PAR) synthesis by the PAR polymerases (PARP) is increased in proportion to stress severity (Hashida, 2009). PARP reaction consumes NAD and ATP, therefore affecting energy homeostasis (De Block, 2005). These authors observed that the downregulation of PARP enhanced stress tolerance probably due to a reduced consumption of NAD and ATP. However PAR takes place in response to ROS and DNA damage (Qin, 2008). Ishikawa *et al.* (2009) observed that overexpression of a PARP pyrophophohydrolase, *AtNUDX7* (*NUCLEOSIDE DIPHOSPHATE LINKED TO SOME MOIETY X*), increased resistance to oxidative stress; whereas the mutant had higher levels of cellular NAD and ATP, but was hypersensitive to oxidative stress. Thus it seems that a tight correlation in the appropriate use of energy is essential to acquire resistance against ROS regardless of their origin.

Polyribosylation of proteins by PARPs is overcome by the antagonistic reaction of the PAR glycohydrolases (PARG). Interestingly one *A. thaliana* clock mutant, *TEJ* (from Sanskrit bright) was identified as a PARG (Panda, 2002). Besides its brighter luminescence that traduced into higher amplitude of all tested clock genes, the period of the rhythms was lengthened independent of light quality and quantity. Furthermore the mutant affected the transcription of clock regulated genes and flowered earlier independent of the photoperiod (Panda, 2002). Therefore these results suggest that a link between energy homeostasis and the circadian clock exists and has not yet been completely defined.

VI. Aim of this work

Several questions regarding the role of *TIC* in clock entrainment remain unanswered. How does *TIC* participate in entraining the clock at dawn? What is the role of *TIC* in entrainment and what is the state of *tic* clock prior to dawn? Does the state of *tic* clock alter other metabolic process and physiological responses that participate in light gating to the clock? Is *tic* response to re-entrainment different from wild type? How does *TIC* exert its time-specific function?

With those questions defined, the objectives of my thesis work were as followed:

Main objective

Characterize *TIC* function in regard of pre-dawn light in the morning entrainment of the circadian clock.

Particular objectives

1. Perform and analyse a microarray transcript profile toward morning anticipation and the effect of advancing the resetting of the clock prior to dawn, in a *TIC* dependent fashion.
2. Characterize *tic* effects and responses derived from its clock arrest during night.
3. Search for TIC protein interactors and generate a hypothesis of a mechanism for TIC action within the circadian clock.
4. Characterize the *TIC*-like gene, *TKL*, in regard of its function in the *A. thaliana* clock.

I addressed those questions during my research as a presentation for this thesis. I found that *tic* responses to light signals were different from the wild type, as well as its transcriptional profile differed prior to dawn. *tic* presented pleiotropic phenotypes with altered responses to ROS, ABA, abiotic and biotic stress. It is plausible that *tic* displayed such physiological defects because of a general disruption in cellular homeostasis. In

support of this, TIC was found to be able to interact with the kinase AKIN10. These results suggested that TIC could be activated by AKIN10 and consequently TIC could exert its function within the circadian clock. Finally I hypothesized that TIC activation would lead to morning entrainment. As an aside, the TIC-related gene, *TKL* was not found to have a function within the clock.

II. Material and Methods

II.A. Material

Unless otherwise stated, all material used was bought from DUCHEFA (media, agar, organic and inorganic salts, organic compounds) or SIGMA (chemicals, hormones, inorganic salts).

When water was used as a solvent, Millipore grade filtered water was used, unless otherwise noted.

Growth media for plants

1) Murashige and Skoog (MS) basal salts
- 4.4 g/L MS
- 0.5 g/L 2-(N-morpholino)ethanesulfonic acid (MES)
- 1 % (w/v) sucrose (MS1) or 3 % (w/v) sucrose (MS3)
- 1 % (w/v) phytoagar

pH adjusted to 5.7 with KOH and sterilized in an autoclave for 20 minutes at 121°C.

Antibiotics, hormones or chemicals were added to the required concentrations for their respective assays.

2) MS1 basal salts for iron tests
- 2.2 g/L MS
- 0.5 g/L 2-(N-morpholine)ethanesulfonic acid (MES)
- 1 % (w/v) sucrose
- 0.9 % (w/v) gelrite (Scott laboratories)

pH adjusted to 5.7 with KOH and sterilized in an autoclave for 20 minutes at 121°C.

Iron solutions or chelators were added to the specified concentrations.

3) Gambourgh B5 (G-B5) with bromocresol purple as a pH indicator.
- 3.163 g/L G-B5 with micro and macroelements including vitamins
- 0.25 g/L 2-(N-morpholine)ethanesulfonic acid (MES)
- 0.2 mM $CaSO4^{\cdot}2H_2O$
- 0.008 % (w/v) bromocresol purple

pH adjusted to 6.5 with NaOH and sterilized in autoclave for 20 minutes at 121°C.

4) Agar-water
- 0.01 % (w/v) agar in water

Growth media for bacteria

1) NYGA
- 5 g/L bactopeptone (Difco)
- 3 g/L yeast extract (Difco)
- 20 ml/L glycerol
- 10 g/L agar

Antibiotics

- Kanamycin 100 mg/mL in H_2O
- Hygromycin 100 mg/mL in H_2O
- Carbenicillin 100 mg/mL in H_2O
- Rifampicin 50 mg/mL in DMSO

Antiobiotics were dissolved in water and filter sterilized through a 0.45 μM filter (Millex), except rifampicin. They were store at -20°C until use.

Hormones and chemicals

- Dimethyl sulfoxide (DMSO)

- Methylviologen dichloride (MV)
  25.7 mg/10 mL H_2O for 10 mM stock solution

- Diphenyleneiodonium chloride (DPI)
  10 mg/3.18 mL DMSO for 10 mM stock solution

- Salicylhydroxamic acid (SHAM)
  15.314 mg/10mL H_2O for 10 mM stock solution

- Hydrogen peroxide (H_2O_2)
  30% w/w solution

- cis-trans (+/-) abscisic acid (ABA)
  24.6 mg/10mL ethanol for 10mM stock solution

- 3-(2Pyridyl)-5,6-diphenyl-1,2,4-triazine-4,4-disulfonic acid sodium salt (ferrozine)
  123.1 mg/50 mL H_2O for a 5mM solution

- 17-β-estradiol
  2.72 g/mL DMSO for a 10mM solution

All except ferrozine were kept at -20°C until use. Ferrozine was kept at 4°C and protected from light.

Buffers and solutions

DNA extraction buffer (DBE)
- 200 mM Tris pH 8.0
- 240 mM NaCl
- 25 mM Ethylendiamintetraacetic acid (EDTA)
- 1% (w/v) dodecyl sodium sulfate (SDS)

10X Tris EDTA (TE)
- M Tris pH 7.5
- 10 mM EDTA

25X Tris borate EDTA (TBE) electrophoresis buffer
- 67.23 g/L Tris
- 34.31 g/L boric acid
- 37.22 g/L EDTA

pH adjusted to 8.0 with KOH

Bleach solution
- 33 % Klorix (commercial sodium hypochlorite solution)
- 0.02 % Triton X-100

50 mM D-luciferin (LABTECH international, UK)
- 1 g D-luciferin (D-[4,5-dihydro-2-(6-hydroxy-2-benzothiazolyl)-4-thiazole-carboxylic acid] in 71.3 ml 0.1 M triphosphate buffer (Na2HPO4/NaH2PO4) adjusted to pH 8.0.

Aliquots of 1.5 mL were stored at -80°C upon use. For the 5 mM working solution the stock was diluted with 0.01% (w/v) Triton-X100.

Fe$_3$EDTA solution
- 1.835 g/500 mL for a 10 mM solution

FeS04$^.$7H$_2$O solution
- 1.39 g/500 mL for a 10 mM solution

MgCl$_2$ 6$^.$H$_2$O
- 20.33 g/L for a 10 mM solution

Lugol solution
Ethidium bromide (10 mg/mL)
Silwet L77 (Lehle Seeds, USA)
Ethanol

Molecular Biology

PCR reagents (all from PEQLAB)

- 10X Buffer
- 25 mM MgCl$_2$
- 5X Enhancer
- 10 mM di-deoxinucleotides (dNTPs)
- Oligonucleotides (from Invitrogen or Sigma)
- Laboratory purified *Thermus aquaticus* DNA polymerase as described by Engelke *et al*. (1990) and Grimm *et al.* (1995)

RNA extraction
- RNAeasy kit from Qiagen (Germany)

RNA driven complementary DNA (cDNA) synthesis, amplification for microarray ATH1 hybridization

All these steps were perfomed according to the instructions of the following kit from Ambion (USA): Ambion MessageAmp II-Biotin Enhanced single round aRNA amplification kit; catalog number: 1791. The kit provided all reagents necessary for cDNA synthesis, purification and biotionylation of cRNA.

cDNA synthesis
- T7 oligo (dT) primer
- Arrayscript
- RNase inhibitor
- 10X first strand buffer
- dNTP mix
- 10X second strand buffer
- DNA polymerase
- RNase H
- T7 enzyme mix
- T7 10X reaction buffer
- Biotin NTP mix
- Nuclease free water

cDNA purification and fragmentation
- Wash buffer
- cDNA binding buffer
- aRNA binding buffer
- 5X array fragmentation buffer
- aRNA and cDNA filter cartridges
- Nuclease free water

ATH1 chips hybridization, staining and scanning

Hybridization
- ATH1 chips (Affymetrix, USA)
- Streptavidin Phycoerythrin (SAPE) staining solution
  - 2X MES stain buffer
  - 50 mg/mL acetylated bovine serum albumin (BSA) (Invitrogen)
  - R-Phycoerythrin Streptavidin (SAPE) (Molecular probes)
  - Nuclease free water

- Antibody solution
  - 2X MES stain buffer
  - 50 mg/mL acetylated BSA (Invitrogen)
  - SAPE (Molecular probes)
  - Goat antibody IgG
  - Biotinylated anti-streptavidin antibody (goat) (Vector Laboratories)
  - Nuclease free water

- Hybridization cocktail
  - DMSO
  - 2X hybridization buffer (prepared according to Affymetrix)
  - 10 mg/mL herring sperm DNA (Promega)
  - 50 mg/mL acetylated BSA (Invitrogen)
  - control oligonucleotide B2 (Affymetrix)
  - 20X eukaryotic hybridization controls (*BioB*, *C*, *D*, *Cre*) (Affymetrix)
  - Nuclease free water

Material for Yeast two hybrid screen

Media
YPDA
- Yeast extract   10 g/L
- Peptone   20 g/L
- Glucose   20 g/L
- Agar   20 g/L

Synthethic minimal and drop out media (from Clontech-Takara, France)
Leucine/Tryptophan (LW), LW/Histidine/Adenine, LW/Histidine

Strains
PJ69-4a (James, 1996)
PJ69-4α (James, 1996)

Solutions

Tris EDTA Lithium acetate
- 1X TE
- 100 mM Lithium acetate

Polyethylene glycol lithium acetate
- 8 mL 40% Polyethylene glycol (PEG)
- 1X TE
- 100 mM Lithium acetate

Salmon sperm carrier DNA (Invitrogen)

Vectors (Gateway derived from Invitrogen, Germany)
pDEST32
pDEST22

Material for *in vitro* pull-down and *in vitro* phosphorylation

Lysis buffer
- 50 mM Tris HCl pH 7.5
- 300 mM NaCl
- 25 mM imidazole
- 10 mM NaF
- 10% glycerol
- 2 mM β-mercaptoethanol
- 1:100 protease inhibitor cockatil

Dialysis buffer
- 50 mM Tris HCl pH 7.5
- 40% glycerol
- 2 mM β-mercaptoethanol
- 0.1 mM EGTA
- 1 mM phenylmethylsulfonyl fluoride (PMSF)

Gluthathione agarose beads

Kinase buffer
- 20 mM HEPES
- 2.5 % Triton X-100
- 10 mM $MgCl_2$
- 50 mM NaF
- 5 mM PMSF
- 5X protease inhibitor cockatil

γ-^{32}P ATP (Amershan-GE Healthcare Life Sciences, Germany)

SDS-Polyacrylamide gel electrophoresis (PAGE) (According to Laemmli, 1970)
- 29:1 acryalamide-bisacrylamide
- Tris-HCl pH 8.8 or 6.8
- 10 % SDS
- 10 % ammonium persulfate (APS)
- TEMED

SDS buffer
- 25 mM Tris
- 192 mM glycine
- 0.1 % SDS

Coomassie staining solution
- 1 % brilliant blue R-250
- 10 % glacial acetic acid
- 45 % methanol

Plant material

The following lines were used throughout the study:

Table I. Wild type and transgenic lines used in this study.

Name	Ecotype	Luciferase marker	Reference
Col-0 (wt)	Col	---	NASC
wt	Col	*CCA1*	(Doyle, 2002)
wt	Col	*CAB*	(Ding, 2007)
wt	Col	*CCR2*	(Doyle, 2007)
tic-2	Col	---	(Ding, 2007)
tic-2	Col	*CCA1*	(Ding, 2007)
tic-2	Col	*CAB*	(Ding, 2007)
tic-2	Col	*CCR2*	(Ding, 2007)
AKIN10	Col	---	Berendzen, K. PhD thesis (2005)
AKIN10	Col	*CCA1*	This thesis
tic-2/AKIN10	Col	*CCA1*	This thesis
AKIN11	Col	---	Berendzen, K. PhD thesis (2005)
AKIN11	Col	*CCA1*	This thesis
tic-2/AKIN11	Col	*CCA1*	This thesis
tkl-1	Col	---	This thesis
tkl-1	Col	*CAB*	This thesis
tkl-1	Col	*CCR2*	This thesis
tic-2/tkl-1	Col	---	This thesis
tkl-2	Col	---	This thesis
gi-2	Col	---	NASC
gi-100	Col	---	unpublished
Ws-2 (wt)	Ws	---	NASC
wt	Ws	*CCA1*	(Doyle, 2002)
tic-1	Ws	*CCA1*	(Ding, 2007)
gi-11	Ws	*CAB*	(Ding, 2007)
tic-1/gi-11	Ws	*CAB*	(Ding, 2007)

Oligonucleotides

The following list includes oligonucleotides used for genotyping plants and for the generation of constructs for expression of recombinant proteins.

Table II. List of oligonucleotides

Name	Gene/insertion	Sequence	Product size (bp)
For genotyping plant transgenic lines			
tic2LP	*tic-2* SAIL 753 E03	TGATTGTAGTGACGCGTGAAC	952
tic2RP	*tic-2* SAIL 753 E03	GAAGAATAATTTTCCGCCGAC	952
tkl1LP	*tkl-1* SALK 028176	GTGCAGTTGTTTTCAAATTGC	1004
tkl1RP	*tkl-1* SALK 028176	TCCTCTTACTCCGATTGAACG	1004
tkl2LP	*tkl-2* SAIL 714 A02	CAGTTGTTTTCAAATTGCATATCAG	959
tkl2RP	*tkl-2* SAIL 714 A02	CTTCTTCTCCTCTTACTCCGATTG	959
LBb1	SALK lines	GCGTGGACCGCTTGCTGCAACT	variable
LB1S	SAIL lines	GCCTTTTCAGAAATGGATAAATAGCCTT GCTTCC	variable
AK10fwd	*AKIN10*	GGATCTTGAGTCGACGGATC	573
AK10rev	*AKIN10*	CATAATTTGGACTTCCACAACTTGT	573
AK11fwd	*AKIN11*	AAATGGGCTCTTGGACTTCAGT	416
AK11rev	*AKIN11*	TCCGTCGACTCAGCATAATCT	416
For constructs for protein expression			
TIC-LP	TIC 5' primer	GGGGACAAGTTTGTACAAAAAAGCAGG CTTAGAAGGAGATAGAACCATGGATAG AAATAGAGAA	variable
TIC-RP250	TIC 3' primer for TIC-250	GGGGACCACTTTGTACAAGAAAGCTGGG TACTAATTAGCTGGAGACGT TGA	750
TIC-RP564	TIC 3' primer for TIC-564	GGGGACCACTTTGTACAAGAAAGCTGGG TACTAACAATTCCTCTCAAACTT	1692
TIC-RP770	TIC 3' primer for TIC-770	GGGGACCACTTTGTACAAGAAAGCTGGG TACTATTGCTGCCTCTGCTGAAA	2410
AK10-LP	AKIN10 full lenght	GGGGACAAGTTTGTACAAAAAAGCAGCT TAGAAGGAGATAGAACCATGGATGGAC AGGCACA	2208
AK10-RP	AKIN10 full lenght	GGGGACCACTTTGTACAAGAAAGCTGGG TATCAGAGGACTCGGAGCTG	2208
AK11-LP	AKIN11 full lenght	GGGGACAAGTTTGTACAAAAAAGCAGG CTTAGAAGGAGATAGAACCATGGATCAT TCATCAAAT	2067
AK11-RP	AKIN11 full lenght	GGGGACCACTTTGTACAAGAAAGCTGGG TATCAGATCACACGAAGCTC	2067

II.B. Methods

Seed surface sterilization

Seed aliquots were surface sterilized by adding the following volumes of solutions. As each solution was added, the tube containing the seed aliquot was shaken in a vortex and spun down. The procedure consisted in washing the seeds with 500 µL ethanol, followed by 400 µL of bleach solution, immediately afterwards they were rinsed three times with 800 µL of sterilized water and finally resuspended in 500 µL of agar/water.

The seeds were kept in the tube or placed on plates with MS1 or MS3 media for 2-3 days at $4^{o}C$ in the dark before releasing to growth conditions.

Growth conditions

The seeds were germinated over MS1 or MS3 under photoperiods of 12 hours light and 12 hours darkness (12:12 LD). Most of the experiments were performed on MS1 media.

When seedlings were 7-day old, they were transferred to soil, then were placed either under long-day (16:8 light/dark), short-day (8:16 light/dark) or intermediate-day (12:12 light/dark) photoperiods. The first two were under greenhouse conditions, whereas for the latter a climatic chamber was used.

Generation of plant resources and transgenic lines.

Plants were crossed for obtaining the desired genotypes by using preferentially the luciferase harbouring line as the male and the other as the female. For this a female flower that had not opened yet was emasculated by removing carefully the sepals, petals, and stamens, while leaving intact the carpel. The later was fecundated with the pollen of a mature flower recognized by its yellow colour.

The obtained siliques from the crosses were harvested and the progeny (F1) was selected by luciferase imaging screen, antibiotic resistance and/or genotyping by PCR. The selected F1 plants self pollinated and their progeny (F2) was screened again for the presence of the desired trait. Either in the F2 population or its progeny (F3), the homozygous plants for a particular trait/marker were obtained. These plants were confirmed as homozygous by repeating the selection tests on their progeny (F3 or F4).

DNA extraction

The plant material was ground using a pistil and sand or metal beads with 400 μL DEB and 75 μL chloroform. The material was shaken in a vortex and centrifuged at 2500 g for 10 min, and finally, the supernatant was recovered and transferred to a clean tube. Then 300 μL isopropanol was added, followed by shaking with vortex before a second centrifugation step under the same conditions. The pellet was recovered by decantation, then it was washed once with 70% ethanol and the pellet was kept by decanting the supernatant. Finally the DNA was allowed to dry for 10-30 min by standing the tubes uncapped at room temperature. The DNA was brought back to solution with either 100μL water or 1X TE.

PCR and Electophoresis

Standard PCR procedures were employed (Sambrook, 2001), which consisted of the following parameters: 1 cycle of $94^{o}C/2$ min, followed by 30 cycles of $94^{o}C/20s$, $60^{o}C/30s$, $72^{o}C/90s$ and a final cycle of $72^{o}C/10$ min.

Plant DNA samples were used to screen for the presence of the desired transgene by amplifying with a specific oligonucleotide pair (table II). The final reaction volumes were 10 or 20 μL at the final concentration of 1X PCR buffer, 1.5 mM Mg_2Cl, 1X enhancer, 0.25 mM dNTPs, 0.5 μM each primer and 0.2 μL Taq Polymerase with 1 μL of DNA solution as template.

Electrophoresis conditions were standard (Sambrook, 2001), as 1% agarose gels with ethidium bromide (0.5μg/mL) were run in 1X TBE at 90 volts. Visualization of the bands was achieved using the BIORAD GEL DOC system.

Microarray samples and ATH1 hybridization

Replicate biological samples of wild type and *tic-2* were grown in MS3 media under 12:12 LD photoperiod for seven days. On the 8th day, the plants were collected, either before lights on (dawn-anticipation assay) or after giving a pulse of light with duration of 2 hours before the expected time for lights on (clock-resetting assay), and frozen in liquid nitrogen (see figure II.1A). Total RNA was extracted using the RNAeasy kit from Qiagen and RNA quality was assessed by examining the integrity of ribosomal bands after electrophoresis.

I

II

Genotype comparison
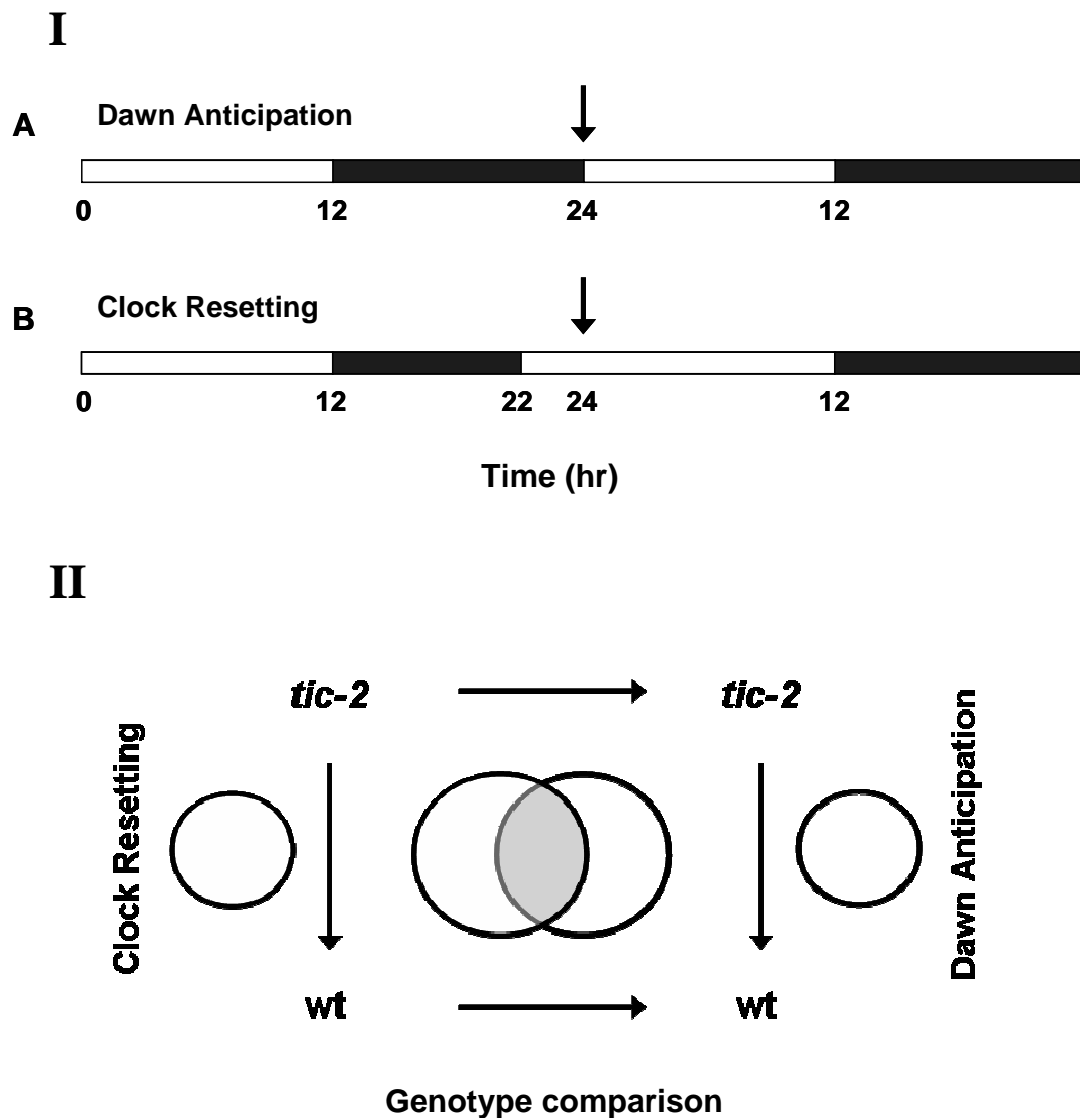
Figure II.1. Schematic representation of the microarray experimental designs and of the pair-wise comparisons performed.

I) Diagram of experimental design. Seedlings grown on MS3 for 7 days under 12:12 LD photoperiod were collected the next day at the indicated time (arrows). Only days 7 and 8 are shown. White and black bars represent respectively, light and dark periods.

A) Dawn anticipation assay. The plants were harvested just before the lights on.

B) Clock resetting assay. The seedlings received a 2 hour light pulse before the predicted onset of dawn and were collected as soon as the light pulse was over.

II) Scheme of the group comparisons for the data analyses. The experimental designs allowed the evaluation of mRNA changes between genotypes under 2 physiological conditions (vertical arrows), as well as the response within genotypes toward an environment change (horizontal arrows). This thesis focused on the comparison between wild type and mutant and their respective lists of differentially expressed genes (depicted by the circles next to the arrows). The overlapping area (light gray) between the lists (center of the figure) corresponds to the mRNA abundance changes in *tic-2* that were independent of the physiological conditions and therefore were called as *tic-2* specific.

The direction of the arrows indicates the way of the comparison (1, *tic-2 vs.* 2, wt); consequently the fold change values describe induction or repression of *tic-2* genes.

The service unit from the MPI Tübingen performed cDNA synthesis, amplification, labeling, hybridization and scanning of the Affymetrix ATH1 chips. Quality control of the chip image after hybridization was ensured.

The cDNA synthesis was executed by using the MessageAmp II-Biotin Enhanced kit from Ambion. For the first strand synthesis, the RNA was mixed with the T7 oligodT primer and incubated for 10 min at 70°C, followed by the addition of the reverse transcription master mix and incubated for 2 hours at 42°C. For the second strand cDNA synthesis, the second strand master mix was incorporated to the reaction followed by an incubation of 2 hours at 16°C. Then the cDNA was purified by mixing with the binding buffer and the solution was spun down through the cDNA filter cartridge which binds the cDNA. The filters were washed and the samples were eluted by adding twice previously warmed water at 55°C. The synthesis of the biotin labeled antisense RNA (aRNA) involved mixing the purified cDNA with the *in vitro* transcription master mix which then was incubated at 37°C for at least 4 hours but less than 14 hours. After incubation water was added to each sample and the aRNA was mixed gently with the aRNA binding buffer and pure ethanol. The samples were purified by passing through the aRNA filter cartridge, followed by washing and elution steps.

Finally for the hybridization to the ATH1 chips, the aRNA samples were mixed with the hybridization cocktail and denatured at 99°C for 5 min followed by 45°C for 5 min. Previously the ATH1 chips were adjusted and room temperature and prehybridized with 1X hybridization buffer at 45°C for at least 10 min. Then the prehybridization buffer was removed from the ATH1 chips and they were loaded with the hybridization mix containing the aRNA. Finally hybridization was performed overnight at 45°C with gently rotation at 60 rpm. After hybridization, the samples were removed from each ATH1 chip and the later was washed with the corresponding buffer and stained according to Affymetrix protocol EukGe-WS2v4 by using the GeneChip Fluidics Station 450. The arrays were scanned with the Affymetrix GeneChip scanner GS300 7G.

Microarray data analysis and mining

The CEL files generated with the Affymetrix GeneChip Operating System (GCOS) were analysed using the Affymetrix Expression Console software. After loading the CEL files, the Robust Multichip Analysis (RMA) algorithm (Irizarry, 2003; Grant, 2007) was applied to the CEL files from the 8 hybridized ATH1 chips. Besides evaluating the image derived from the ATH1 chip hybridizations, box plots, MvA expression plots, were used to

evaluate signal intensity between the 8 ATH1 chips and for detecting artefacts, respectively. mRNA spike controls were analysed for an equal hybridization signal intensity between and within arrays and for the quality of biological material (Affymetrix Expression Console manual; Grant, 2007; Allison, 2006). Then I proceeded with the normalization after which the 8 chips had equal signal intensity as evaluated by box plots of expression. Spearman's correlation and PCA were used to visualize the similarity of the expression profiles within the samples (Allison, 2006, Cordero, 2008). Volcano plots were used to visualize the fold change of expression and the statistical significance of the later (Allison, 2006; Grant 2007).

The microarray statistical analysis was performed using Flexarray software version 1.1 (Blazejczyk, 2007). To perform the complete pipeline with this software, the CEL files instead of the CHIP files previously generated with GCOS, were employed for the analysis. The CEL files were normalized with the three available algorithms: MAS 5.0, GC-RMA and Probe Logarithmic Intensity ERor (PLIER) followed by an ANOVA test. By comparing the output gene-lists obtained, and based on published records of the most robust algorithms used for microarray expression analysis (Allison, 2006; Grant, 2007; Cordero, 2008), I selected the GC-RMA algorithm for the rest of the analysis.

After GC-RMA normalization, a Cyber-T statistical test (Cordero, 2008) was applied to pair-group comparisons. These consisted in comparing the same genotype under both treatments and between the genotypes under the same experimental condition, generating 4 different data sets (see figure II.1B). In all cases, a False Discovery Rate (FDR) filter with p-value equal or below 0.05, which statistically reduces the false negative calls (Grant, 2007), and a filter based on log2 fold change were applied. Therefore a gene was called as differentially expressed when it met the requirements of having a p-value equal or below 0.05 and a fold change above or equal 2 or below or equal 0.5. A second set of gene-lists were generated by applying a less stringent filter which consisted in a fold change of above or equal 1.5 or below or equal 0.66, while still enforcing a FDR p-value of 0.05.

The gene-lists were analysed for overrepresented Gene Ontology (GO) terms using the FatiGO tool from Babelomics (Al-Shahrour, 2006). This tool allowed the comparison of the gene-lists to the genome for functional enrichment of particular GO terms by performing a Fisher test and a multiple test correction. Other GO analyses were done with GOTerm Finder and Genecodis (Nogales-Cadenas, 2009). Also the lists were analysed for pathways or reactions overrepresented in them using the Skypainter tool from Reactome

(Tsesmetzis, 2008) and MAPMAN (Thimm, 2004). The 4 gene-lists generated with a threshold of a p-value equal or below 0.05 and a fold change above or equal 2 or below or equal 0.5 after FDR correction, were analysed with Babelomics, Skypainter and MAPMAN. The lists from the *tic-2 vs.* wt comparisons and its derived *tic-2* specific gene-list with the less stringent threshold (mentioned above) were evaluated with all the mentioned programs.

Rhizosphere acidification test

Seedlings grown on half strength MS1 solidified with gelrite (see methods MS1 for iron test) for 5 to 6 days were transferred to the same base media, but supplemented with 200 μM $FeSO_4$, 200 μM Fe_3EDTA or 300 μM ferrozine, and grown for two more weeks. After this time lapse, the plants were carefully transferred to G-B5 media with bromocresol purple as pH indicator and grown for 2 or 3 days. The later is the time required to observe a change of colour in the media due to the rhizosphere acidification response toward iron availability. A decrease in pH in the media caused a colour change from red to yellow while an increase from red to purple.

Germination assays

Stratified seeds were spread over MS1 media containing increasing concentrations of methylviologen or ABA (0 to 10 μM, between 100 to 300 seeds per concentration), or H_2O_2 (0 to 1 mM) and placed under 12:12 LD.

Germination was scored after 7 days considering as a germinated seed those that had opened and green cotyledons.

Drought tolerance assay

Pots containing equal amounts of soil were weighed before seedling transfer. To obtain the total amount of grams of dried soil, pots were placed in an oven at 60-70 ^{o}C for one week. Similarly, pots that were watered until the soil was saturated, were weighed to define the total amount of water that the soil could hold. The difference in weight between both was considered as the grams of water required to have a soil at 100% water capacity.

Plants that were between 3 to 4 week old and grown under 12:12 LD were shifted to new watering regimes. The plants were watered by weighing the pots individually and adding the amount of water in grams required for reaching the desired soil water capacity (65%, 30%, or 15% soil water capacity). The plants were kept under this regimen for 20 to

35 days by monitoring weight and adding water at least each two days. In parallel, the amount of water added was recorded as gram weight.

Starch qualitative measurement

Plants grown under short day conditions (8:16) were harvested immediately after dawn, before dusk or after a 2 hour prolongation of the night period. Rosettes were immediately submerged in 80% ethanol, followed by two or three more changes of ethanol and left overnight at $4^{o}C$. The next day, if the tissues were not complete for chlorophyll extraction, another wash with ethanol was performed. Otherwise the samples were shortly washed in water and then stained with lugol solution. The samples were briefly washed in water before images were acquired.

Infection with *Pseudomonas syringae*

Plants were grown on soil between 4 and 5 weeks on short days (8:16) before infecting them with the bacteria. The infection was performed at dawn and at dusk, respectively, by spraying the bacterial suspension over the leaf area (Tornero, 2001; Zipfel, 2004). Before infection, the plants were covered with a lid previously sprayed with water to obtain high humidity at least 3 hours before the performing the infection.

Psedomonas syringae (*P. syringae*) strain DC300 (virulent strain, compatible interaction) and AvrRps4 (avirulent strain, incompatible interaction) were grown overnight one day before the infection (Hinsch, 1996). Bacterial cultures were harvested with $MgCl_2$ and set to an optical density of 0.2 at 600 nm in this solution with 0.04% silwet. The bacteria were sprayed throughout the leaves surface, kept covered under the humidified lids without any perturbation for 3 or 4 hours to let dry the leaves surface. This protocol is a slight modification from Tornero *et al.* (2001) and Zipfel *et al.* (2004).

Leaf discs of 0.6mm from three biological replicates each one from 3 leaves were washed in 70% ethanol, rinsed twice with water and finally collected in a tube with 1.5 mL 10 mM $MgCl_2$ /0.01% silwet. They were incubated at 650 rpm for 1 hour at $28^{o}C$. An aliquot of 20 μL was taken from each tube and was spotted on to NYGA media. Bacterial Colony Forming Units (CFU) for day 0 were counted after incubation for one day at $28^{o}C$ followed by an incubation for another day at room temperature.

For the CFU count at 3 days after infection, the same protocol as above was followed with the exception that a dilution series after the incubation of the bacteria took

place. The dilution was a 1:10 series from 10^{-1} to 10^{-5} in 10 mM $MgCl_2$. All dilutions were plated on NYGA media with its respective antibiotic.

Luciferase imaging

Transgenic plants harbouring a clock promoter gene fused to the luciferase gene construct were used for monitoring clock periodicity by measuring bioluminescence with a TOPCOUNT scintillation counter from Perkin Elmer. The promoter:luciferase constructs used are listed in table I in this section. This protocol, briefly described below, is as Hanano *et al.* (2006).

The experiments consisted in transferring 7 day old seedlings entrained to 12:12 LD cycles to previously ethanol sterilized and dried 96 well black microtiter plates (Perkin-Elmer), containing MS1 or MS3 media with or without a particular concentration of a chemical or hormone. For statistical analysis, between 24 to 48 seedlings per genotype for each concentration were transferred by distributing them in rows. 15 μL of filter sterilized luciferin 5 mM were added to each well and the plate was sealed with transparent film which was perforated for allowing gas exchange.

Once the plates were set up, they were placed in a TOPCOUNT with trichromatic LED panels having red and blue light at a fluence of 1-1.5 μE each as a light source. For this, the plates were stacked by alternating the experimental set up with reflector plates consisting of a mirror that reflects the light source in an equal distribution. The equipment was set up to measure each plate after 1 minute of delay for avoiding chlorophyll autofluorescence and by reading each well for 5 seconds. The plates were entrained for 1 o 2 days in the topcount under red and blue light for 12 hours and 12 hours of darkness before setting the experiment to constant light (LL).

Analysis of clock rhythms

For visualization of the luminescence patterns, the data from the scintillation counter were processed with the EXCEL macro TOPTEMP II (available under the website http://millar.bio.ed.ac.uk/Downloads.html). The estimation of period values was performed using the Biological Analysis Software System (BRASS) macro in Excel (Southern and Millar, 2005). This application includes the Fast Fourier Transformation Non Linear Least Square (FFT-NLLS) analysis tool (Plautz, 1997). The analysis for period estimates was performed by selecting a time window of at least a minimum of 60 hours, but ideally equal or larger than 72 hours. Standard analysis parameters included period limits between 15-35

hours with a confidence probability of 95%. Rhythms were assessed by comparison of Relative Amplitude of Error (RAE) weighted means of the period lengths (calculated by BRASS) in addition to comparisons of individual period and of RAE values. The RAE is a ratio of the amplitude's error in relation to an estimate of the most probable amplitude that describes the fit of the actual data to a theoretical cosine curve. Therefore, the RAE is a measure to evaluate rhythmicity, where a RAE equal to 0 is a perfect cosine curve and RAE equal to 1 is arrhythmic.

Yeast two hybrid (Y2H) screen

Amplified cDNA corresponding to the *TIC* amino terminal fragments and full-length *AKIN10*, both with flanking *att*B sites, were cloned to the pDONR201 vector through the gateway BP reaction and later mobilized to pDEST32 and pDEST22 destinations vectors through the gateway LR reaction according to the manufacturer (Invitrogen). In both steps, recombinant colonies were selected on media with the appropriate antibiotic.

Competent yeast cells were obtained by inoculating a YPDA media with either PJ69-a or PJ69-α and incubating at 30°C at 2000 rpm overnight. The next day, fresh media was inoculated with the yeast cultures and incubated 30°C at until an OD between 0.4 and 0.6 was reached. Cultured yeast cells were centrifuged at 1000 rpm for 5 min at room temperature. Then the pellet was resuspended and washed with 50 mL of distilled H2O. After centrifugation at 1000 rpm for 5 min at room temperature, 1X TE/LiAc was added to the cell pellet, and this was resuspended by pipetting. The freshly prepared yeast competent cells were used for the transformation within 1 hour.

For yeast transformation, 100 ng of each destination vector were mixed with previously denatured salmon sperm carrier DNA. Yeast competent cells PJ69-4a and PJ69-4α were mixed with pDEST32-N-TIC, pDEST22-AKIN10, respectively, and mixed by vortexing for 10 s. Then, 600 μL of freshly PEG/LiAc was added to DNA-yeast mixture, and subsequently it was mixed with vigorous vortexing for 30 s. The cells were incubated at 30°C for 30 min with shaking at 200 rpm. After incubation, 70 μL of DMSO was added and the tube containing the cells was placed at 42°C in a water bath for 15 min and followed by ice for 1 minute. The cells were centrifuged at maximum speed for 30 s and, the pellet was resuspended with 500 μL 1X TE. 100 μL of resuspended cells were spread on the selective media. For pDEST32-N TIC transformants, cells were spread on the SD-

Leu media, and for pDEST22-AKIN10 transformants, cells were plated on the SD-Trp media. In both cases, transformants were grown at $30\,^{\circ}$C for 2 to 3 days.

The yeast transformants were mated by inoculating fresh YPDA media with both strains and incubated overnight at $30\,^{\circ}$C. The following morning, the culture was plated on SD-LW, SD-LWHA and SD-LWH with a range of concentrations of the histidine biosynthetic inhibitor according to the manufacturer (Clontech).

GST pull-down

Recombinant histidine tagged AKIN10 (His-AKIN10) protein was obtained as described by Berendzen (2005). The vector that produces GST tagged TIC amino fragment (GST-TIC) recombinant protein was obtained by amplifying a TIC amino fragment and introduced it to a pGEX-2T vector (GE Healthcare). GST-TIC was isolated according to the manufacturer guidelines. Purified recombinant proteins of GST-TIC and His-AKIN10 were mixed with gluthathione sepharose beads and incubated at room temperature for 30 minutes. After incubation, the mixture was centrifuged and the supernatant was recovered. The gluthathione sepharose beads were washed with buffer and centrifuged. This washing step was repeated three times. After this, 2 X SDS loading buffer was added to the column to elute the protein samples. Finally the proteins were separated by SDS-PAGE electrophoresis after being denatured by boiling and the gel was stained with Commassie blue following standard procedures (Sambrook, 2001).

in vitro **protein kinase assay**

Equal amounts of His-AKIN10 and GST-TIC described above were mixed and labelled with 5μCi γ-^{32}ATP in 1X kinase buffer using as a control a separate sample of His-AKIN10 without substrate. The kinase reaction was performed at room temperature and stopped by addition of 4X SDS loading buffer added with 100 mM EDTA (Berendzen, 2005). The samples were resolved by SDS-PAGE electrophoresis. The gel was dried between sheets of Whatman paper under vacuum and finally exposed to a film for autoradiography (Sambrook, 2001).

Internet resources

The following websites were used for retrieving sequences and generating the alignment. All parameters were set as default.

http://blast.ncbi.nlm.nih.gov/

http://align.genome.jp/

http://www.ebi.ac.uk/Tools/clustalw2/index.html

http://www.cbs.dtu.dk/services/MaxAlign/

The following web-pages were used to download free software or make online analyses. When online analyses were performed, parameters were set as default.

http://genomequebec.mcgill.ca/FlexArray/

http://www.babelomics.org/

http://arabidopsisreactome.org/

http://bar.utoronto.ca/

http://mapman.gabipd.org/web/guest/home

http://genecodis.dacya.ucm.es/analysis/

http://go.princeton.edu/cgi-bin/GOTermFinder

Contributions

Dr. Zhaojun Ding and Dr. Jieun Shin performed independent yeast two hybrid screens, Zhaojun Ding also performed *in vitro* experiments with recombinant TIC protein.

Dr. Csaba Koncz kindly provided the estradiol inducible *AKIN10* and *AKIN11* lines. The cDNA library for the yeast two hybrid screen was a gift from Dr. Hans Sommer.

I worked together with Katharina Heidrich in the infection assay with *Pseudomas syringae*.

III. RESULTS

General overview and restatement of the biological phenomena under study

time for coffee (*tic*) was described as a short period mutant with a low amplitude of *CAB:LUC* expression (Hall, 2003). The phenotype of *tic* resembled that of the double mutant *cca1/lhy*, as the mutant was found to have a short hypocotyl and chlorotic leaves. It was concluded that TIC was required during the late night as by release assays, *tic* clock was found to be reset between late night and early morning (Hall, 2003). Further characterization of *tic* showed that the expression of evening and morning clock genes, such as *GI*, *TOC1*, *ELF3* and *LHY*, *CCA1*, was altered, as all displayed and advanced phase of expression relative to the wild type (Ding, 2007). Additional genetic analyses of *tic* demonstrated that it was required for clock progression through pre-dawn events and to maintain clock rhythms (Ding 2007).

Even though it was shown that *TIC* had a time-specific participation in the clock, *TIC* transcript and protein levels were not found to oscillate through the day. Additionally TIC protein was found to be constitutively nuclear localised (Ding, 2007). Therefore TIC time-specific action in the oscillator must be triggered by an as of yet unknown mechanism. As the transition from dark to light is the main environmental cue that entrains the circadian clock on a daily basis (Salomé, 2005), and the clock in *tic* stops just before this transition takes place, *TIC* time-specific activity may be a key player in clock entrainment.

To understand the role of *TIC* in clock entrainment, I envisioned that a microarray gene-expression profile toward the anticipation of dawn, as well as triggering the resetting of the clock prior to the expected sunrise, could help elucidate the transcriptional changes that take place and are dependent of *TIC*. Thus from the analysis of *tic* transcriptome under these conditions, it would be possible to infer the role of *TIC* in response to clock resetting under ever changing photoperiods.

III.A. *time for coffee* **gene expression analysis unraveled a mutant with a pleiotropic phenotype.**

1) Microarray data analysis

To gain insight into *TIC* function in clock entrainment, a transcript profiling analysis was performed using the *A. thaliana* Affymetrix ATH1 GeneChip (ATH1). Taking into account that the clock in *tic* had been shown to stop around late night, two different time-points were selected (see figure II.1-I). The dawn-anticipation assay, in which samples were collected before the dark period ended, was designed with the purpose to detect the transcriptomic alterations in *tic* due to clock arrest. The clock-resetting assay that consisted in giving a 2 hr light pulse out of a normal diurnal cycle (2 hr before the expected time), had the aim of revealing the transcriptomic changes consequent of clock resetting, as well as defining *TIC* involvement in this re-entrainment. Additionally the gene expression changes that were dependent on *TIC* regardless of the experimental conditions, served to genetically characterize the mutant. I found that *tic* gene expression was not only altered within the circadian clock, but that it resulted in disrupted gene expression of several metabolic pathways and stress responses. Thus *tic* transcriptomic profile unraveled a mutant with a complex phenotype and provided a striking example of the pervasiveness of the circadian clock in modulating plant development.

The gene-expression analyses consisted of pair-wise comparisons between *tic-2* and wild type: i) before the break of dawn and ii) as a response to the resetting of the clock; iii) as well as between the conditions (clock resetting *versus* dawn anticipation) in each genotype (figure II.1-I). For this, RNA was extracted from duplicate biological samples for each physiological condition. Amplified cDNA from each RNA sample was hybridized to an *A. thaliana* Affymetrix ATH1. This generated a total of 8 microarray hybridizations. After hybridization, the quality of the arrays was evaluated. This consisted in a visual examination of the hybridized ATH1 chips with the Affymetrix GeneChip scanner (Affymetrix manual 2006; Allison, 2006). The 8 ATH1 chips fulfilled the quality standards and consequently the derived CEL files from the scanned images were used for gene-expression analysis.

To assess the quality of microarray hybridizations, of the biological material as well of the reproducibility and reliability of the samples, further quality tests were performed. These included the evaluation of the scanned image derived from the ATH1

chip hybridizations, signal intensity box plots, MvA expression plots and mRNA spike controls (see methods). Spearman's correlation and Principal Component Analysis (PCA) were used to visualize the similarity of the expression profiles within the samples (Allison, 2006; Cordero, 2008).

The PCA plot simplifies the input data and clusters it based on the extent to which the samples relate to each other. The PCA showed that the experimental conditions had a larger effect on the transcript profiles than the genotypes (see figure III.1A). The experimental conditions explained ~60% of the variability of the transcriptional changes observed, while the genotype background explained only ~25% (figure III.1A). The samples from the dawn-anticipation assay (black symbols) were separated by a larger distance (in the X axis) from those of the clock-resetting assay (white symbols) than between themselves (Y axis) (figure III.1A). Furthermore within each genotype, *tic-2* showed a larger difference between its transcript profiles than the wild type (the white and black circles are farther away from each other in the X axis than the white and black diamonds). In conclusion, the PCA analysis showed that the expression profiles of the biological duplicate samples were similar, indicating biological reproducibility in the experiments. Though the treatments had a larger effect on gene expression, the genotypes also showed specific effects in patterns of transcript accumulation.

Statistical analyses were performed on the microarray data files. For this, I generated 4 lists of genes differentially expressed from all the possible pair comparisons (figure II.1-II). The number of differentially expressed genes reflected the earlier finding with the PCA plot, as the experimental conditions had a larger effect on global gene expression (figure III.B). The pair-wise comparisons showed a larger number of misexpressed genes due to the conditions than to the genotypes (compare the total number of differentially expressed genes between left and right Venn diagrams in figure III.1B). When the clock-resetting assay was compared to the dawn-anticipation assay, the number of transcripts found as differentially expressed between these conditions was around 3,000 and 2,000 genes in *tic-2* and wild type, respectively (figure III.1B, left panel). Therefore the mutant exhibited an exacerbated response to the environmental shift relative to the wild type. When the genotypes were compared under the same experimental conditions, the number of genes differentially expressed was around 1100 and 1400 in the resetting and anticipation assay, respectively (figure III.1B right panel). The overlapping area of this Venn diagram became of interest as it reflects those genes that are misexpressed in *tic-2* regardless of the experimental setup. This set of genes, that herein I called as "*tic-2*

A **Two dimensional Principal Component Analysis Plot**

B

Venn diagrams of differentially expressed genes
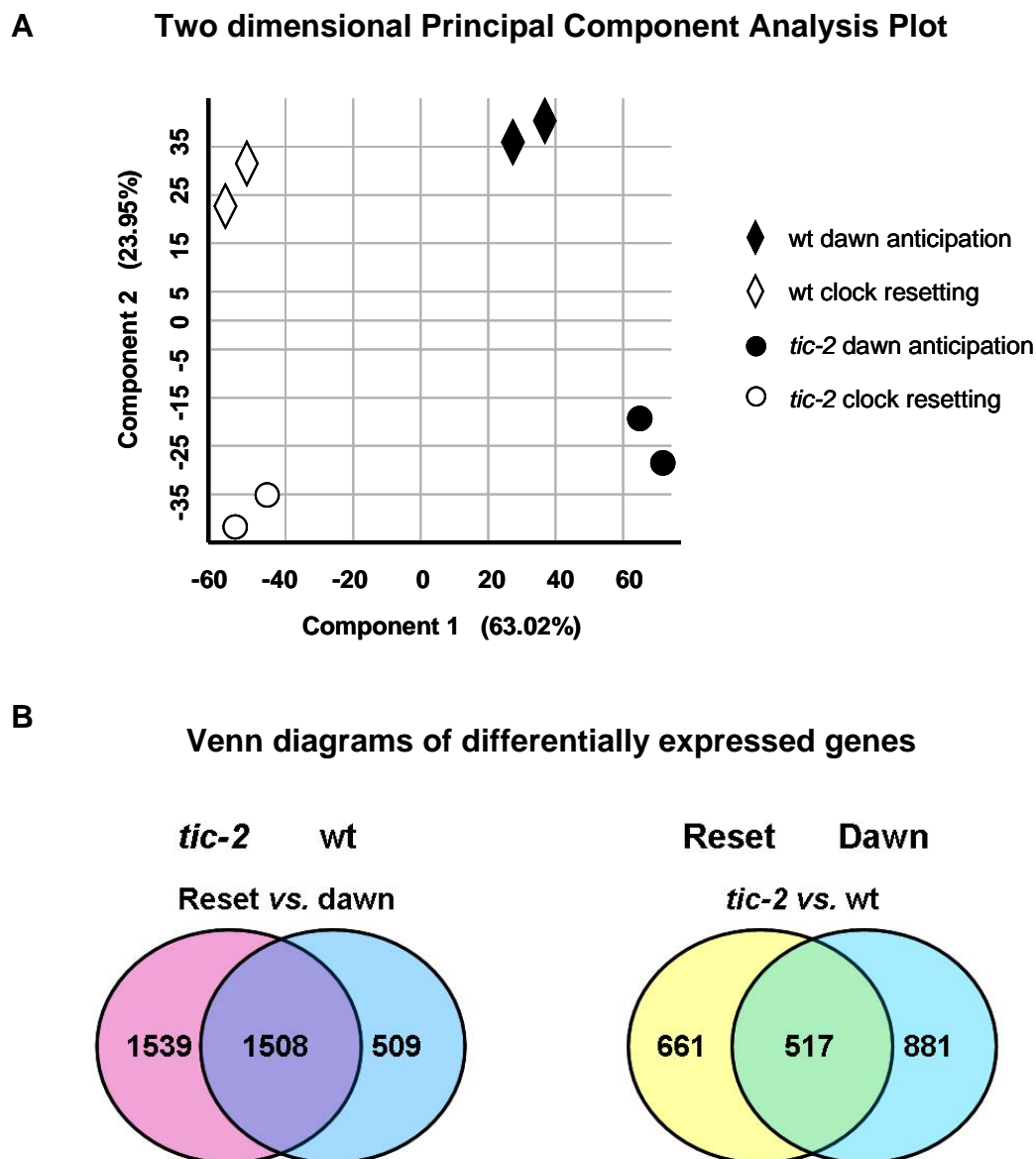
Figure III.1. Overview and analysis of the microarray data.
A) The principal-component analysis (PCA) plot simplifies and describes the microarray datasets in a two-dimensional view by separating the data based on their similarity. The plot showed that replicate samples cluster together, confirming previous analysis of the quality of the hybridization. The PCA also demonstrated that the experimental conditions (clock-resetting *vs.* dawn-anticipation) had a major effect on transcript expression patterns relative to the comparison between genotypes. The environmental conditions roughly explained 60% of the variability (component 1, X axis), while the variability due to the genotype was around 25% (component 2, Y axis). Note that the distance between *tic-2* expression profiles was larger than in the wild type (wt).
B) Venn diagrams showing the overlap of genes differentially expressed in comparisons between both experimental conditions in each genotype (left), or when the genotypes were compared to each other in a single condition (right). The first comparison (left) shows that *tic-2* had a higher number of genes differentially expressed than wt (3,000 and 2,000, respectively). The right panel illustrates that the number of genes differentially expressed between *tic-2* and wt was around 1,000 and that less than half of them were constitutively modified in *tic-2* regardless of the physiological conditions.

46

specific," could explain the genetic difference between *tic-2* and wild type that by PCA analysis was found to be responsible of ~25% of all transcriptome changes (figure III.1A). From the four generated gene-lists, the *tic-2 versus* wild-type comparisons and their overlapping area (*tic-2* specific) were the main focus of this thesis.

Considering that *tic-2* was isolated in a screen for clock mutants, I first examined the expression of clock genes and clock-related genes in the 4 lists of differentially expressed genes. Table III summarizes the fold-change expression values found between the four comparisons (figure II.1-II). In the genotype comparisons (first two columns of table III), I found that *tic-2* resulted in increased expression of almost all circadian clock and clock-related genes with a 2 to 8 fold increase relative to wild type. The overexpressed genes included the evening genes *GI*, *ELF3*, *TOC1*, *LUX*, *CCR2* and the pseudo response regulator (*PRR)* family. Interestingly, *LUX*, a myb like transcription factor (Hazen, 2005), was within the 10 genes that displayed the highest overexpresion in *tic-2*. In contrast, the morning gene *LHY* was found to be repressed, whereas *CCA1* mRNA abundance resembled that of wild type. Two further genes that exhibited reduced expression in *tic-2* were *FLOWERING LOCUS C* (*FLC*) and *TIC* gene itself. The observed *TIC* transcriptional repression in *tic-2* could be an artefact of the 25 length oligonucleotide design of the ATH1 and the T-DNA insertion, though the gene repression was only observed in 2 of the 4 comparisons (table III). Analysis of the clock-resetting *versus* dawn-anticipation comparisons showed that the behaviour of both genotypes toward light was similar. Induction of light-responsive genes, such as *GI* and *PRR9* was detected in both genotypes (table III). These expression profiles corroborated earlier findings that *tic* results in abnormal clock-gene expression (Ding, 2007) and the microarray analysis here presented expanded the list of clock genes affected in the *tic-2* background.

To obtain a global view of the transcriptional changes that occurred in *tic-2*, the gene-lists were analysed for enrichment of Gene Ontology (GO) terms. GO is a structure vocabulary that describes genes products based on their association with cellular component or localisation, molecular process involved and biological function across databases in a species independent manner (Ashburner, 2000). The GO analysis was performed with gene-lists derived from two different fold-change thresholds (see methods), as a limited number of genes taken into account diminish the probability of finding overrepresentation of GO terms or pathways. Nevertheless, both thresholds were reliable in avoiding false positives and the gene-lists were analyzed with several programs. For the GO enrichment analysis, I focused on the lists of differentially expressed genes obtained

Table III. Clock genes fold change (log2) values

Table III. Fold change values of core clock genes and clock associated genes.
Fold changes were calculated from the expression values of each pair comparison. The values represent induction or repression respective to the first element in each comparison. Gene expression values (log2) are shown in a color intensity code (red induced, pale red <2.0, dark red >2.0; green repressed, light green <2.0, dark green >2.0) for each of the 4 comparisons. Note that most of the genes were induced in *tic-2*.

nd stands for not detected as a differentially expressed gene after statistical analysis. The analysis had as a threshold a two fold change with a p-value below or equal to 0.5 and a False Discovery Rate (FDR) below or equal to 0.5.

Gene name	Atg code	Dawn tic-2 vs. wt	Resetting tic-2 vs. wt	tic-2 Reset vs. Dawn	wt Reset vs. Dawn
LHY	At1g01060	-1.406535	nd	nd	nd
CCA1	At2g46830	nd	nd	nd	nd
TOC1	At5g61380	2.929029	2.906518	nd	nd
GI	At1g22770	1.932598	3.284617	4.113093	2.761074
ELF3	At2g25930	1.699737	1.526682	nd	nd
LUX	At3g46640	4.604814	4.365481	-1.15689	nd
PRR9	At2g46790	2.281379	1.299152	3.534076	4.516303
PRR7	At5g02810	4.016162	3.468417	1.274093	1.821838
PRR5	At5g24770	1.288404	nd	nd	nd
PRR3	At5g60100	2.806262	3.086767	nd	nd
TIC	At3g22380	nd	-1.57826	-2.13448	nd
FLC	At5g10140	-1.534988	-1.48306	nd	nd
CCR2	At2g21660	1.191844	nd	nd	nd
CHE	At5g08330	1.293302	1.656979	-2.06761	-2.431283
REV2	At5g37260	nd	nd	-2.69796	-4.11639
ZIK4	At3g04910	nd	nd	nd	-1.06022
CK2 β	At3g60250	nd	nd	-1.70903	nd
MAPK7	At2g18170	1.289645	1.127339	nd	nd
LIP1	At5g64813	nd	nd	-1.0147	nd

from the comparison between genotypes. Particular attention was placed to the GO categories from and the list of genes specific to *tic-2*. Table IV displays a summary of the GO terms and pathways that appeared with a biological significance as scored with a low p-value in the lists of differentially expressed genes. The GO analysis allowed the of study *tic-2* global gene expression in an unbiased manner.

From the GO analysis, I observed that *tic-2* exhibited different responses to environmental and cellular stimulus than the wild type (table IV). Concerning the environmental stimuli, stress responses toward diverse environmental cues, such as light, water and oxidative stress were highlighted categories. Involving light stimulus and signalling, the photoreceptors *PHYTOCHROME A* (*phyA*) and *PHOTOTROPIN 1* (*PHOT1*), as well as signalling molecules such as *PHYTOCHROME INTERACTING FACTOR 4* (*PIF4*) and *NON PHOTOTROPIC HYPOCOTYL 3* (*NPH3*) were induced in *tic-2*. GO terms associated to responses to salt stress and water deprivation were present in the 4 gene-lists, but to a higher extent in the genotype comparison analyses. Therefore responsive genes to these stimuli such as *DEHYDRATATION RESPONSIVE ELEMENT BINDING PROTEIN 2A* (*DREB2A*), *COLD REGULATED 15A and B* (*COR15A* and *COR15B*) and a group of *EARLY RESPONSE TO DEHYDRATATION* genes (*ERD7, ERD3, ERD4, ERD10)* were upregulated in *tic-2* (table V). Genes defined as involved in responses to oxidative stress displayed a complex pattern of expression. Some genes, such as *CATALASE 1* and *CATALASE 3* (*CAT1*, *CAT3*), *SENESCENCE RELATED 1* (*SEN1*) were upregulated. However the vast majority of genes in the oxidative stress category were downregulated, including peroxidases (*L-ASCORBATE PEROXIDASE*, *PER20*, *PER73*) NADPH oxidases as *RESPIRATORY BURST OXIDASE HOMOLGUE* (*RBOHD* and *RBOHC*), gluthathione-S-transferases and *CUPPER-ZINC SUPEROXIDE DISMUTASE* (*CSD2*) (table V). Therefore *tic-2* transcriptional profile exhibited a marked difference toward environmental signals relative to the wild type.

With regard to GO terms involved in responses to endogenous cellular stimulus, some categories of hormones were highlighted. An example was ABA, whose GO term enrichment showed genes that were both up and down-regulated. Besides the ABA related responses to environment mentioned above, ABA metabolic genes as *ABA DEFICIENT 2* (*ABA2*), phosphatases such as the *SNF1-RELATED PROTEIN KINASES* (*SNRK2.2,* and *SNRK 2.3*), as well as ABA responsive genes as *ABA INSENSITIVE 1* (*ABI1*) and *RESPONSE TO DESICCATION* (*RD22*) were misregulated (table V). Another major GO term in the data set, mostly with induced genes, was iron homeostasis (table IV). The

Table IV. Summary of the Gene Ontology terms with a significant p-value present in the differentially expressed gene lists.

The 4 lists of differentially expressed genes were loaded to online tools that indentify overrepresentation of GO terms within the input data by applying algorithms and statistical tests. The table presents a summary of the main terms or pathways that were significant as they presented a low p-value through one or more of the independent analysis (see methods).

The column at the right indicates if the overrepresented terms were identified in set of genes derived from: the experimental conditions (dawn anticipation/clock resetting), genes that were exclusively induced (Up) or repressed (Down), that had induced and repressed genes within the GO category (full gene-list) or only present in the mutant (*tic-2* specific).

Gene Ontology Annotation	Observations
Biological process	
circadian rhythm (GO:0007623)	Up / *tic-2* specific
regulation of circadian rhythm (GO:0042752)	Up / *tic-2* specific
response to stress (GO:0006950)	Full gene-list
response to endogenous stimulus (GO:0009719	Full gene-list
response to abiotic stimulus (GO:0009628)	Full gene-list
response to temperature stimulus (GO:0009266)	Full gene-list
response to light stimulus (GO:0009416)	Up
response to water deprivation (GO:0009414)	Full gene-list
response to hormone stimulus (GO:0009725)	Full gene-list
response to jasmonic acid stimulus (GO:0009725)	Down
response to abscisic acid stimulus (GO:0009737)	Full gene-list
response to salt stress (GO:0009651)	Full gene-list
response to wounding (GO:0009611)	Down
response to oxidative stress (GO:0006979)	Down
response to reactive oxygen species (GO:0000302)	Down
cellular iron ion homeostasis (GO:0006879)	Up / *tic-2* specific
iron ion transport (GO:0006826)	Up / *tic-2* specific
iron ion homeostasis (GO:0055072)	Up
di-, tri-valent inorganic cation transport (GO:0015674)	*tic-2* specific
transition metal ion transport (GO:0000041)	*tic-2* specific
biological regulation (GO:0065007)	Up
regulation of cellular process (GO:0050794)	Up

regulation of nucleobase, nucleoside, nucleotide and nucleic acid metabolic process (GO:00192190)	Up
regulation of primary metabolic process (GO:0080090)	Up
carbohydrate metabolic process (GO:0005975)	Full gene-list
starch metabolic process (GO:0005982)	*tic-2* specific
cellulose and pectin-containing cell wall loosening (GO:0009828)	Full gene-list
secondary metabolic process (GO:0019748)	Down
terpenoid metabolic process (GO:0006721)	Down
isoprenoid metabolic process (GO:0006720)	Down
flavonoid biosynthetic process (GO:0009813)	Down
Molecular Function	
transcription factor activity (GO:0003700)	Up
DNA binding (GO:0003677)	Up
structural constituent of cytoskeleton (GO:0005200)	Up
transcription regulator activity (GO:0030528)	Full gene-list
oxidoreductase activity, acting on peroxide as acceptor (GO:0016684)	Down
peroxidase activity (GO:0004601)	Down
Pathways and Reactions (KEGG or AraCyc)	
sterol biosynthesis	Down / *tic-2* specific
plastoquinone biosynthesis	Dawn anticipation
ascorbate biosynthesis	Dawn anticipation
vitamin E biosynthesis	Dawn anticipation
flavonoid biosynthesis	*tic-2* specific
S-adenosylmethionine (SAM) cycle	Dawn anticipation
starch degradation in leaves	*tic-2* specific
spermine biosynthesis	Down / *tic-2* specific
glucosinolate biosynthesis from phenylalanine, tryptophan and homomethionine	Clock resetting
leucine degradation	*tic-2* specific
polyamine biosynthesis	Down / *tic-2* specific
chlorophyllide a biosynthesis	Up/ *tic-2* specific
fatty acid metabolism	*tic-2* specific
phenylpropanoid biosynthesis	Down / *tic-2* specific
metabolism of xenobiotics and drugs cytochrome P450	*tic-2* specific

overexpression of ferritins (*FER1, FER3, FER4*), *NICOTIANAMINE SYNTHASE 2* (*NAS2*), as well as the *IRON RESPONSIVE TRANSPORTER 1* (*IRT1*) and *METAL TRANSPORTER NATURAL RESISTANCE ASSOCIATED MACROPHAGE PROTEIN 1* (*NRAMP1*) were specific to *tic-2* as they were induced in both experimental conditions (table V). Taken together, the GO enrichment analysis suggested that *tic-2* had altered responses to environmental stress conditions.

Along with the stress responses, the gene expression profiles suggested an energy imbalance in *tic-2*. This was noted by the misregulation of transcripts that encode structural or catalytic proteins of mitochondria such as *ALTERNATIVE OXIDASE 1A* (*AOX1A*), ATP/AMP transporters, cytochrome c biogenesis proteins and some enzymes of the citric acid cycle, also known as tricarboxilic acid cycle (TCA). Similarly genes involved in the biosynthesis of plastoquinone and antioxidants, such as ascorbate and tocopherols were missexpressed, while genes that participate in the synthesis and salvage of nicotinadenin-dinucleotide (NAD) such as *L-ASPARTATE OXIDASE* (*AO*) and *NICOTINATE PHOSPHORIBOSYL TRANSFERASE* (*NAPRT*), respectively, were repressed only in the dawn-anticipation assay (table V).

Primary and secondary metabolic processes were affected in *tic-2*, as seen by GO terms derived from the mutant comparison to wild type. Genes required for chlorophyll synthesis, such as *PROTOCHLOROPHYLLIDE OXIDOREDUCTASE A* and *B* (*PORA, PORB*) and *UROPORPHYRINOGEN DECARBOXYLASE* (*HEME1*) were increased in *tic-2*, whereas transcripts from photosynthetic genes such as *LIGHT HARVESTING COMPLEX/CHLOROPHYLL A/B-BINDING PROTEIN* (*CAB4, CAB3*), ferredoxin and others were increased or reduced in the genotype comparisons (table V). In the same comparison, carbohydrate metabolism, in particular starch degradation, presented several genes overexpressed and this included *STARCH EXCESS* (*SEX1, SEX4*), and amylases (*AMY3, BAM4*). Similarly some *DARK INDUCED GENES* (*DIN4, DIN10*), involved in dark to light transitions and starvation (Baena-González, 2007), were induced in *tic-2*. Interestingly genes involved in nucleic acid metabolism, including both DNA and RNA, were misexpressed in *tic-2*, as well as several genes within the cell cycle (table V). In general, *tic-2* transcriptome displayed overexpression of genes involved in the categories of DNA repair and expression of transcription factors (table IV), whereas the regulation of transcription had both induced and repressed elements. Some particular examples from these processes are listed in table V. Surprisingly, not only these basic processes were transcriptionally altered, but also constituents of the cytoskeleton, in particular tubulin

filaments. Thus these analyses suggested that *tic-2* has alterations in essential metabolic processes.

Secondary metabolism, in particular terpene, flavonoid and phenylpropanoid metabolism, was highlighted by GO enrichment, as genes in these pathways were differentially expressed between *tic-2* and wild type (table IV). These pathways appeared with a group of genes that mainly presented decreased transcript levels. Some examples include *NARANGENIN-CHALCONE SYNTHASE* (*CHS*) and *FLAVONOL SYNTHASE 1* (*FLS1*) (table V). The expression profile also suggested that polyamine biosynthesis would be restrained in *tic-2* as the expression of *ARGININE DECARBOXYLASE 1* and *2* (*ADC1*, *ADC2*) and *SPERMIDINE SYNTHASE* (*SPDS3*) was reduced (table IV and V).

All together, the microarray transcript profiles gave an insight into several and unexpected metabolic alterations that occurred in *tic-2*, either concomitant to the mutation or environmental dependent. This global gene expression analysis suggested that the alteration of the circadian rhythms have a pervasive consequence in plant development and metabolism equilibrium or that *tic-2* results in a pleiotropic disruption of gene expression due to a homeostatic function of *TIC* in *A. thaliana*.

2) General *tic-2* phenotypic and physiological characterization

The microarray transcript profile analysis suggested that *TIC* mutation caused effects in gene expression beyond the circadian clock. Prior to this work, *tic* had not been extensively characterized regarding its growth phenotype (Hall, 2003). Nonetheless *tic* displayed a dramatically different morphology (figure III.2). Therefore I decided to examine *tic-2* phenotypes under different physiological treatments. Similarly based on the gene expression data and the GO categories described above, I explored *tic* physiology and responses toward environmental and chemical perturbations.

2.1) *tic-2* phenotype under different photoperiods

To obtain an expanded phenotypic characterization of the *tic* allele in Col-0 background (*tic-2*), plants were grown under different photoperiods and their development was followed by macroscopic observations. When grown in soil, the *tic-2* mutant presented

A

Col-0   *tic-2*

B

8:16

12:12

Col-0

16:8
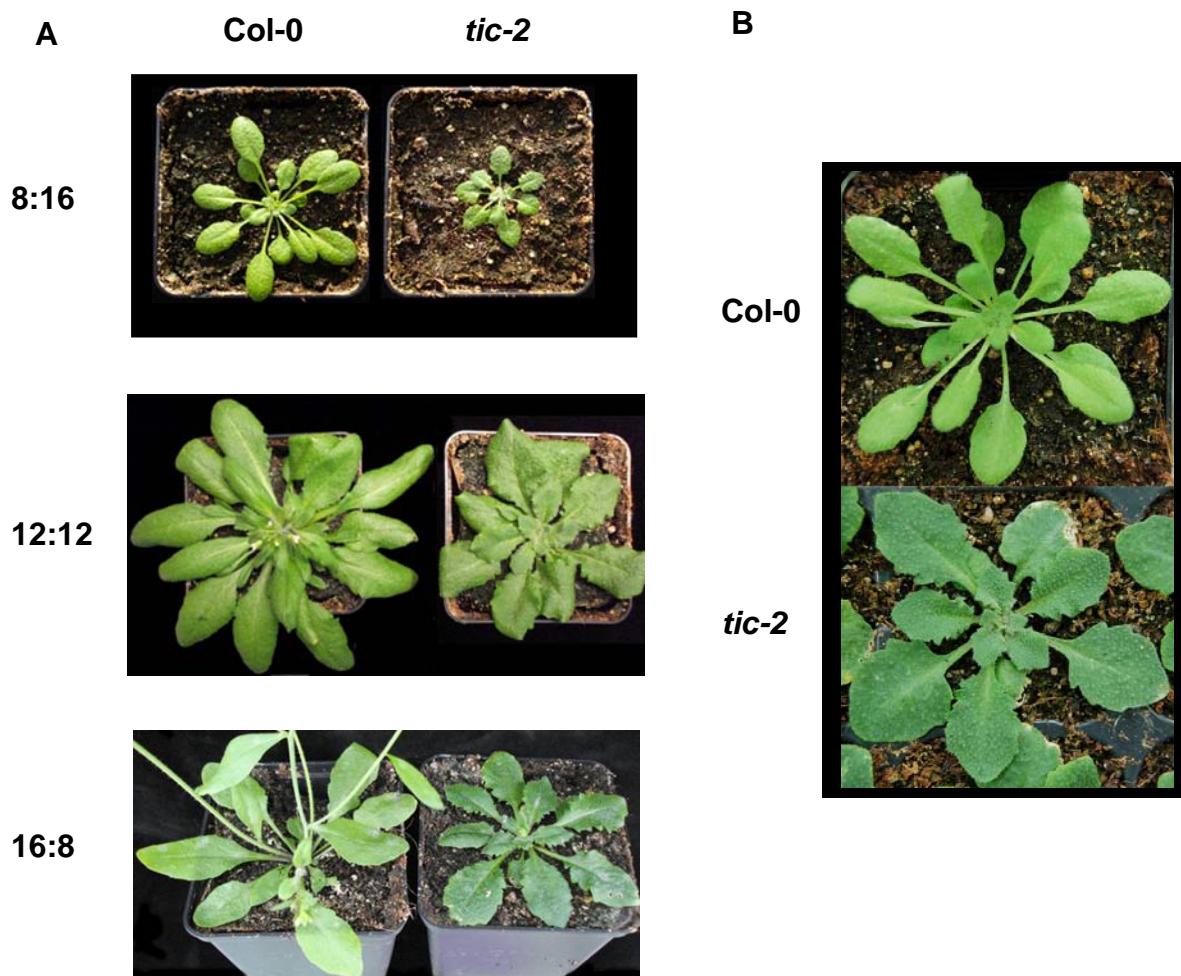
tic-2

Figure III.2. *tic-2* **rosette morphology and development.**
A) Growth development of Col-0 wild type and *tic-2* under different photoperiods. The rosette of *tic-2* presented a smaller size and a reduced number of leaves relative to wild-type rosette. *tic-2* developed darker green leaves and presented leaf serration. Both traits were enhanced as the photoperiod was lengthened. *tic-2* growth was slower than the wild type and consequently displayed a late-flowering phenotype (note the wild-type bolt had emerged under 12:12 LD and wild type had already flowered in 16:8 LD, while *tic-2* had not). All plants in panel A were sown at the same time on MS1 media and after 7 days, were transferred to the greenhouse under the depicted photoperiods.
B) Photographs of Col-0 and *tic-2*.Photographs were taken to plants at a different age of development. Note the difference in leaf structure and colour in *tic-2* compared to wild type as mentioned in A.

a dark green colour, compared to the wild type, and *tic-2* displayed serration of its the leaves (figure III.2). Furthermore the growth rate of *tic-2* was slower as the rosette size and the number of leaves were reduced in time after sowing compared to wild type. Consequently *tic-2* made its transition to flowering later than the wild type. These developmental characteristics are presented in figure III.2A, as the photographs were taken when the plants were of the same age (around 4 weeks after sowing). Note that under a 12:12 photoperiod, wild type already bolted, while *tic-2* had not yet committed to flower under a 16:8 photoperiod. *tic-2* developmental defects were observed regardless of the photoperiod length, though the longer the light period, the darker the coloration of the leaves was relative to the wild type (figure III.2). These results suggested that *tic-2* has a slower developmental programme than wild type. This and the leaf serration could be a consequence of *tic-2* defects in the circadian clock.

2.2) *tic-2* had a starch excess phenotype

The transcript profile and GO terms indicated alterations in the carbohydrate metabolism, particularly starch degradation, in *tic-2*. Genes such as *SEX1, SEX4, AMY3* and *BAM4*, all of them involved in starch catabolism (Smith, 2007), were overexpressed in *tic-2*. This led me to evaluate if starch levels were altered in *tic-2*. As starch content in *A. thaliana* leaves displays a diurnal pattern with maximum and minimum levels at dusk and dawn, respectively (Zeeman, 2007), I grew plants under short-day conditions (8:16). From these plants, whole rosettes were collected at three time-points: at dawn, before dusk and after an extension of the night by 2 hours. The later triggers a starvation response, as plants consume almost all of their starch prior to the expected dawn and consequently have exhausted their carbohydrates resources (Zeeman, 2007). These time-points were chosen to observe the maximum and minimum amount of starch throughout a day in wild type and *tic-2*. Starch content was evaluated by iodine staining after removing chlorophyll from the plants with ethanol.

Interestingly and contrary to the predictions from the gene expression pattern, *tic-2* presented a starch excess phenotype. This term was applied to mutants that were impaired in starch breakdown and consequently presented a dark brown coloration after lugol staining at the end of the night, as in the case of the mutant *sex1* (Caspar, 1991; Yu, 2001). Tissues rich in starch, composed of polysaccharides amylose and amylopectin retain iodine

within its structure acquiring a dark brown/purple colour, whereas starch free tissues remain pale (Caspar, 1991). At dawn, the time in which the starch content reaches its minimum level in the wild type, *tic-2* still showed starch accumulation in its leaves (figure III.3). Similarly two alleles of the clock mutant *gigantea* (*gi)* displayed the previously reported starch excess phenotype for this gene (Eimert, 1995). At dusk, all samples presented a dark coloration, indicating that starch synthesis occurred through the light period. Strikingly even initiating a starvation response by extending was not enough to trigger starch remobilization both in *tic-2* and *gi*, as their rosettes still appeared stained (figure III.3 bottom row). Therefore I concluded that *tic-2* was not impaired in starch biosynthesis, but manifested a defect in its catabolism. Consequently this caused starch accumulation, leading to the observed starch excess phenotype.

2.3) Iron homeostasis in *tic-2*

Iron homeostasis appeared as one of the main statistically different GO terms specific to the mutant, in addition to the circadian rhythm category (table IV). The genes involved in iron metabolism that were overexpressed included the ferritins (*FER1*, *FER3*, *FER4*) as well as the iron transporter *IRT1* and the nicotianamine synthase *NAS2* (table V). All of these genes appeared as highly induced in *tic-2* regardless of the experimental conditions. Therefore their expression defects were specific to *tic-2*. During this work, Duc *et al.* (2009) established a tight correlation between *TIC* and iron homeostasis by confirming that ferritin expression is under *TIC* control. All together, *TIC* is an essential component for iron metabolic regulation.

Ferritins are expressed under iron excess conditions or after iron resupply to iron starved plants (Kim, 2007). In order to test if the cause of high ferritin expression was a response to defective iron uptake, the later was tested through a simple pH test. Iron uptake in *A. thaliana* involves the secretion of protons to the rhizosphere, which acidify the media allowing the mobilization of insoluble iron (Yi, 1996). To test for the acidification response, *tic-2* and wild-type plants were grown on media supplemented with iron (200 μM FeSO$_4$ or 200 μM Fe$_3$EDTA) or grown under iron-deficient conditions, through the use of the iron chelator ferrozine. After growing under these conditions, the plants were transferred to a control media with a pH indicator to assess for their rhizosphere acidification response toward iron availability. The acidification response was evaluated by
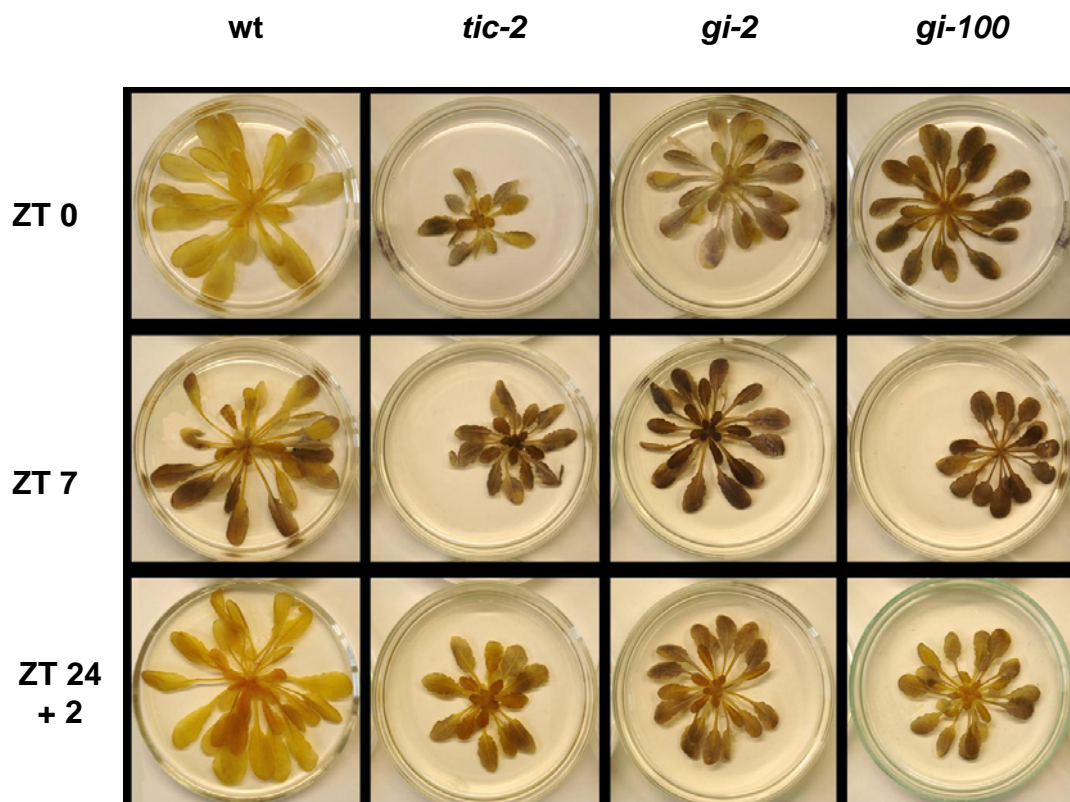
Figure III.3. *tic-2* **displayed a starch excess phenotype.**
Plants were grown in the greenhouse under short day (8:16) conditions for 45-50 days before sampling. Whole rosettes were taken as dawn broke (ZT 0), and one hour prior to dusk (ZT 7) for assessing diurnal starch accumulation. After dusk onset, another set of samples were kept in darkness until ZT 2 the next day (2 hours after subjective dawn), therefore extending the night duration (bottom row).
Whole rosettes were submerged in ethanol for removing chlorophyll prior to lugol staining. After staining, starch accumulation in the leaves was revealed as a dark brownish coloration due to iodine binding to starch molecules. The photographs demonstrated that *tic-2* displayed a starch excess phenotype as starch was observed in the leaves of *tic-2* at dawn, time of the day at which starch content reaches its minimum (compare the brown coloration of leaves in *tic-2* to the yellowish colour shown by the wild type at ZT 0). A night extension of two hours (bottom row) was not enough to observe starch remobilization in *tic-2*. As a positive control for starch accumulation, two alleles of *gigantea* (*gi*), previously shown to have a starch excess phenotype (Eimnert, 1995), are shown.

the change of colour in the media from red to yellow. This colour change is a consequence of the release of protons to the media by the roots. Wild-type plants acidified more their surrounding than *tic-2* (figure III.4). Unexpectedly, wild-type plants displayed an increased acidification response both under control conditions and with an available source of iron such as $FeSO_4$ when compared to plants previously grown on an insoluble form of iron as Fe_3EDTA or with the iron chelator (figure III.4). This behaviour was different from the one reported by Yi *et al.* (1996). Though *tic-2* had a lower acidification response compared to the wild type, a similar pattern was observed. A higher acidification response was observed in $FeSO_4$ treated or control mutant plants than with ferrozine and Fe_3EDTA treatments (figure III.4). This implied that the acidification response toward iron availability was not impaired in *tic-2*. Therefore from this, I concluded that iron uptake was not compromised in *tic-2* and was not the cause of high ferritin expression.

2.4) *tic-2* manifested hypersensitivity to oxidative stress.

The gene-expression profile led me to hypothesize that oxidoreductase metabolism and responses to oxidative stress were impaired in *tic-2*. To confirm this, seeds from *tic* mutant in Col-0 and Ws-2 backgrounds were germinated on MS1 media supplemented with methylviologen (MV). This compound, commercially known as paraquat, produces oxidative stress by capturing electrons from photosystem I, while reacting with oxygen, which in turn produces superoxide damaging the chloroplast (Nelson, 2000; Buchanan, 2000). The germination of the mutant was arrested at lower concentrations relative to the wild type. *tic-1* was twice as susceptible, as it reached its half lethal dose below 0.5 μM MV, whereas the half lethal dose in wild type was just below 1.0 μM MV (figure III.5A). As a control for resistance to oxidative stress by methylviologen, I used the *gi* mutant, which was previously shown to be resistant to this chemical (Kurepa, 1998). *gi* displayed the expected resistance to the chemical presenting a half lethal dose around 4.0 μM MV (figure III.5A). Interestingly the double mutant *tic-1/gi-11* mimicked the susceptibility of *tic-1* single mutant (figure III.5A). This result suggested that *tic-1* would act downstream of *gi-11* in regard of resistance to oxidative stress or that effect of the mutation of the former is dominant in this respect.

wt **tic-2** **Distribution in each plate**

top illuminated

bottom illuminated

A	B
C	D

A) ½ MS1 (control)
B) 200 μM FeSO$_4$
C) 300 μM Ferrozine
D) 200 μM Fe$_3$EDTA
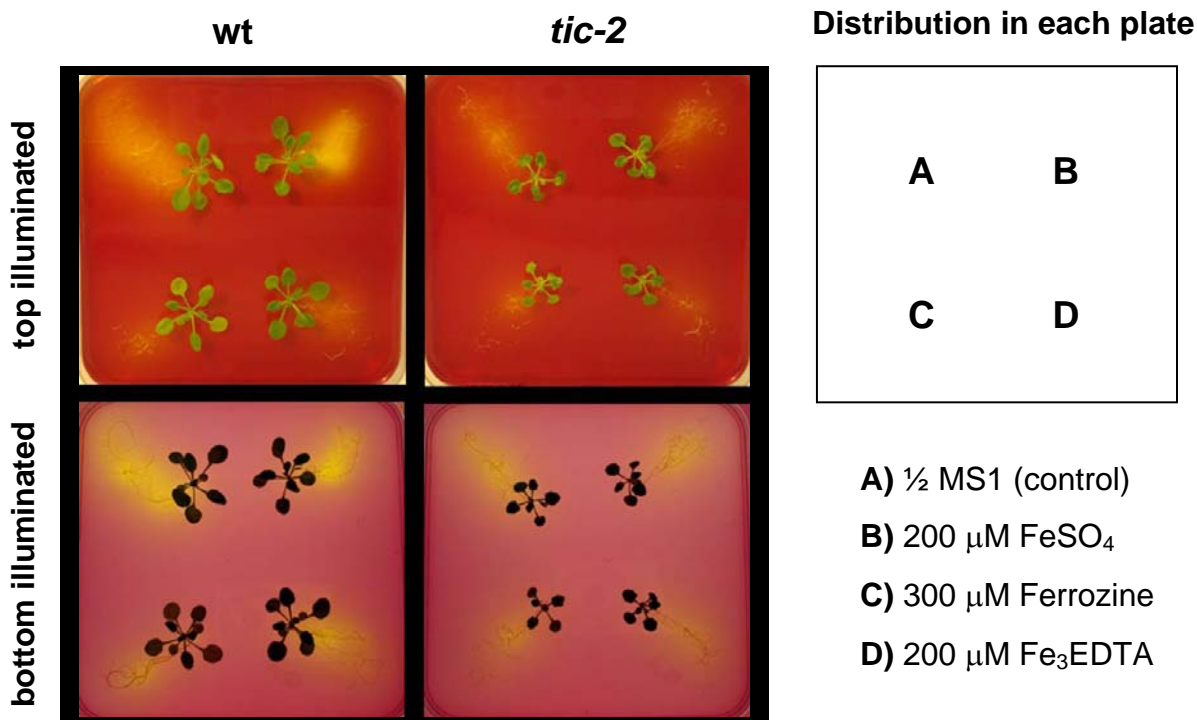
Figure III.4. Rhizosphere acidification response toward iron availability.
Seedlings that were grown for 5 to 6 days on MS1 media for iron tests were transferred to media supplemented with iron (200 μM FeSO$_4$ or 200 μM Fe$_3$EDTA) or with an iron chelator (ferrozine) and grown for a further two weeks. After this period, plants were transferred to Gambourg B5 media with a pH indicator. The transfer was done in the order and positions presented on the scheme (upper right) for each genotype. The pictures were taken three days after transferring to G-B5 media, the time lapse required for observing the acidification response.
The upper panels are photographs taken with top illumination to show the red colour of the media, the aspect of the plants and the change of pH. The lower panels are pictures of the plates presented above, but with bottom illumination. This created a higher contrast of the rhizosphere acidification response, aiding in the visualization of the change of colour of the media from red to yellow.
In general Col-0 wild-type plants (wt) acidified to a greater extend the media than the mutant. The acidification response in both genotypes was diminished with Fe$_3$EDTA, which is an insoluble source of iron, and with the iron chelator, ferrozine. Though the rhizosphere acidification was diminished in *tic-2* compared to wild type, the response itself was not compromised.
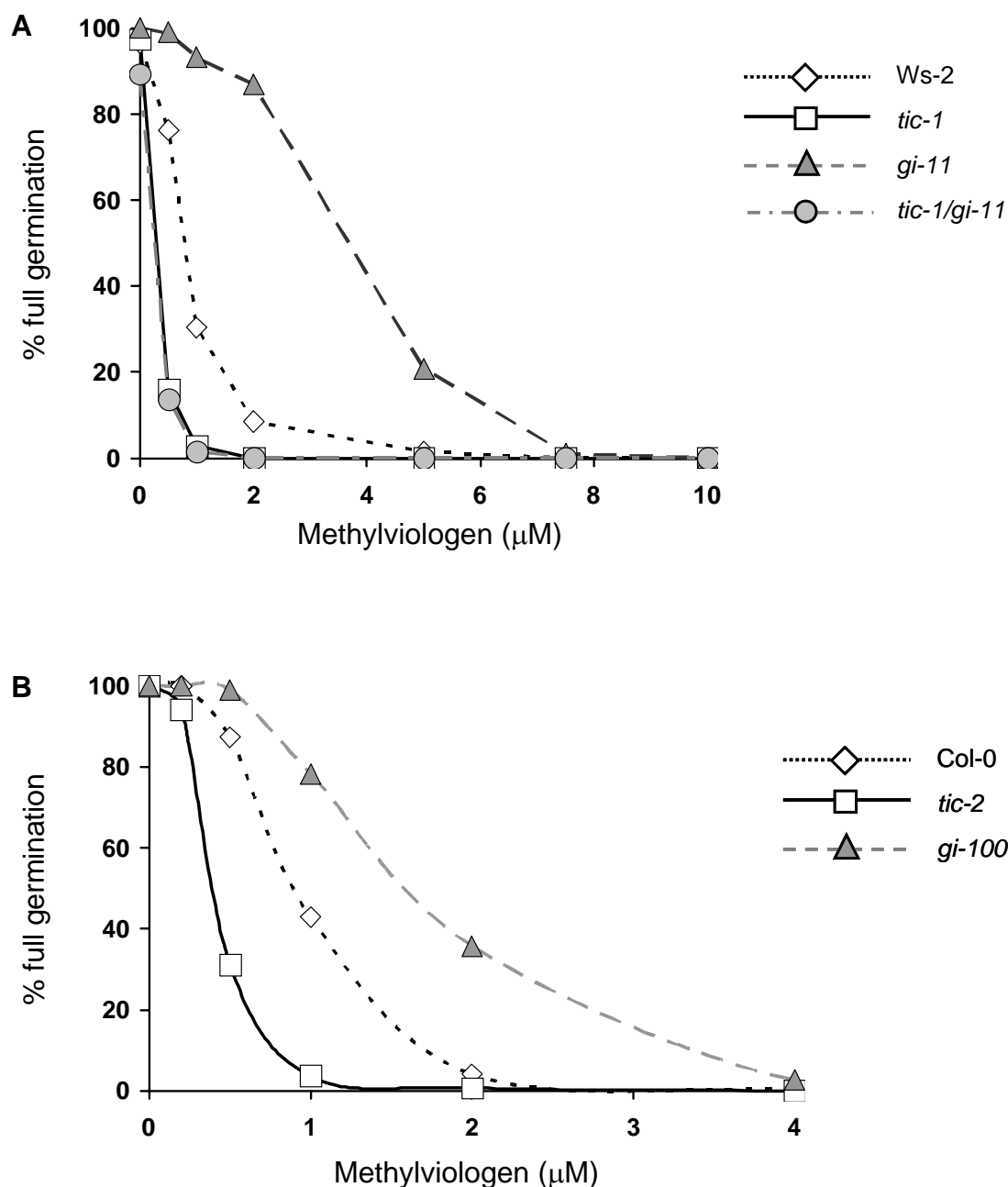
Figure III.5. *tic* **failed to fully germinate under oxidative stress conditions.**
A) Percent of full germination of wild type, *tic-1*, *gi-11* and *tic-1/gi-11* on MS1 supplemented with methylviologen (all lines in Ws-2 background)
B) Percent of full germination of wild type, *tic-2* and *gi-100* on MS1 supplemented with methylviologen (lines in Col-0 background)
A) and B) Germination rate of seeds released to a 12:12 photoperiod over media with different concentrations of methylviologen dichloride. In both ecotypes, *tic* displayed a hypersensitivity to the oxidant, reaching its half lethal doses at half the concentration than the respective wild types. The *gi* mutants are shown as a control for resistance to oxidative stress by methylviologen (Kurepa, 1998). Germination was scored 7 days after the end of the stratification.

C
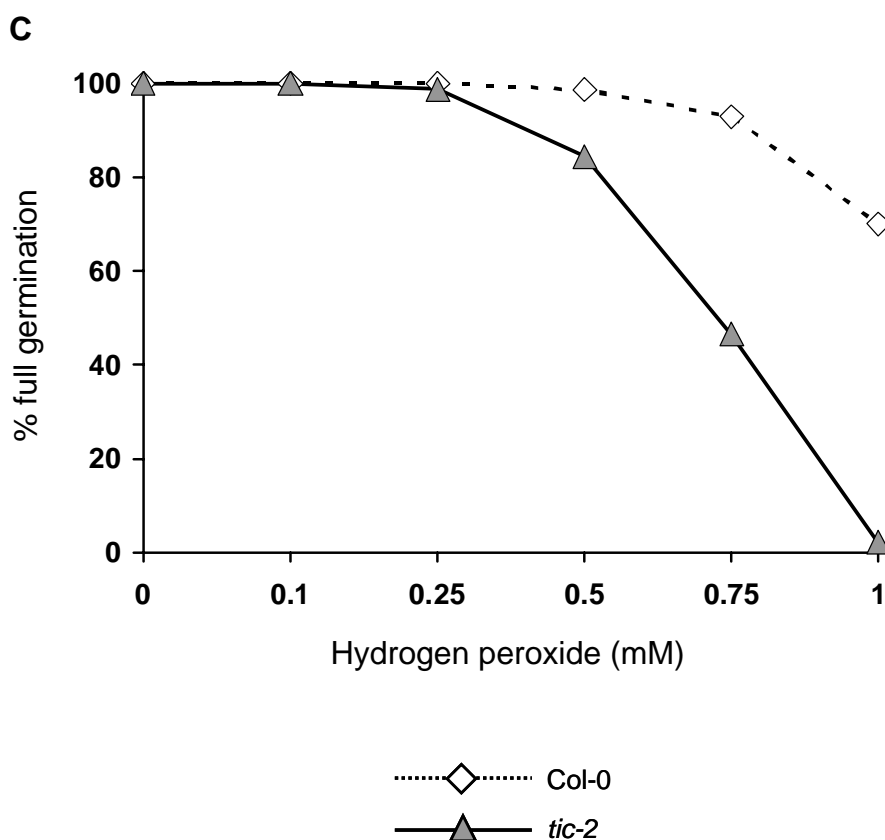
Figure III.5. (continuation). *tic* **failed to fully germinate under oxidative stress conditions.**
C) Percent of full germination of Col-0 wild type and *tic-2* on MS1 supplemented with H_2O_2. The germination of *tic-2* was arrested at lower concentrations than the control. Germination rate of seeds was scored 7 days after they were released to a 12:12 photoperiod over media with increasing concentrations of hydrogen peroxide.

The experiment with methylviologen was repeated with lines in the Col-0 background. Similar results were found in this ecotype (figure III.5B). The main difference observed was that the *gi* allele in Col-0 was more susceptible to MV the allele in Ws-2. This dissimilar behaviour has been previously reported (Kurepa, 1998).

In order to test the susceptibility of *tic* to other forms of oxidative stress, I performed another germination assay by adding hydrogen peroxide (H_2O_2) to the media and monitored the percentage of seed survival. I found a similar trend in susceptibility to H_2O_2 as to MV (figure III.5C). *tic-2* germination rate diminished at lower concentrations relative to wild type, reaching its half lethal dose around 0.75 mM H_2O_2. At this concentration wild type was unaffected (figure III.5C). While *tic-2* germination was arrested at 1 mM H_2O_2, wild type viability was only slightly affected. From these experiments, I concluded that *tic-2* was hypersensitive to superoxide radicals and peroxide, two different sources of oxidative stress.

2.5) ABA related responses in *tic-2*.

In the gene-ontology data mining, ABA appeared as one hormone-stimulus pathway that was modified in *tic-2* (table IV). I focused on ABA because other abiotic processes related to ABA-mediated responses, such as water deprivation and salt stress, were also highlighted as overrepresented GO terms in the data sets (table IV). Therefore I tested the effect exogenous ABA application. For this, I scored the germination rate of wild type and mutant on MS1 media supplemented with increasing concentrations of this hormone. *tic-2* germination was arrested at lower concentrations than the wild type, resulting in an ABA hypersensitive phenotype (figure III.6). The mutant sensitivity to ABA was ~2 fold compared to wild type. Notably, *tic-2* responded to ABA as low as 1 µM, a concentration that had no effect on the wild type. Furthermore at 5 µM ABA, *tic-2* germination was completely arrested, whereas wild-type seeds still germinated. This result provided evidence of altered ABA signalling in *tic-2*, in support of the bioinformatic analysis.

Further analysis showed that genes such as *DREB2a, COR15a, ERD3, ERD7, RD22, ABI1, SNRK2.2* and *SNRK2.3* were upregulated in *tic-2* (table V). This suggested that the mutant may be tolerant to drought. Consequently I tested drought tolerance in wild type and mutant plants grown under different soil water capacities. For this, plants were
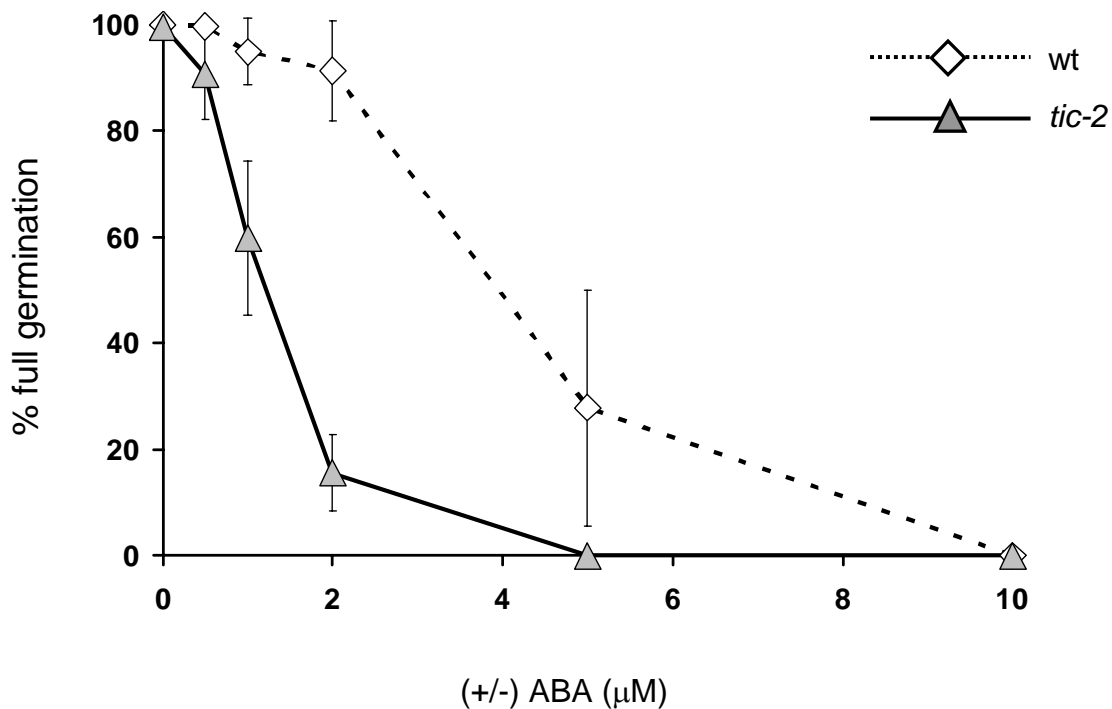
Figure III.6. Germination of *tic-2* displayed hypersensitivity to ABA.
Rate of germination on MS1 supplemented with (cis/trans) ABA. Germination was scored
7 days post-stratification. The germination of *tic-2* was arrested at lower concentrations of
ABA than the wild type (wt).
Error bars indicate standard deviation from three experiments with 100-300 seeds per
genotype per concentration.

watered with the required amount to keep a constant soil water capacity (SWC) over the course of the experiment (see methods). *tic-2* demonstrated to be tolerant to slight and severe drought conditions (figure III.7). When wild type and *tic-2* plants were kept at 65% SWC, a well watered soil, they developed normally. At 30% SWC, the growth of wild type was slightly reduced compared to itself at 65%, but without compromising its physiology. On the other hand, at 30% SWC *tic-2* development appeared identical to itself at 65% (figure III.7). Interestingly when wild-type plants were under severe drought at 15% SWC, their leaves appeared wilted and necrotic, whereas the leaves of *tic-2* were still turgid and general plant fitness was not obviously compromised (figure III.7). When both wild type and mutant plants were left without watering for 21 days, the symptoms of wild type toward drought were enhanced, while *tic-2* was basically unaltered (figure III.7). This indicated that *tic-2* was drought tolerant.

To assess if the drought tolerance observed in *tic-2* was related to its water loss, the total amount of water used during irrigation to maintain a constant SWC was recorded. The total water consumption from the mutant during the mild drought period or control conditions was significantly less than that of wild type (figure III.7B and 7C). The amount of water added to the soil of *tic-2* plants to keep the SWC at 65% and 30% was around 50% of wild type (figure III.7B and 7C). This data indicated that *tic-2* could loss less water through transpiration. Taken together, these physiological tests suggested that *tic-2* had altered ABA responses that lead to hypersensitivity to the hormone while germinating, and resistance to drought through higher levels of gene expression related to this condition.

2.6) Susceptibility to biotic stress infringed by *Pseudomonas*.

ABA and reactive oxygen species (ROS) production play a crucial role in plant defence mechanisms (Ton, 2009). As *tic-2* displayed hypersensitivity toward ROS (figure III.5) and ABA (figure III.6) and had altered ABA related-responses (figure III.7), I decided to examine how the mutant would behave in response to biotic stress. Therefore I performed a bacterial infection trial by subjecting wild type and mutant plants to *Psedomonas syringae* strains, either virulent or avirulent (DC3000 and DC3000 AvrRps4, respectively) (Hinsch, 1996). For each plant/bacterial strain combination (4), the infection was executed at dawn or at dusk (8 total) and colony forming units (CFU) were counted to measure bacterial growth.

Soil Water Capacity (%)
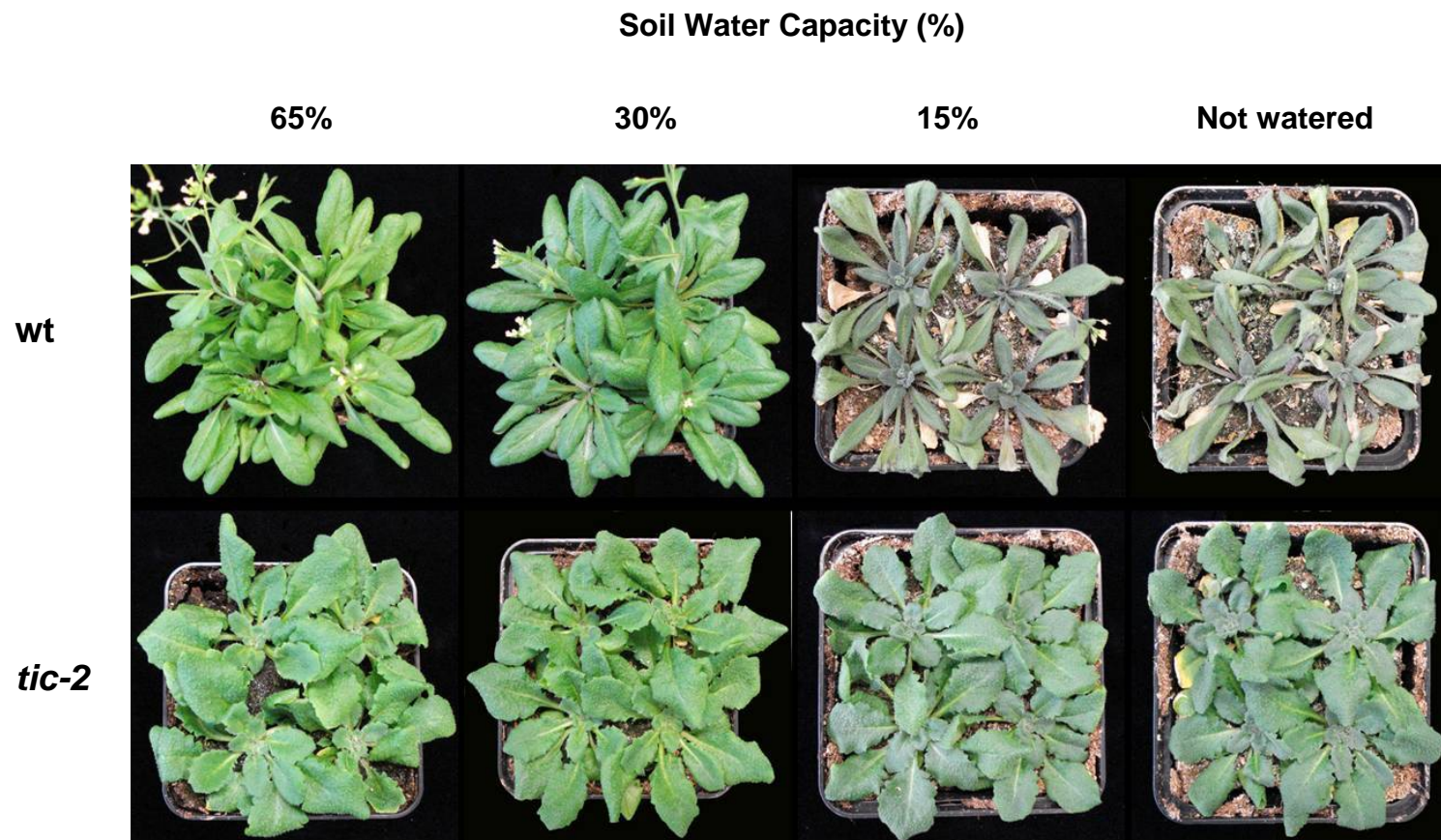
Figure III.7. *tic-2* **showed tolerance to drought conditions.**
Plants were grown for 3-4 weeks under a 12:12 photoperiod and normal watering. Immediately afterwards, watering was continued by adding the volume of water required to reach the desired soil water capacity. The photographs shown were of wild type and *tic-2* plants grown for 3 weeks under the specified soil water capacities.

B

C
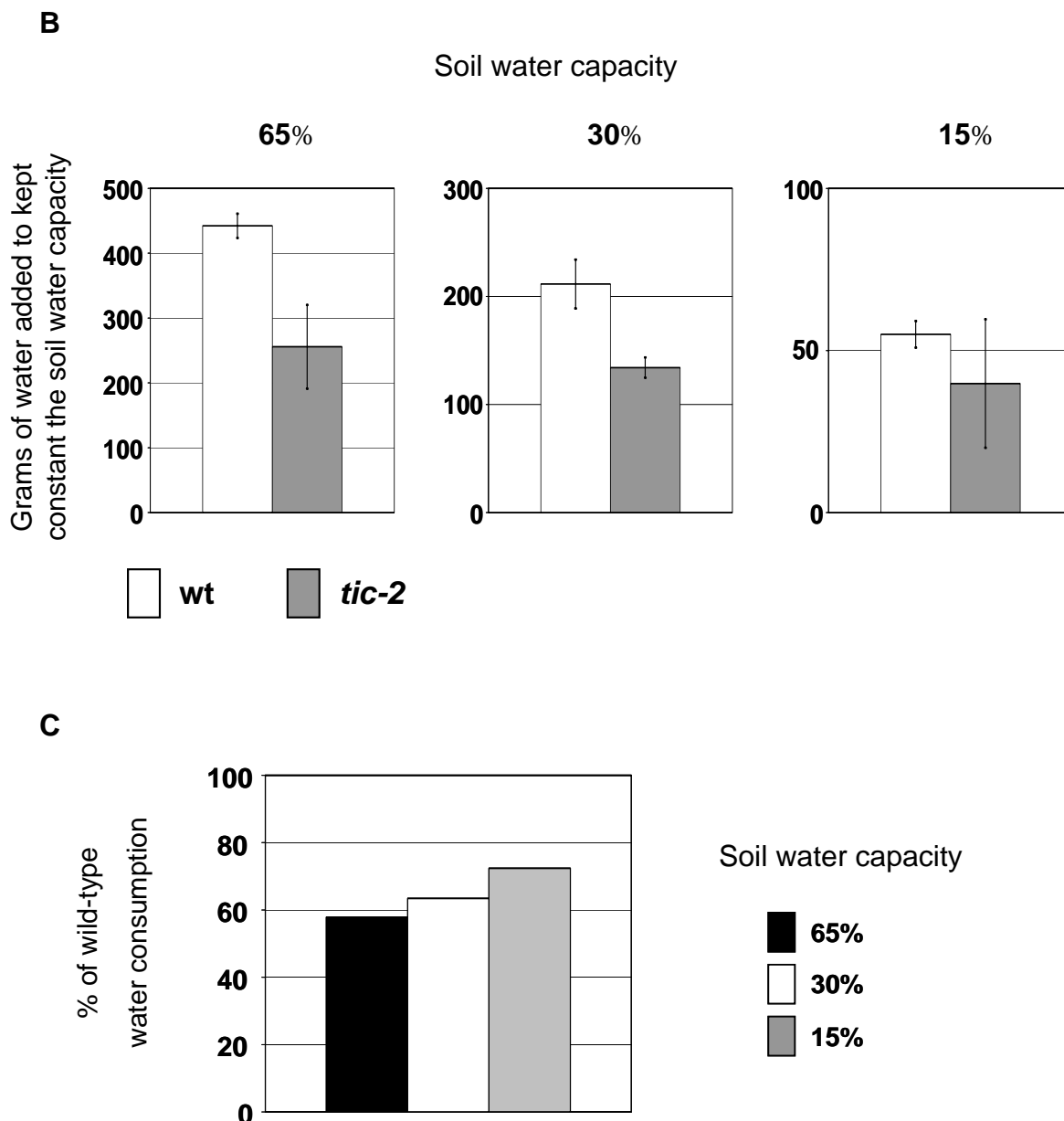
Figure III.7. (continuation). *tic-2* **showed tolerance to drought conditions.**
B) Total amount of water added to keep the desired soil water capacity constant through the duration of the experiment (3 weeks). The soil water capacity is shown on the top of each panel. Note that at 65% and 30% soil water capacity, *tic-2* water consumption (in gray colour) was significantly less through the 3 week period. Averages are from 2 independent experiments, each one with 3 or 4 pots with 4 plants per genotype per condition. Error bars represent standard deviation.
C) *tic-2* water consumption plotted as the percentage of wild type (wt) water consumption. The total grams of water added to the wild type were considered as the 100%, the grams of water added to *tic-2* were taken as the percentage of wild-type total amount in each condition.

Three days after inoculation, the infection rate with the *P. syringae* virulent strain revealed a time-dependent effect on wild-type plants, producing ~10 times less CFU in the evening than in the morning (figure III.8). This time-dependent effect was not observed with the avirulent strain. Furthermore as expected, the avirulent strain produced less CFU than the virulent one. In contrast, *tic-2* showed a higher susceptibility to the bacterial infection with the *P. syringae* virulent strain than wild-type plants. Also the time-dependent susceptibility effect was not observed in *tic-2*, as demonstrated by similar rates of infection at dawn and dusk (figure III.8). Concerning the effect of the avirulent bacterial strain on *tic-2*, a higher variability between assays was observed. However infection rates were slightly higher in *tic-2* than those with wild type and no time-dependent effect was observed. In conclusion wild-type plants showed a time-dependent susceptibility to a virulent *P. syringae* strain. In contrast, *tic-2* was hypersensitive to *P. syringae* infection and no time-dependent infection susceptibility was observed.

3) Effect of chemicals causing oxidative stress or blocking electron transfer in circadian periodicity.

tic circadian-clock defects included an early phase and low amplitude rhythms (Hall, 2003), but the mechanism underlying these effects are still unknown. In this work, I demonstrated that *tic* showed hypersensitivity to oxidative stress (figure III.5). Considering that diurnal physiological process, such as photosynthesis and respiration, produce ROS, I hypothesized that ROS would have an effect on circadian rhythms. Furthermore, it is before and after the light to dark transitions when the clock is more susceptible to entrainment, and *tic* clock is arrested before dawn, which coincides with the time when photosynthesis will restart and will be source of ROS production. Therefore I tested the effect of compounds that produce oxidative stress on circadian periodicity. These compound were methylviologen (MV), hydrogen peroxide (H_2O_2), salicylhydroxamic acid (SHAM) and diphenyleneiodonium chloride (DPI). The first two cause oxidative stress, while SHAM and DPI inhibit proteins involved in ROS dissipating processes and oxidoreductase activities, respectively. SHAM blocks specifically the alternative oxidase (AOX1a), which provides plants with a non conservative energy passage of electrons from complex II, avoiding overreduction of the mitochondrial electron transport chain
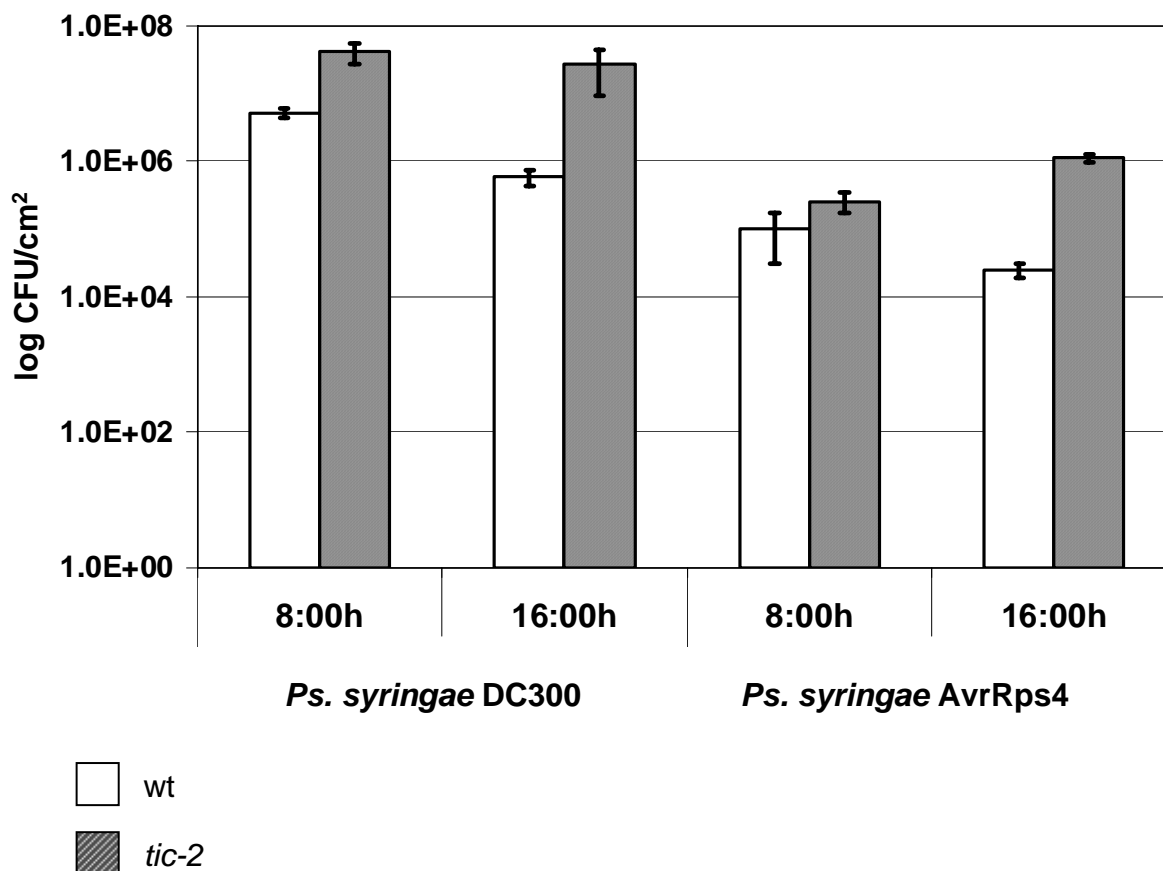
Figure III.8. *tic-2* **was hypersensitive to** *Pseudomonas syringae* **infection.**
Wild type and *tic-2* plants were inoculated with a virulent (left side, DC3000) and an avirulent
(right, DC3000 AvrRps4) strain of *P. syringae* at the break of dawn or before dusk by spraying a
solution of the bacteria over the leaves. Bacterial growth was recorded as Colony Forming Units
(CFU) per area 3 days after infection.
Bacterial growth with the virulent strain was higher in *tic-2* than the wild type. Besides *tic-2*
susceptibility to the pathogen, note that the CFU counts were similar both at dawn and dusk
(compare gray bars within the virulent strain), whereas the wild type presented a gating or
diurnal effect on bacterial growth, being less susceptible to infection at dusk (white bars within
the virulent bacteria).
The CFU counts with the avirulent strain were lower compared to the virulent infection.
Error bars indicate standard error of three replicates each one consisting of three leaves.

complexes (Nelson, 2000). DPI binds to flavoproteins and is an inhibitor of NADPH oxidases, NADPH-ubiquinone oxidoreductase and nitric oxide synthase (Riganti, 2004).

To test the effect of redox-altering compounds on wild type and *tic-1* clock rhythms, I selected the *CCA1:LUC* as a reporter of the pharmacological action of these compounds on clock period. I selected *CCA1* as a reporter for clock-gene expression because it was the only clock-gene not found to be misexpressed in *tic-2* microarray data (table III). Ws-2 wild type and *tic-1* seedlings were grown for 7 days on MS1 under a 12:12 photoperiod. Then they were transferred to media with or without the above mentioned compounds and luciferin was added. Bioluminescence was recorded under constant light conditions after one day of further entrainment (see methods).

CCA1:LUC driven rhythms of wild-type plants displayed an oscillating pattern with a peak of expression at dawn, whereas *tic-1* plants showed a rhythm with low amplitude that dampened through time (figure III.9 follow the pattern of the black symbols), as previously described (Hall, 2003). The pharmacological effects were thus compared to these two baselines.

The addition of H_2O_2 produced a lengthening effect of clock periodicity at low H_2O_2 concentrations in wild type (figure III.9A and C blue diamonds, 0.10 mM). This effect was reversed by increasing the H_2O_2 concentration and then it provoked a shortening of the period (figure III.9A and C pale blue and yellow diamonds, 0.25 mM 0.50 mM, respectively). Notably the amplitude of the wild-type rhythms was decreased regardless of the H_2O_2 concentration applied (figure III.A). Addition of H_2O_2 to *tic*, compound to which I previously showed it has germination susceptibility (figure III.5C), did not affect its periodicity, except at high concentrations that markedly compromised plant fitness (figure III.9B and C). Thus the wild-type oscillator was sensitive to a dose response of H_2O_2 in a complex manner and *tic-1* was resistant to this effect.

Methylviologen application affected in a different manner the circadian periodicity of wild type and *tic-1*, when compared to the effect of H_2O_2 addition. In the wild type, MV provoked an increase of period in a dose-dependent fashion (figure III.10). Rather than observing a constant increase in period length, MV effect "was buffered," meaning that a given concentration threshold had to be surpassed for observing a significant response. The wild-type period was lengthened at 0.5 μM (dark yellow) with a second increase at 2-5 μM (pink and white, respectively). The period was shortened at a concentration of 10 μM (pale blue) (figure III.10A and C). Besides the effect on period, a reduction of amplitude was observed in a dose-dependent manner (figure III.10A). Though *tic-1* showed a similar
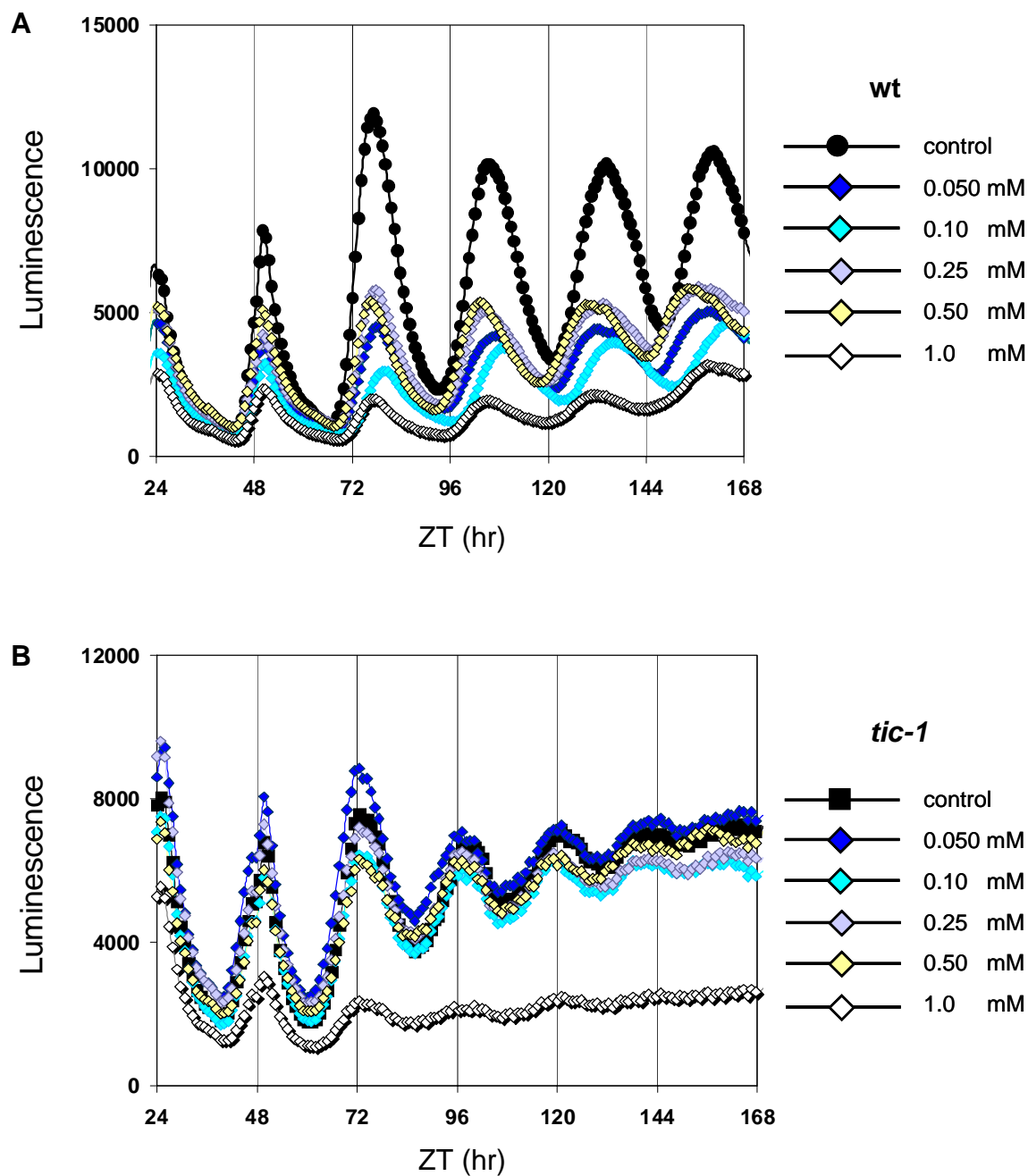
Figure III.9. Dose response of hydrogen peroxide on circadian periodicity.
A) *CCA1:LUC* luminescence rhythms of Ws-2 (wt) under constant light after transferring seedlings to MS1 media with increasing concentrations of H_2O_2.
B) *CCA1:LUC* luminescence rhythms of *tic-1* under constant light after transferring seedlings to MS1 media with increasing concentrations of H_2O_2.
The key code at the left of the panels shows the H_2O_2 interval of concentrations. Note that the amplitude of the rhythms in wild type diminished at the lowest H_2O_2 concentration, whereas in *tic-1* this effect was not visible.
The first 24 hours shown were under LD, from ZT 48 on, the conditions were constant light.

C
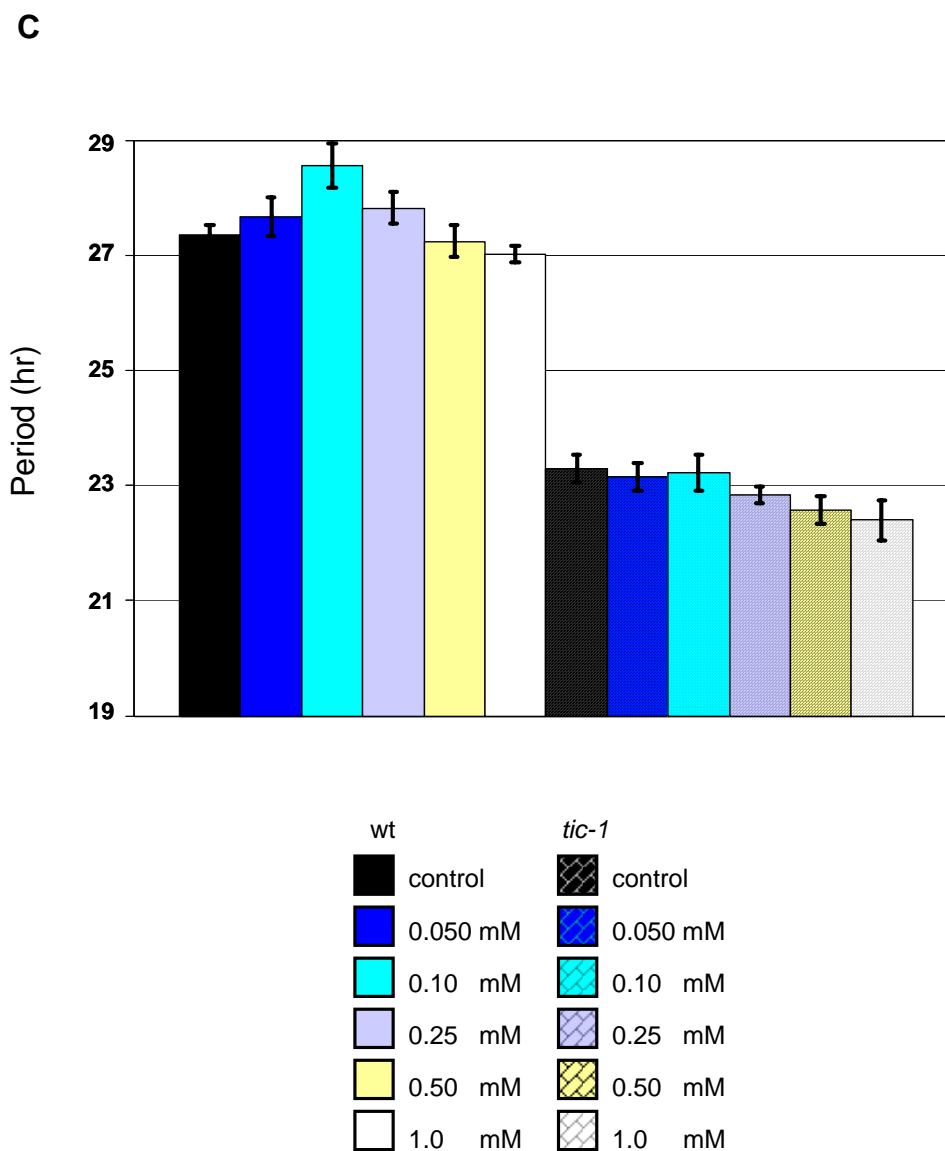
Figure III.9. (continuation). Dose response of hydrogen peroxide on circadian periodicity.

C) Bar chart summarizing the change of period length in wild type and *tic-1* after addition of H_2O_2. At the bottom of the graph the colour key specifies the H_2O_2 concentrations employed per treatment. Note that at low concentrations, H_2O_2 lengthens period of wild type, at higher concentrations the circadian clock pace was restored and then reduced, whereas the addition of H_2O_2 did not produce such an effect on *tic-1*.

Error bars indicate standard error from a population between 28 to 48 plants per treatment.
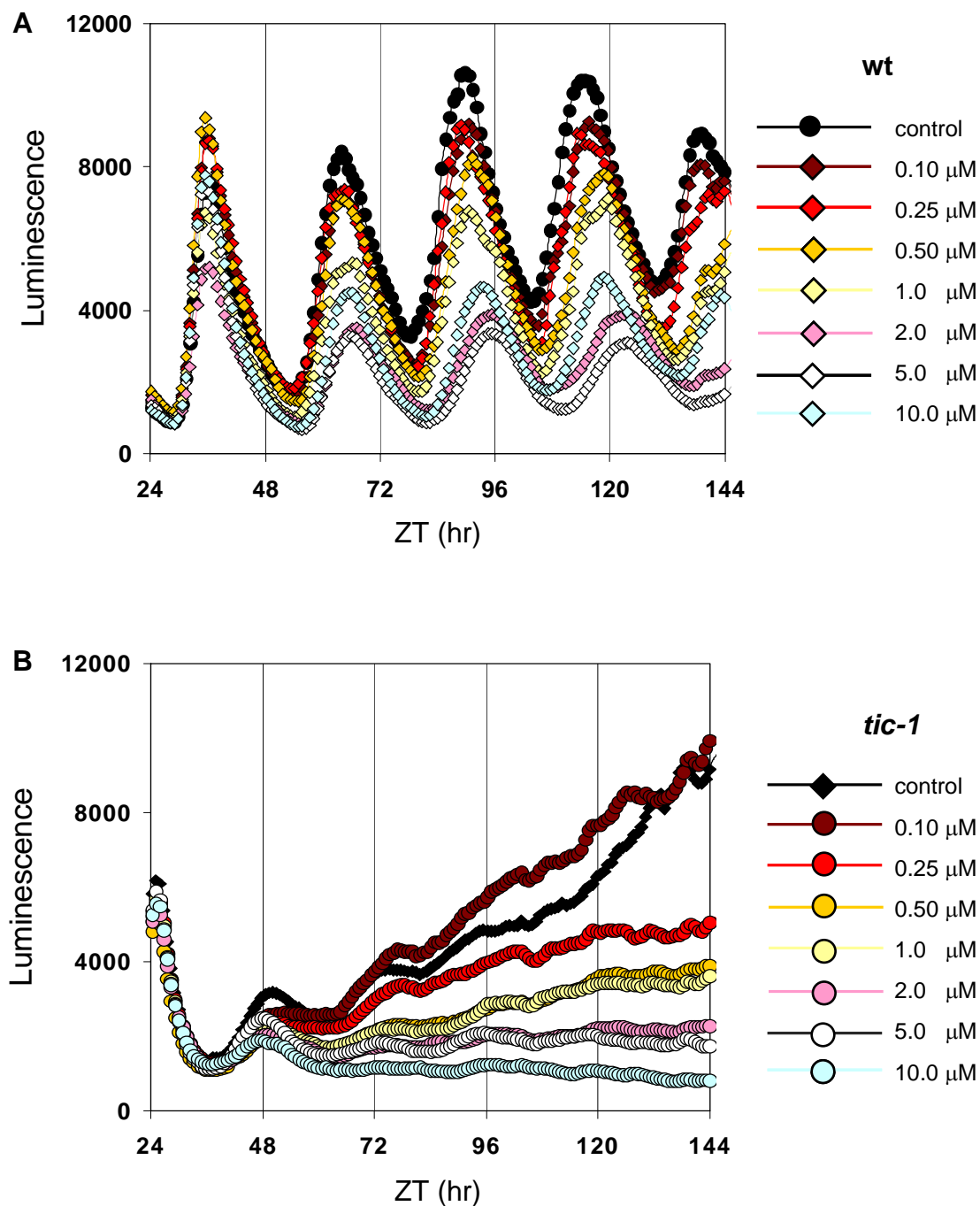
Figure III.10. Dose response of methylviologen on circadian periodicity.
A) *CCA1:LUC* luminescence rhythms of Ws-2 (wt) under constant light after transferring seedlings to MS1 media with increasing concentrations of methylviologen.
B) *CCA1:LUC* luminescence rhythms of *tic-1* under constant light after transferring seedlings to MS1 media with increasing concentrations of methylviologen.
The codes at the left of the panels specify the concentration of methylviologen per treatment.
The first 24 hours belong to an LD cycle before transfer to LL at ZT 48.

C

Effect of Methylviologen on period length
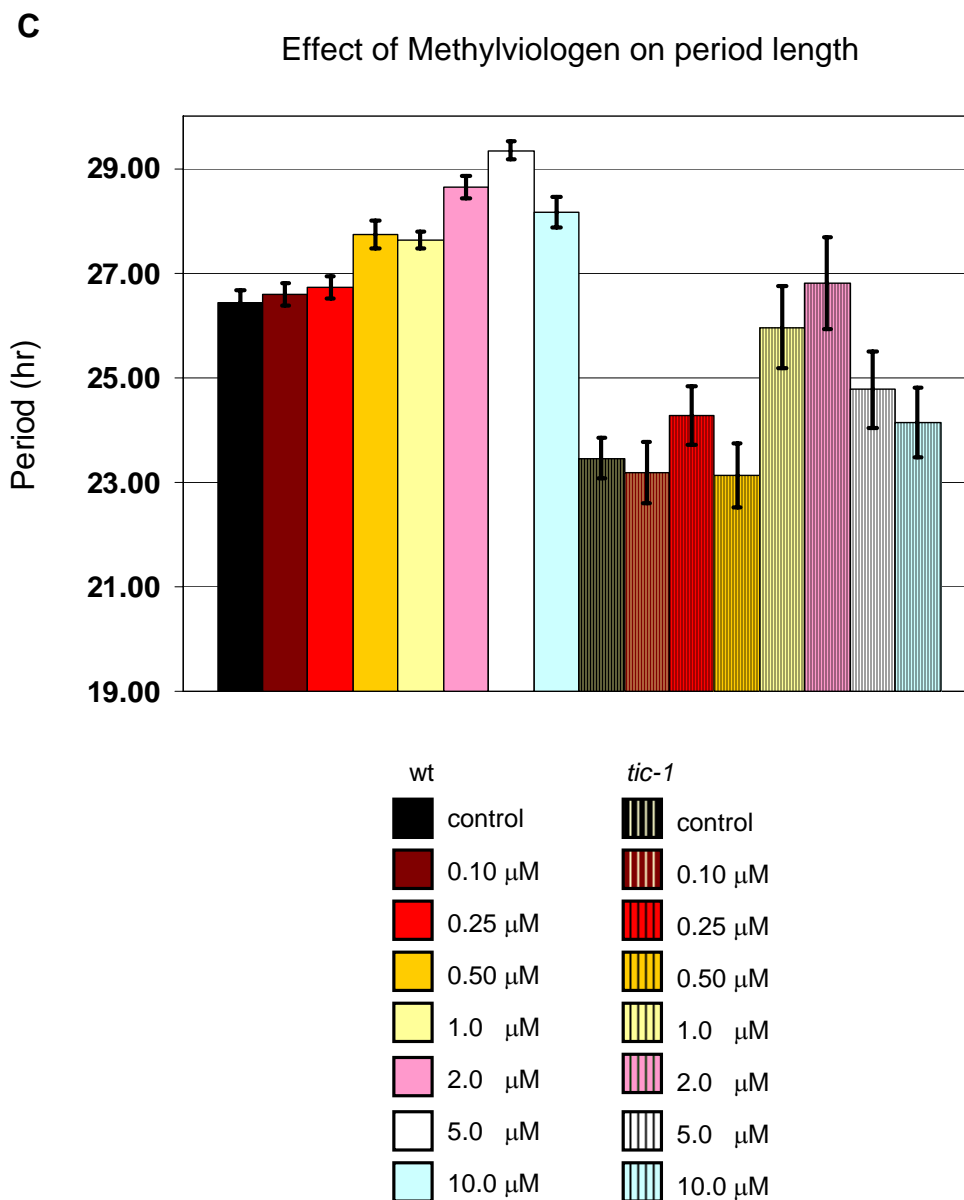
Figure III.10. (continuation). Dose response of methylviologen on circadian periodicity.
C) Chart summarizing the period length in wild type and *tic-1* upon treatment with methylviologen. At the bottom of the graph the colour key displays the MV concentration gradient. Plain and stripped colours indicate wild type and *tic-1,* respectively.
The pro-oxidant increased the period length in both genotypes. Note that wild type had two thresholds for these increases (0.50 μM and 2.0 μM, dark yellow and pink respectively), while in *tic-1* a clear threshold was reached until 1.0 μM of methylviologen (pale yellow). Furthermore, *tic-1* displayed hypersensitivity to oxidative stress as seen by the decrease in period length at a lower concentration than wild type (compare white bars).
Error bars indicate standard error from a population between 28 to 48 plants per treatment.

trend as wild type, the lengthening effect of period took place at lower concentrations (1-2 μM pale yellow and pink, respectively) (figure III.10B and C). Also the period was shortened at lower concentrations (5 μM, white) (figure III.10C), probably reflecting the susceptibility of the mutant to this chemical as I previously described in a germination assay (figure III.5). Taken together, both wild type and *tic-1* circadian clock were responsive to methylviologen as this provokes a lengthening of the periodicity. However the specificity of this effect was dependent of the genotype.

Periodicity was also assessed with DPI, an inhibitor of NADPH oxidases and other flavoproteins. DPI had no effect on period length in the wild type at the range of concentrations tested in this study (figure III.11A and B). However an effect on amplitude was observed at higher concentrations (figure III.11A, lime and green figures). Contrary to these results, DPI caused a lengthening of *tic-1* periodicity at a concentration of 1.0 μM (figure III.11B and C, dark green). Also no clear effect on amplitude was found in *tic-1* except at 1.0 μM. These results suggested that *tic-1* period was more susceptible to the effect of DPI (figure III.11). It remains to be tested if the period of wild type could be affected by DPI at higher concentrations.

As briefly stated above, the mitochondrial bound AOX1a can be inhibited by SHAM. This chemical became of interest as the expression of *AOX1a* was found to be induced in *tic-2* (table V). When SHAM was applied to wild type, no clear effect on period length was found (figure III.12A and C). A slight shortening of period length occurred at 2.0 μM (figure III.C). Interestingly this period shortening effect was stronger on the mutant and it took place at the lowest concentrations used in this study (figure III.12B and C pale blue and light gray). From these results, I concluded that *tic* was hypersensitive to SHAM, as *tic* could require higher activity of the AOX1a to sustain its ROS hypersensitive phenotype.

The results from the chemical perturbation of the clock rhythms showed that the circadian clock can be affected by ROS and specific inhibitors. These effects can alter clock periodicity and/or amplitude. The results suggested that the extent of the effect of these compounds would depend on the metabolic status of the plant as a mutant hypersensitive to oxidative stress like *tic* displayed different patterns of responses than wild type.
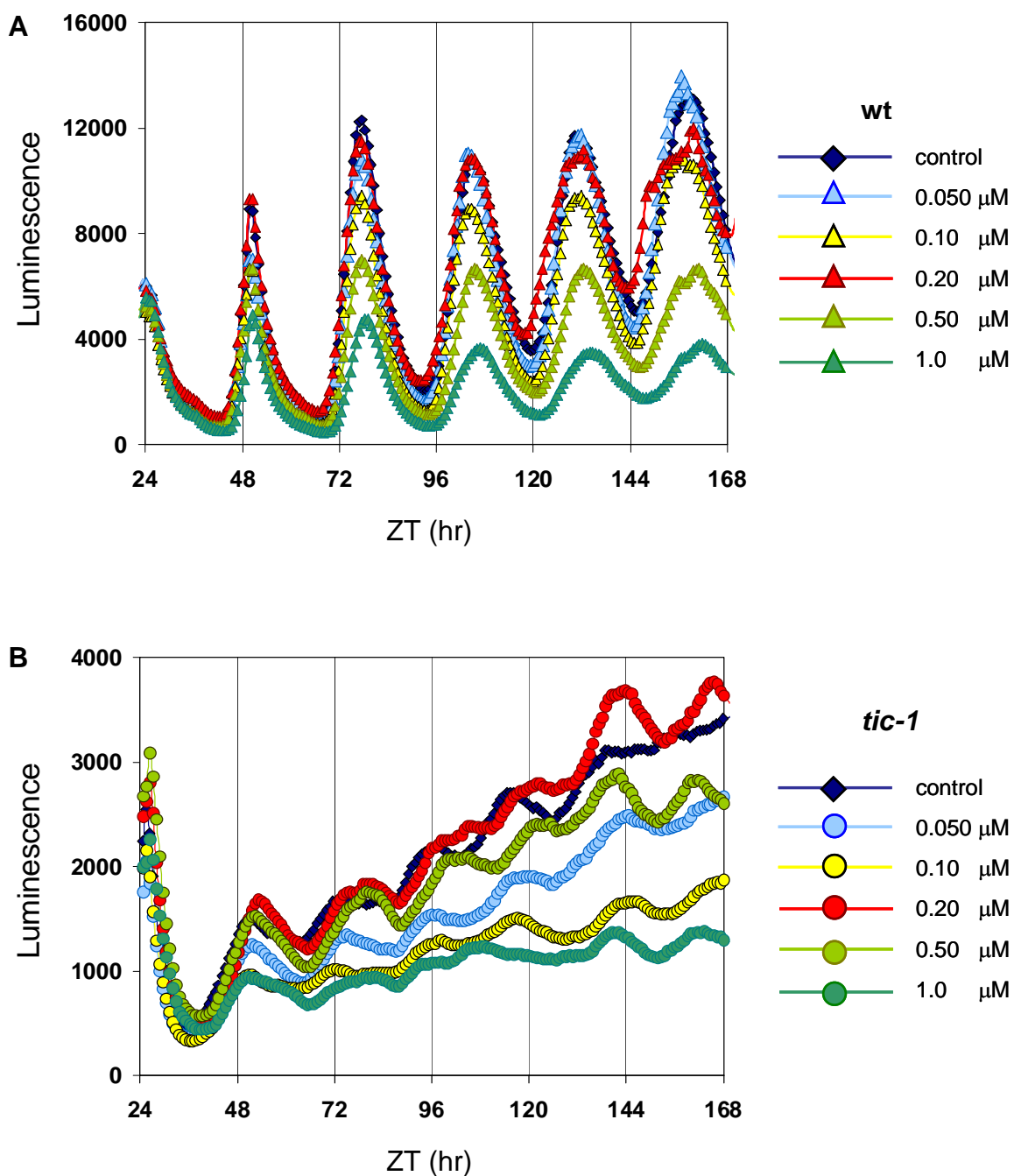
Figure III.11. Dose response of DPI on circadian periodicity.
A) *CCA1:LUC* luminescence rhythms in Ws-2 (wt) after transferring seedlings to increasing concentrations of DPI under constant light.
B) *CCA1:LUC* luminescence rhythms in *tic-1* after transferring seedlings to increasing concentrations of DPI under constant light.
The key code at the left of the panels shows the DPI concentration used per treatment.
The first 24 hours shown were under LD, from ZT 48 on, the conditions were constant light.

C   Effect of DPI on period length
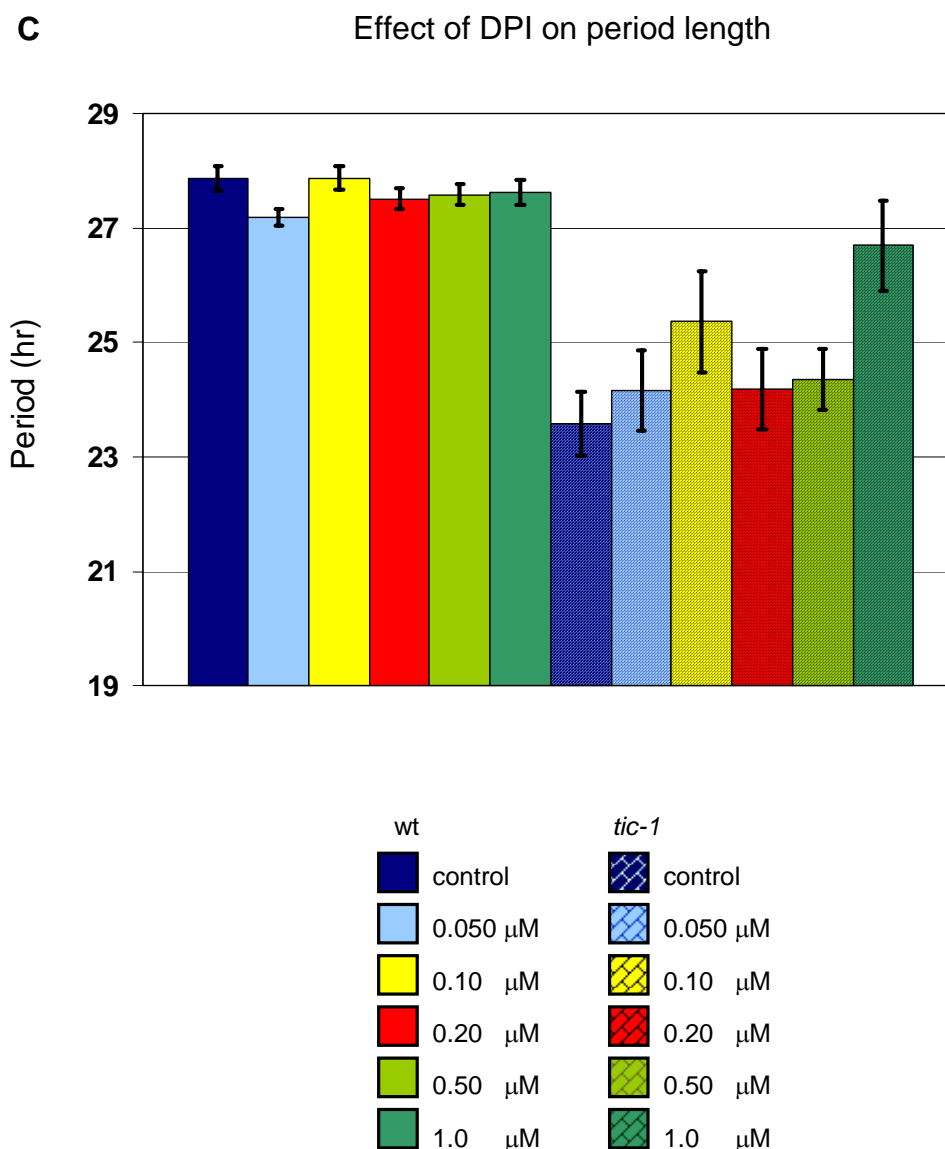
Figure III.11. (continuation). Dose response of DPI on circadian periodicity.
C) Bar chart summarizing the change of period in wild type and *tic-1* after chemical
perturbation by DPI. The inhibition of NADPH oxidases and ROS production by the
addition of DPI at the concentrations tested were not found to have an effect on circadian
periodicity on either the wild type or the mutant.
The period shortening in wild type (pale blue) nor the lengthening seen in *tic-1* (yellow
bar with pattern) in the presented chart, were observed to such an extent in biological
replicate experiments.
Error bars indicate standard error from a population between 28 to 48 plants per treatment.
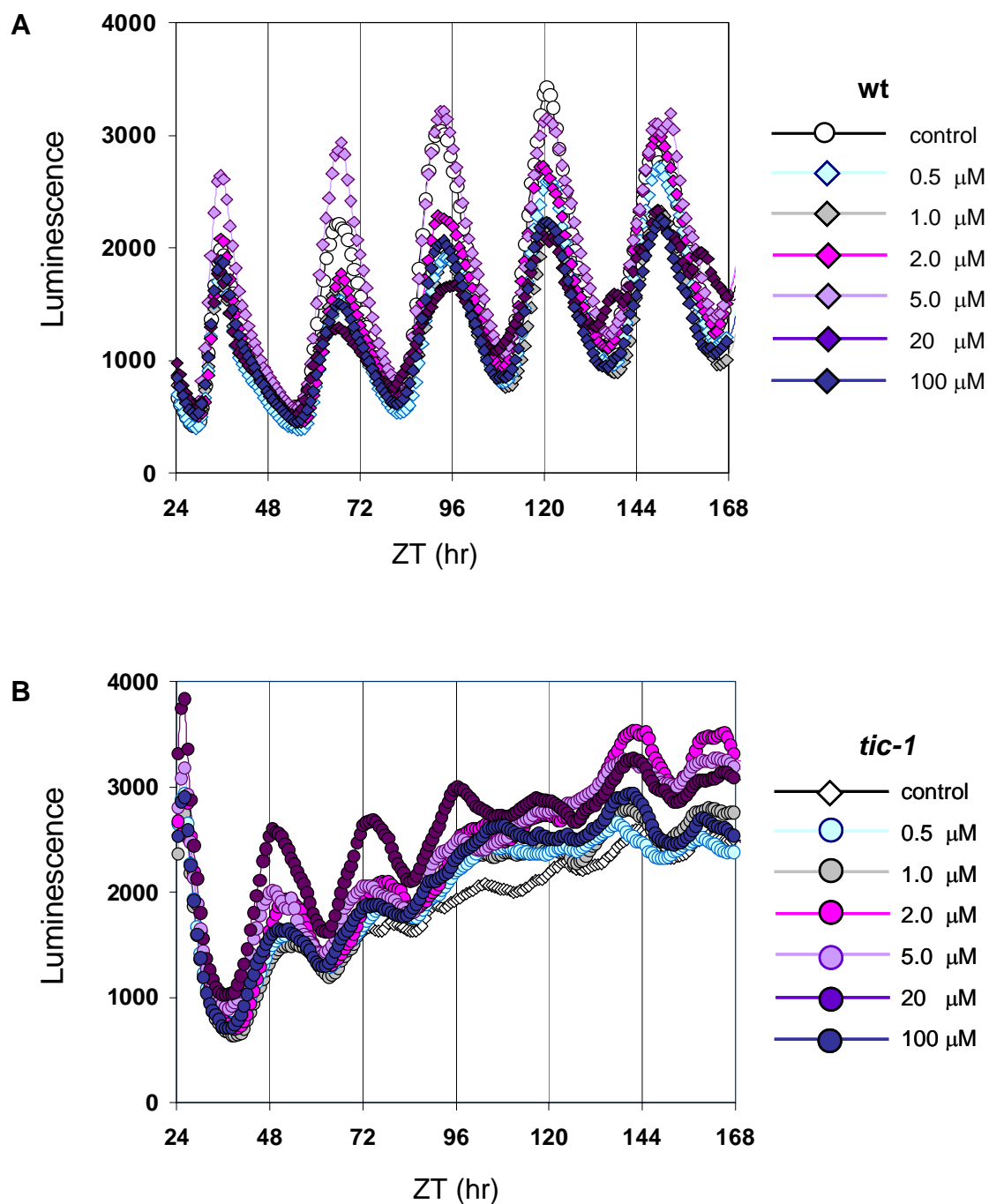
Figure III.12. Dose response of SHAM on circadian periodicity.
A) *CCA1:LUC* luminescence rhythms of Ws-2 (wt) under constant light after transferring seedlings to MS1 media with increasing concentrations of SHAM.
B) *CCA1:LUC* luminescence rhythms of *tic-1* under constant light after transferring seedlings to MS1 media with increasing concentrations of SHAM.
At the left of the panels a colour key shows the SHAM interval of concentrations used.
The first 24 hours shown were under LD, from ZT 48 on, the conditions were constant light.

C Effect of SHAM on period length
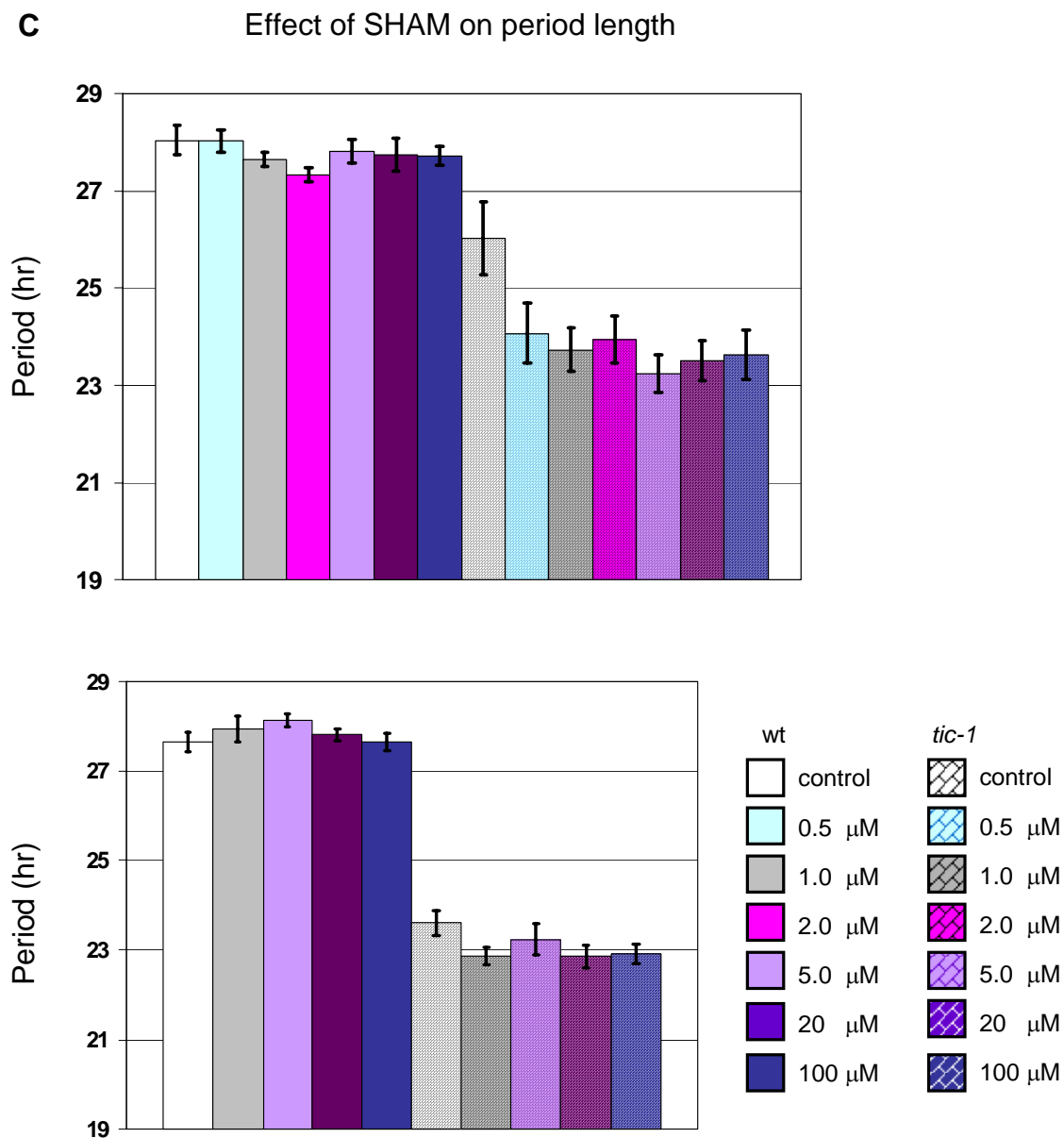
Figure III.12. (continuation). Dose response of SHAM on circadian periodicity.
C) Chart summary of the effect of SHAM on period length in wild-type and *tic-1*. The top and bottom panel show different experiments. Not all the concentrations (shown at the left in boxes with a colour key) were applied to both assays. Note that wild-type behaviour was different, as the period length reduction was not observed in the lower panel, though the 2.0 μM concentration (fuchsia) was not used in this experiment. Although the period lengths varied in *tic-1* between assays, a tendency for period reduction upon SHAM treatment was observed even at low concentrations.
Error bars indicate standard error from a population between 28 to 48 plants per treatment.

III.B. TIME FOR COFFEE interaction with the sucrose non-fermenting (SNF1) related protein kinase (SnRK) AKIN10.

TIC function in the circadian clock is time-specific, playing its role before dawn and therefore affecting entrainment. It was noticed that the dysfunctional clock in *tic* could be restarted late in the night (Hall, 2003). Many circadian-clock components are controlled by the oscillator, as their transcript levels cycle through a ~24 hour period, this includes *CCA1*, *LHY*, *TOC1* and *GI* (Más, 2008). This cycling of mRNA levels participates in establishing the transcriptional feedback loop of the circadian clock. However some circadian clock elements do not cycle at their transcript level, but nonetheless their proteins exhibit a rhythmic pattern of degradation in a daily basis. Then this mechanism drives their oscillation (Más, 2008). Therefore in the clock fine tuning, the cyclic degradation of clock protein products and/or their phosphorylation provides a lagging step in the observed transcriptional-translational loops.

Previously it was reported that neither *TIC* mRNA nor TIC protein oscillate through the day (Ding, 2007). These results indicated that TIC exerted its time-specific function by an unknown mechanism. As TIC was found not to be under circadian control, two time-specific scenarios for TIC function are plausible. In one scenario, an event could trigger TIC activation and only then TIC would exert its function in the clock. In a second scenario, TIC would be constitutively active and its function would be attenuated by a rhythmic factor. Either situation could explain the observed clock arrest in *tic*. Therefore post-translational modifications may control TIC activation or protein stability in the first and second scenarios, respectively. Consequently for TIC to be post-translationally modified, TIC would interact with another protein in a time-specific manner. TIC sequence encodes for a protein of about 1550 amino acids and this sequence did not suggest a putative function. No identifiable domains of hypothetical function were present in TIC sequence in the current protein databases with exception of a P-loop GTP binding domain in its carboxy terminus (Ding, 2007 and this work). Therefore identifying TIC protein interacting partners could provide an insight into the mechanism of its morning regulation of the circadian clock.

1) Yeast two-hybrid screen for TIC protein interactors

With the aim to reveal factors that could render TIC its time-specific activity and more generally to understand TIC mechanism of action, a yeast two hybrid (Y2H) screen was performed. A Y2H screen was selected as it allows the identification of novel protein interactors even when no particular targets for the protein or domain of interest are known (Sambrook, 2001). The Y2H screen was performed between a fragment of the amino terminus of TIC (770 amino acid in length) and a cDNA library (Li, 2009). The TIC fragment was fused to the DNA activation domain as the "bait" as the cDNA library was randomly fused to the DNA binding domain as a "prey." From the Y2H screen, several candidate protein interactors were found. The list of TIC protein interactors included several transcription factors and other elements associated to stress or transcriptional control. Some of those interactors that were represented by several clones in the screen are presented in table VI.

To examine if any of the TIC Y2H interactors could be involved in TIC developmental programme and/or function in the circadian clock, I search for T-DNA mutants in the genes of these encoded proteins. Then I isolated homozygous mutants and examined their growth. Rationalizing that these proteins could interact with TIC and *tic* resulted in a stress phenotype (figure III.2), I screen the mutants under greenhouse conditions for growth phenotypes that may resemble that of *tic-2*. T-DNA transgenic lines for candidates involved in transcription, DNA binding, response to oxidative stress or of unknown function, were not available at the European Arabidopsis Stock Centre (NASC) when this work was performed (table VI). The T-DNA available mutants corresponded to two transcription factors, *MYC2/JIN1* and *BIM1*. However further analysis of *MYC2/JIN1* and *BIM1* was not pursued as they did not show a *tic*-like phenotype consisting either in dark green leaves, slow growth rate or leaf serration.

In the particular case of the protein kinase AKIN10, null mutants do not exist because the mutation is lethal (Csaba Koncz, personal communication). Fortunately, the laboratory of Dr. Csaba Koncz had generated genetic resources through an estradiol inducible system (Zuo, 2000) and gave access to these lines for this research. This system was generated by the fusion of the DNA-binding domain of the bacterial LexA, the transactivating domain of VP16 and the regulatory region of an estrogen receptor (Zuo, 2000). AKIN10 has a homologue kinase, AKIN11 (Le Guen, 1992). AKIN10 and AKIN11 are two SnRK1s [(Sucrose non fermenting 1) Relative Kinase] that share sequence

Table VI. List of candidate TIC protein interactors

The amino terminus of TIC protein was used as bait in a yeast 2 hybrid screen. The displayed locus corresponds to interactors found that concurrently appeared with multiple positive clones.

§ T-DNA insertion lines SALK_040500 and SALK_061267 for *MYC2* and SALK_051585 and SALK_132178C for *BIM1* were screened under 16:8 photoperiod without displaying phenotypic resemblance to *tic-2*.
* T-DNA insertion lines were not available when the present research was performed and therefore these mutants were not tested.

ATG code	Name	Description
At1g32640	*JIN1*/ *MYC2* [§]	MYC-related transcription factor with a basic helix-loop-helix leucine zipper motif. Its transcription is induced by dehydration stress and ABA treatment. Negative regulator of blue light–mediated photomorphogenic growth and blue and far-red-light gene expression. Regulates JA dependent functions. Negatively regulates Trp metabolism and biosynthesis of Trp derived secondary metabolites. Positively regulates flavonoid biosynthesis, resistance to insects, and response to oxidative stress. Regulates other transcription factors expression.
At4g16780	*HAT4*	Homeodomain-leucine zipper protein that is rapidly and strongly induced by changes in the ratio of red to far-red light. Also involved in cell expansion and cell proliferation and in the response to auxin.
At5g08130	*BIM1* [§]	Basic helix-loop-helix family protein involved in brassinosteroid signalling. It synergistically interacts with BES1 to bind to E box sequences.
At3g01090	*SNRK1.1*/ *AKIN10*	SNF1-related protein kinase that physically interacts with SCF subunit SKP1/ASK1 and 20S proteosome subunit PAD1. Master regulator of energy signalling.
At2g40820	unnamed	Unknown
At1g17760	*CSTF77*	(Cleavage stimulation factor 77) Encodes a homolog of the mammalian protein CstF77, a polyadenylation factor subunit. RNA processing factor of antisense *FLC* transcript. Mediates silencing of the floral repressor gene *FLC*.
At5g43130	*TBP-4* [*]	TATA Binding Protein-associated factor 4. Transcription.
At4g38710	unnamed [*]	Glycine rich protein. Unknown.
At5g05610	*AL1* [*]	Member of the Alfin-Like family of nuclear-localized PhD domain containing homeodomain proteins. Binds to H3K4 di or trimethylated DNA.
At5g55070	unnamed [*]	2-oxoacid dehydrogenase family protein. Involved in response to oxidative stress. Located in cytosol, ribosome and mitochondria.

similarity to their relatives in yeast and mammals, but diverged from plant SnRK2 and SnRK3 (Polge, 2007). Given their similarity, both inducible lines were provided.

In this inducible system, the transgenic lines of the protein kinases *AKIN10* and *AKIN11* are strictly transcriptionally induced upon application of β-estradiol, an estrogen. Besides the resource availability of *AKIN10* transgenic lines, AKIN10 was of interest as it has been involved in energy homeostasis in the night to day transition (Baena-González, 2007). This coincides with TIC time-specific function. Thus both, the availability of these resources and its biological significance made AKIN10 one of the most interesting TIC interacting partners. Thus AKIN10 characterization and its interaction with TIC were tested.

The interaction between the amino terminus of TIC and AKIN10 was confirmed in yeast. For this, a series of 3 deletion fragments of the amino terminus of TIC (1–250, 1-564, 1-770 amino acids) were used (figure III.13 upper panel). This was because the TIC full-length protein and the carboxy terminus of TIC were difficult to express *in vitro*, suggesting these regions were not suited for Y2H studies. Briefly for the Y2H, TIC fragments were fused to the DNA binding domain using the pDEST32 vector and the full length AKIN10 and its homologue kinase AKIN11 were fused to the activation domain using the pDEST22 vector. Both constructs were introduced to yeast strains and the yeast were mated under selective conditions. In these conditions, only if the tested proteins interacted with each other, yeast could grow on an auxotrophic media. As seen in figure III.13B, the transformation of yeast with the empty vectors was not sufficient for promoting growth. Both AKIN10 and AKIN11 supported yeast growth when using the TIC-770 amino fragment and a similar result was obtained with the TIC-564 fragment. However only AKIN10 interacted with the TIC smallest fragment (TIC-250) as seen by yeast growth with AKIN10 and no growth with AKIN11 (figure III.13). In conclusion, this test confirmed TIC interaction with AKIN10 and implied a tighter binding between these than TIC with AKIN11.

Further confirmation of the Y2H interaction between TIC and AKIN10 was obtained through an *in vitro* pull-down assay. For this, a small amino-terminal fragment of TIC protein was fused to a GST tag and the full length AKIN10 to a histidine (His) tag. Both recombinant proteins were incubated together and the mixture was passed over a GST column. After elution, the mixture was separated trough SDS-PAGE electrophoresis. It was observed that both proteins were present and this indicated they could form a complex (figure III.14).

A

Full length, 1550 aa

TIC 1-770, 770 aa

TIC 1-564, 564 aa

TIC 1-250, 250 aa
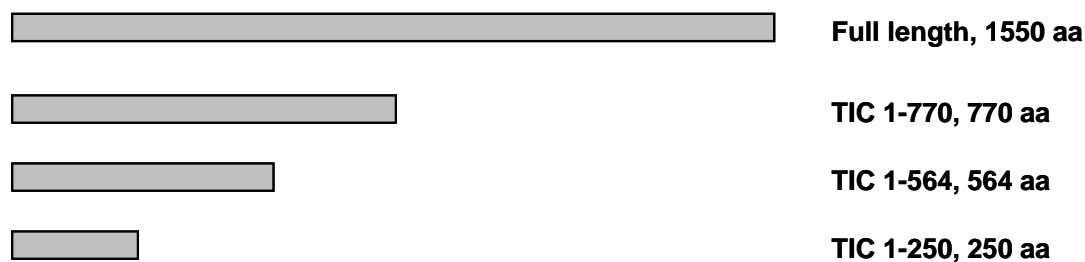
B
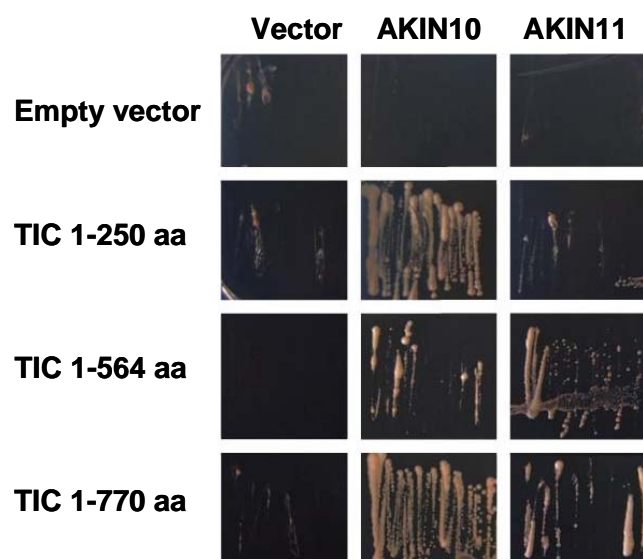
Figure III.13. TIC amino terminus can interact with the kinase AKIN10 in a yeast two hybrid assay.
A) TIC protein deletion fragments used for generating constructs for the yeast two hybrid (Y2H) assay confirmation. The fragment TIC-770 was used for screening the cDNA library by a Y2H assay. TIC full-length sequence is shown as a reference.
B) Yeast two hybrid screen confirmation of the interaction of TIC amino terminus with AKIN10. Even the smallest TIC fragment, TIC-250, was sufficient to interact with AKIN10. Note that both TIC-250 and TIC-750 interaction with AKIN10 allowed yeast growth, while the TIC-250 interaction with the homologue kinase AKIN11 was not sufficient for sustaining yeast growth.
TIC was fused to the DNA binding domain using the pDEST32 vector (bait) and the full-length AKIN10 and AKIN11 to the activation domain using the pDEST22 vector (prey)
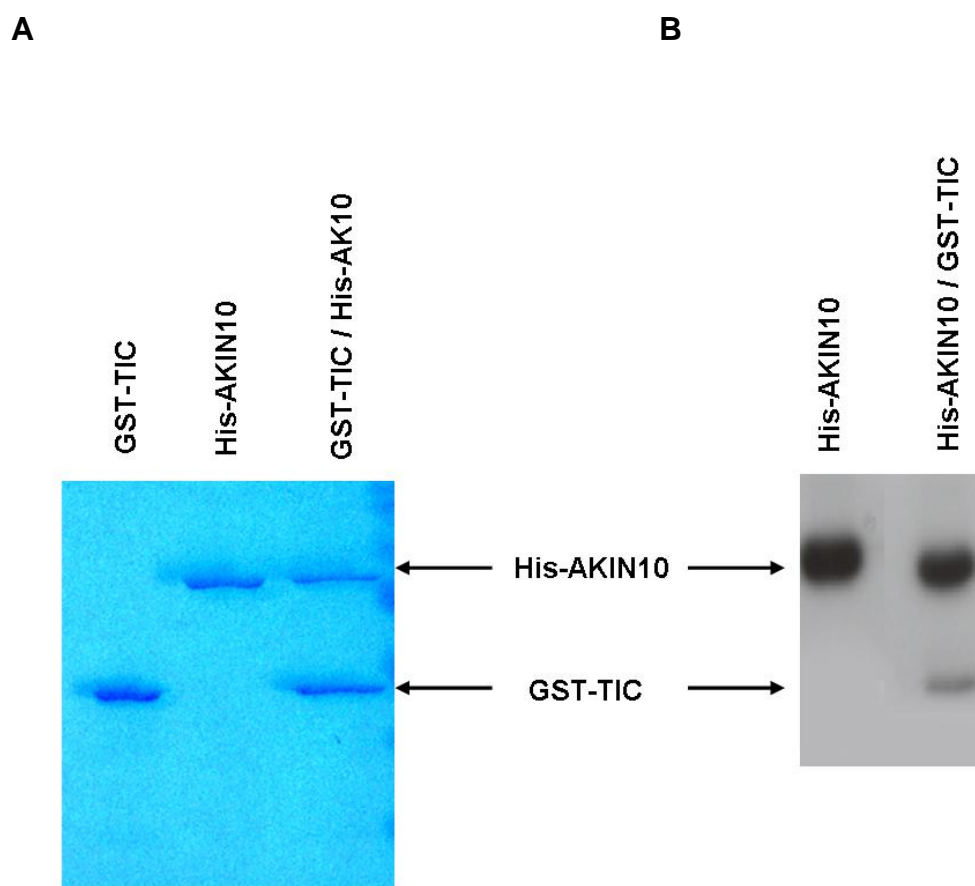
Figure III.14. TIC amino terminus interaction with the kinase AKIN10 was confirmed by *in vitro* pull-down and AKIN10 could phosphorylate TIC in an *in vitro* kinase assay.

A) SDS-PAGE electrophoresis of the pull-down assay between the GST tagged TIC amino terminus fragment and histidine tagged full-length AKIN10.

B) *in vitro* phosphorylation of TIC amino terminus by AKIN10. Autoradiography of ATP radiolabelled proteins after electrophoresis. Due to the kinase autocatalytic activity, AKIN10 appeared with a strong signal as a consequence of high P^{32} incorporation to the protein. The autoradiography revealed a fainter lower molecular weight band corresponding to TIC after phosphorylation by AKIN10.

Note that TIC protein migrated faster as only a fragment of the amino terminus of low molecular weight was used for these constructs.

Once the proteins were shown to interact, the nature of the kinase activity of AKIN10 suggested that it could use TIC as a substrate. To test this hypothesis, both purified recombinant proteins were mixed together and an *in vitro* phosphorylation assay using radioactive ATP was performed. After incubation, proteins were separated by electrophoresis and revealed by autoradiography. A band of higher molecular weight that migrated at the size of AKIN10 was found. This band was a product of the AKIN10 autocatalytic kinase activity as it contained radiolabelled ATP. When the recombinants proteins were incubated together, a band of lower molecular weight was also revealed by autoradiography, demonstrating that AKIN10 could trans-phosphorylate TIC amino fragment (figure III.14). This result indicated that *in vitro* conditions TIC could serve as a substrate for AKIN10. Therefore from these *in vitro* studies it was suggested that AKIN10 interaction with TIC could led to a mechanism of TIC action through phosphorylation.

2) AKIN10 activity affected clock period and this effect was TIC dependent.

AKIN10 was demonstrated to interact with TIC in a Y2H assay, as well as by an *in vitro* pull down, and that TIC could act as substrate for AKIN10. These results suggested that AKIN10 could affect the circadian clock through TIC. To study the physiological role of AKIN10 on the clock, the homologue kinases AKIN10 and AKIN11 were assessed for their effect on clock periodicity. Besides their sequence similarity, both kinases share functions as central regulators in response to darkness and stress (Baena-González, 2007). Therefore though it was found by Y2H that TIC interacted with AKIN10, but not to the same extent with AKIN11 (figure III.13), both kinases were evaluated in regard of the clock. For this, estradiol inducible lines of the catalytic subunit of the kinases were crossed to lines harbouring the *CCA1:LUC* luciferase construct. Then as mentioned above, the transcriptional induction of the kinases could be specifically triggered by the addition of β-estradiol. For monitoring clock rhythms, the *CCA1:LUC* was selected as a reporter because the mRNA levels of *CCA1* were not found to be different between *tic-2* and wild type (table III).

To test the effect of AKIN10 and AKIN11 on the clock, seedlings were transferred to control media or media added with β-estradiol. After one day of entrainment, the seedlings were released into constant light conditions. As long as the kinases were not induced, the *CCA1:LUC* reporter showed no difference on period length, nor the waveform of the rhythmic oscillation (figure III.15A). To test the effect of the induction of kinases on
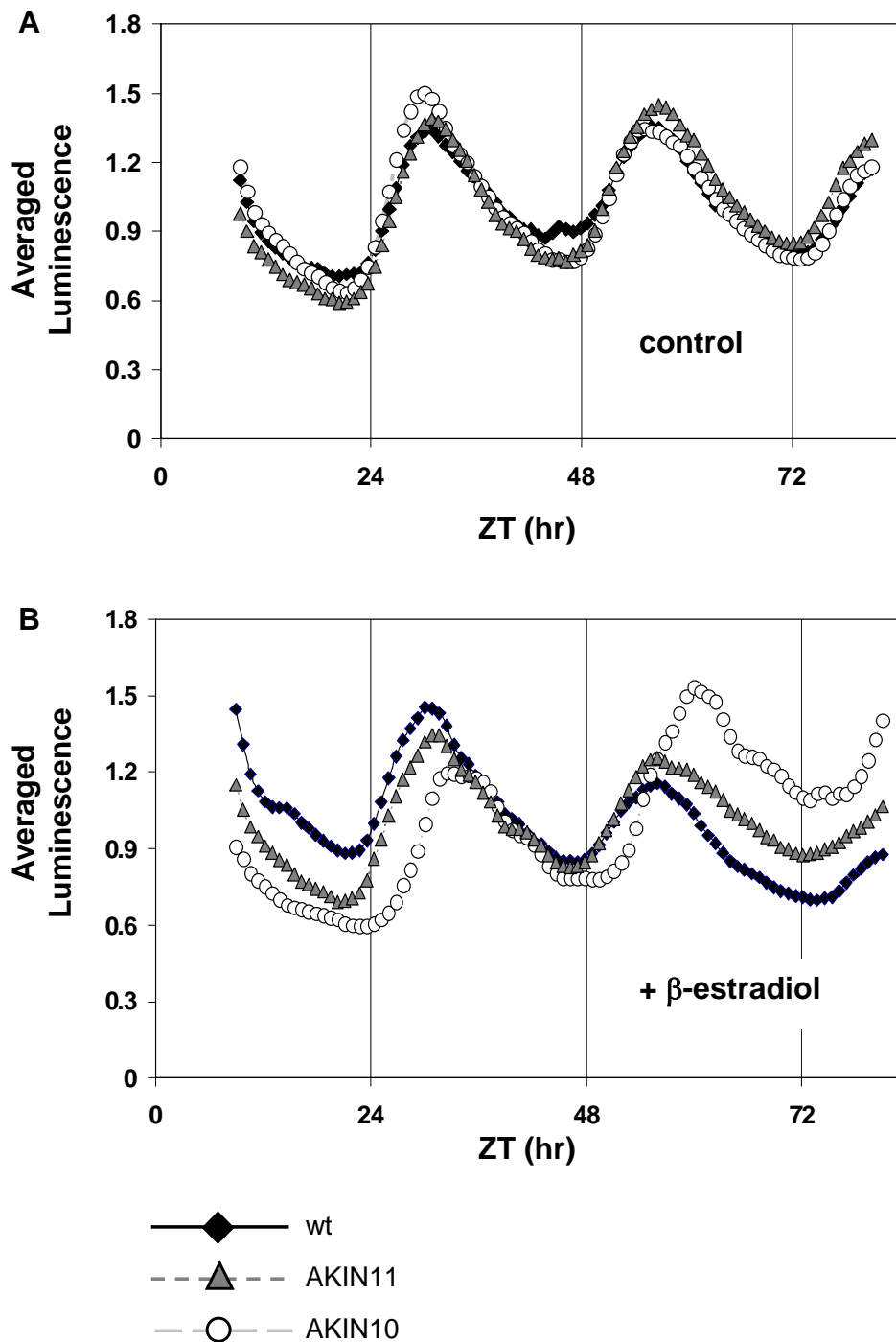
Figure III.15. The induction of the SNF1 related kinase AKIN10, but not AKIN11 lengthened clock periodicity.
A) *CCA1:LUC* luminescence rhythms of wild type (wt), *AKIN10* and *AKIN11* under constant light.
B) *CCA1:LUC* luminescence rhythms of wild type, *AKIN10* and *AKIN11* under constant light after transcriptional induction of the protein kinases with 5 μM β-estradiol. Induction of *AKIN10* (white circles), but not *AKIN11* (gray triangles), caused a lengthening effect on clock periodicity.

the circadian-clock driven rhythms, wild type and the *AKIN10* and *AKIN11* transgenic lines were exposed to media with β-estradiol. Addition of the β-estradiol did not affect wild-type *CCA1:LUC* expression (figure III.15B). Thus the addition of the chemical *per se* did not alter the clock. Interestingly induction of AKIN10 led to a lengthening of the period, indicating that the kinase could affect the circadian clock (figure III.15). On the other hand, after exposure of AKIN11 to β-estradiol, no effect on the clock period was observed. From these results, I concluded that only the induction of the *AKIN10*, but not *AKIN11* provoked a lengthening of clock periodicity (figure III.15B).

As TIC was found to interact with AKIN10 and the later to have an effect on the clock, I hypothesized that AKIN10 effect on the clock would be through the activation of TIC. To test this, transgenic lines of *tic-2* harbouring the *CCA1:LUC* construct were crossed to the β-estradiol inducible *AKIN10* lines and the triple *tic-2*/*AKIN10*/*CCA1:LUC* transgenic line was isolated. Then 7 day old seedlings of the triple transgenic with its respective controls were transferred to control and β-estradiol added media and released into constant light after one further day of entrainment. As seen from figure III.16, under non inductive conditions, I found that *AKIN10* presented a period as wild type with robust oscillations of *CCA1:LUC* driven expression as was observed before (figure III.15). Both *tic-2* and *tic-2/AKIN10* displayed a low amplitude expression of *CCA1:LUC* that tended to arrhythmia (figure III.16). Upon induction and as stated above, wild type was not perturbed and *AKIN10* displayed a lengthening effect of the period (figure III.16B, for clarity the data has been replotted in figure III.16C). Interestingly the *AKIN10* lengthening effect on the period was not observed in *tic-2/AKIN10*, as this line had a similar pattern of *CCA1:LUC* expression as *tic-2* single mutant (figure III.16B). This can be clearly observed in figure III.D and E by comparing the period length of *AKIN10* with or without β-estradiol induction to that of the wild type and to the double mutant *tic-2/AKIN10* under the same conditions. Therefore from these experiments, I concluded that AKIN10 effect on clock period was dependent on *TIC*.

A

B
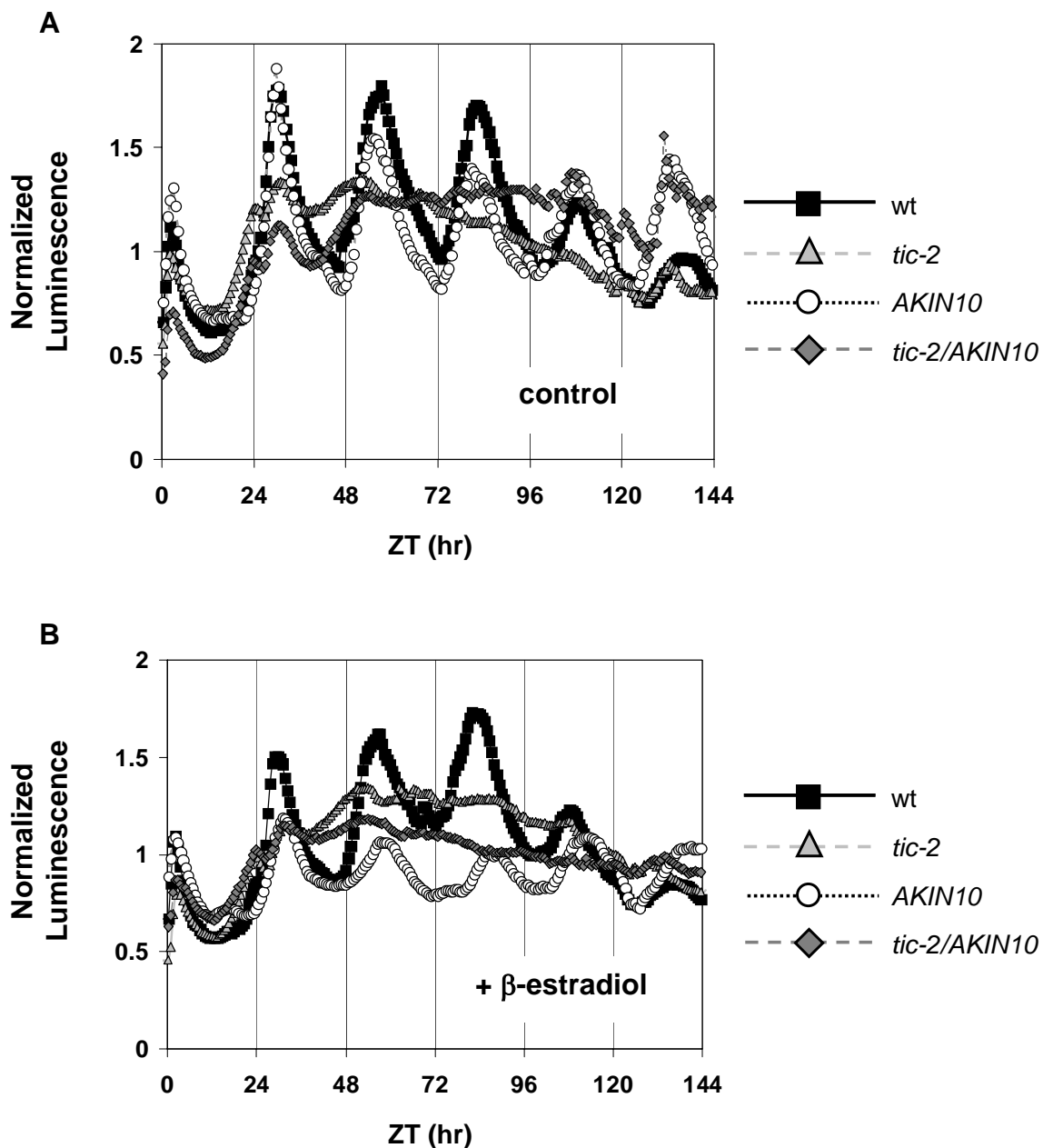
Figure III.16. The clock period lengthening effect by the induction of AKIN10 required TIC.
A) *CCA1:LUC* luminescence rhythms of wild type (wt), *tic-2*, *AKIN10* and *tic-2/AKIN10* under constant light.
B) *CCA1:LUC* luminescence rhythms of wild type, *tic-2*, *AKIN10* and *tic-2/AKIN10* under constant light after transcriptional induction of the kinase with β-estradiol.
The first 24 hr shown belong to an LD cycle before transfer to constant light after ZT 24.

C

D

E
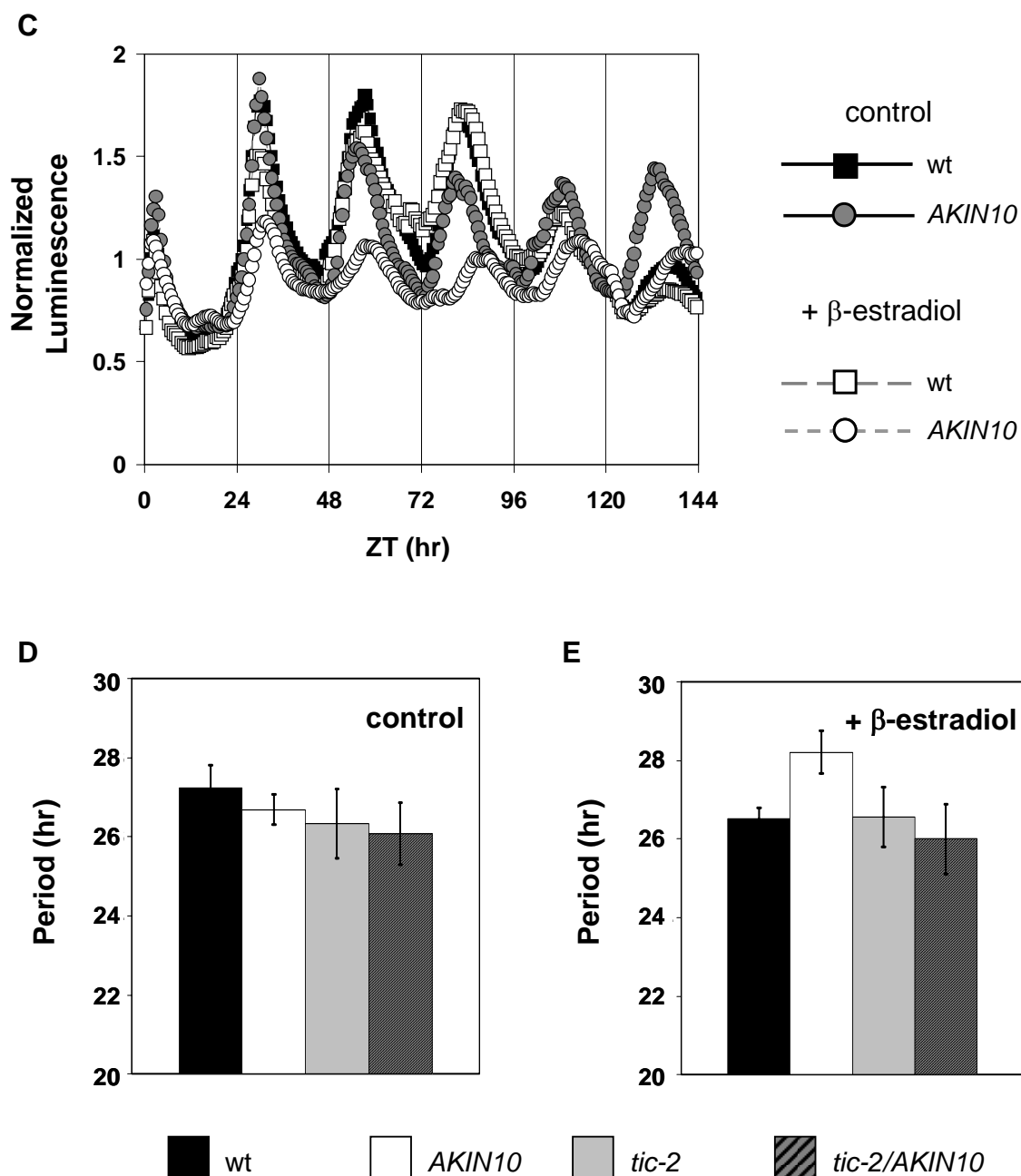
Figure III.16 (continuation). The clock period lengthening effect by induction of AKIN10 required TIC.

C) Data of wild type and *AKIN10* with (white figures) and without (full figures) addition of β-estradiol re-plotted from B and A respectively. Notice that the graphs overlap each other with exception of the induced *AKIN10* (white circles).

D and E) Periods estimates of *CCA1:LUC* rhythms by FFT-NLLS analysis with (E) and without (D) addition of β-estradiol. Note that the transcriptional induction of *AKIN10* lengthened the period compared to wild type (white *vs.* black bars), and that this effect required TIC (dark gray hatched bars).

Error bars indicate standard error from a population between 28 to 48 plants per treatment.

III.C. The TIC-like gene, *TICKLE*, (*TKL*) was not found to have a role in the circadian clock period rhythms.

       As many plants have experienced several genome duplications over evolutionary time, groups of genes with a high degree of similarity are often present in their genomes. Commonly these gene families diverged from a homologous ancestor. Some genes acquired new functions, but many others had redundant or partially redundant functions. Because *TIC* was described as a gene product that encodes for a protein of unknown function, TIC protein sequence was analyzed through a BLAST search with the aim to detect related sequences (Ding, 2007). It was found that *TIC*, which encodes for a hypothethical protein of 1550 amino acids, was restricted to the plant kingdom. Furthermore, it was shown that *TIC* is a single gene in the *A. thaliana* genome and the only paralog sequence with similarity to *TIC* was termed *TICKLE (TKL)*, an acronym derived from TIC-like (Ding, 2007). As these two genes displayed sequence similarity, it was suggested that TKL could have a role within the circadian clock. Here I present efforts to assess if TKL could have either an independent or overlapping function with TIC in regard of the circadian clock.

1) Expansion of the phylogenetic relationship of TIC like sequences.

       Considering that the availability of genomes and sequences has increased in the last years, I performed a new search for sequences related to *TIC*. Using the translated *TIC* sequence, I ran a BLAST search through all available sequence data from NCBI. I found that the only significant matches were from sequences from the plant kingdom. I found TIC-like sequences within all the Viridiplantae, ranging from black cottonwood (poplar) and castor oil, to grape, rice and wheat and even the common moss (figure III.17). Unfortunately though cucumber, papaya, maize, algae and other plant species genomes have been sequenced in the last years (www.ncbi.nlm.nih.gov/genomes/PLANTS and (www.phytozome.net), TIC-like sequences from these genomes have not yet been annotated.

       The retrieved sequences were aligned by using ClustalW from the Kyoto University Bioinformatics Center (http://align.genome.jp/) and by ClustalW2 from the European Bioinfromatics Institute (EBI) a division of the European Molecular Biology Laboratory (EMBL) (http://www.ebi.ac.uk/Tools/clustalw2/index.html). Both multiple

A
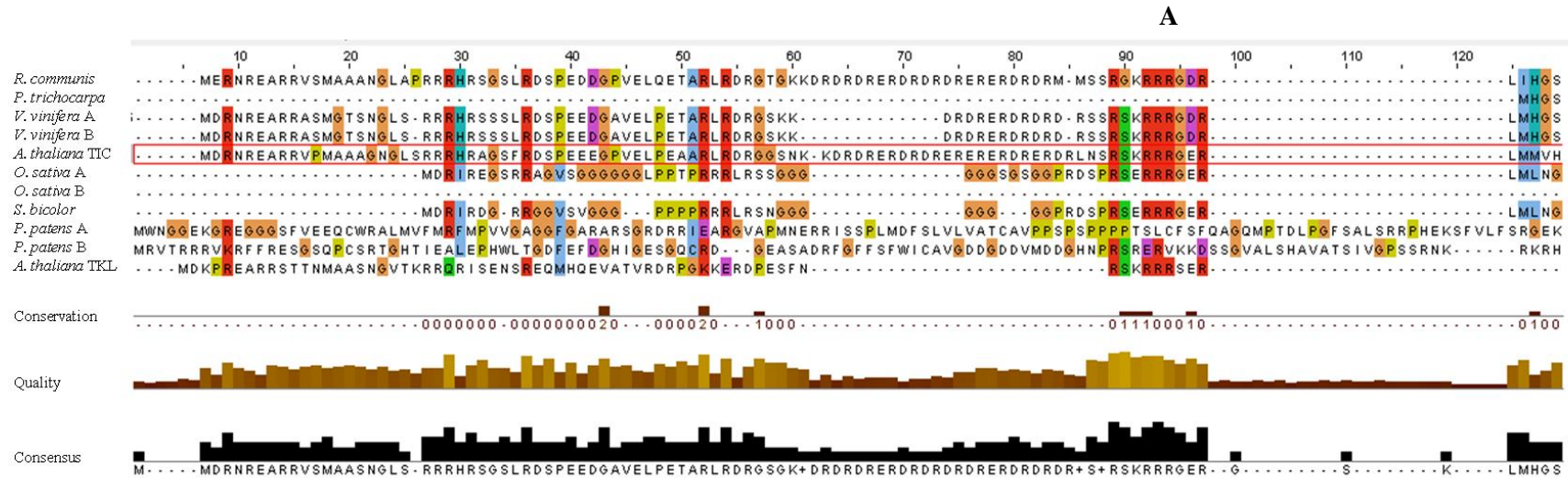
Figure III.17A. Alignment of *TIC* translated sequence and TIC related sequences.
TIC sequence is indicated with a red box. At the bottom of the alignment, bars indicating the degree of conservation between sequences, quality of the alignment per residue and a consensus sequence (from top to bottom respectively) are provided. Numbers bellow the conservation bars reflect the degree of variability for each amino acid residue. 0 = No conservation, 9 = high conservation, * = 100% conservation. The degree of amino acid conservation and the quality are also indicated with a scale colour from dark brown to yellow indicating 0 to 100% identity between the presented sequences. At the top of the alignment, numbers indicate the amino acid residue based on the consensus sequence.
Block A (see discussion)

Arabidopsis thaliana (thale cress) TIC and TKL, *Ricinus communis* (castor oil plant) putative ATP binding protein (XP_002516769.1), *Vitis vinifera* (grape) predicted and unnamed protein (XP_002277982.1 (A) and CBI26227.1 (B), respectively), *Populus trichocarpa* (black cottonwood or balsam poplar) predicted protein (XP_002311616.1), *Oryza sativa* (rice) hypotetical protein OsJ_24809 (A) and Os07g0571100 (B), *Sorghum bicolor* (sorghum) hypotetical protein 02g036890, *Physcomitrella patens* (common moss) predicted proteins XP_001760051.1 (A) and XP_001758408.1. (B).
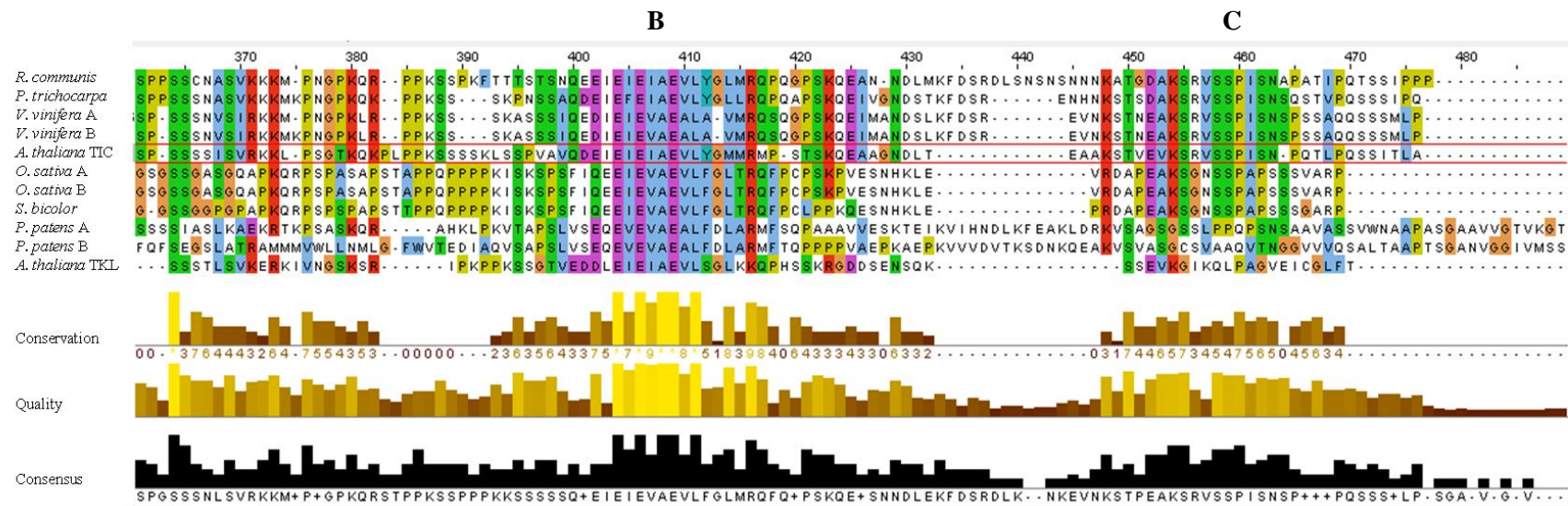
Figure III.17B. Alignment of *TIC* translated sequence and TIC related sequences (continuation).

A fragment of the sequences alignment between amino acids 365 and 485 is shown.

TIC sequence is indicated with a red box. For legends and features below the alignment see figure III.17A.

Note that TIC serves as bridge for the conservation of amino acids residues between the eudicotyledons and the monocotyledons, which are located above and below TIC sequence, respectively. All sequences from tracheophytes were separated from those of briophytes with exception of *A. thaliana* TKL sequence.

Note segments of high conservation scattered between highly divergent areas.

Block B and C (see discussion).

Arabidopsis thaliana (thale cress) TIC and TKL, *Ricinus communis* (castor oil plant) putative ATP binding protein (XP_002516769.1), *Vitis vinifera* (grape) predicted and unnamed protein (XP_002277982.1 (A) and CBI26227.1 (B), respectively), *Populus trichocarpa* (black cottonwood or balsam poplar) predicted protein (XP_002311616.1), *Oryza sativa* (rice) hypotetical protein OsJ_24809 (A) and Os07g0571100 (B), *Sorghum bicolor* (sorghum) hypotetical protein 02g036890, *Physcomitrella patens* (common moss) predicted proteins XP_001760051.1 (A) and XP_001758408.1. (B).

D
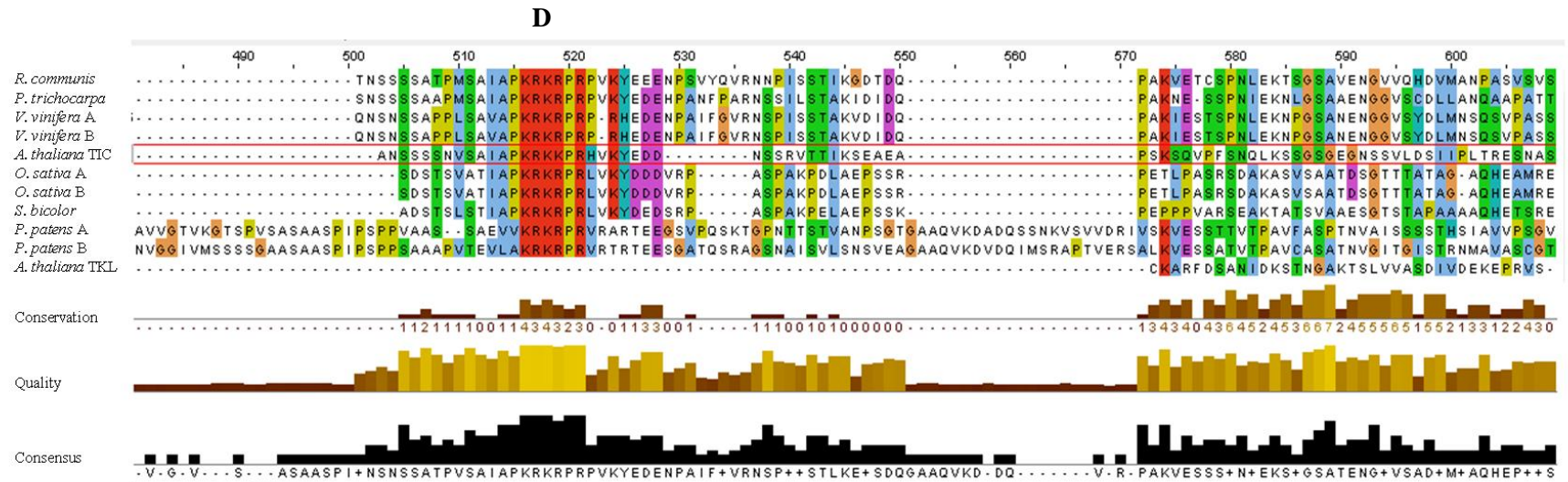
Figure III.17C. Alignment of *TIC* translated sequence and TIC related sequences (continuation).
A fragment of the sequences alignment between amino acids 485 and 605 is shown.
TIC sequence is indicated with a red box. For legends and features below the alignment see figure III.17A.
Note that as *P. patens* proteins were larger, several areas of the alignment only contain these sequences creating gaps in the alignment.
Also in this region is clear that TKL do not posses a block highly conserved between all the other species (amino acids 500 to 550).
Block D (see discussion)
Arabidopsis thaliana (thale cress) TIC and TKL, *Ricinus communis* (castor oil plant) putative ATP binding protein (XP_002516769.1), *Vitis vinifera* (grape) predicted and unnamed protein (XP_002277982.1 (A) and CBI26227.1 (B), respectively), *Populus trichocarpa* (black cottonwood or balsam poplar) predicted protein (XP_002311616.1), *Oryza sativa* (rice) hypotetical protein OsJ_24809 (A) and Os07g0571100 (B), *Sorghum bicolor* (sorghum) hypotetical protein 02g036890, *Physcomitrella patens* (common moss) predicted proteins XP_001760051.1 (A) and XP_001758408.1. (B).
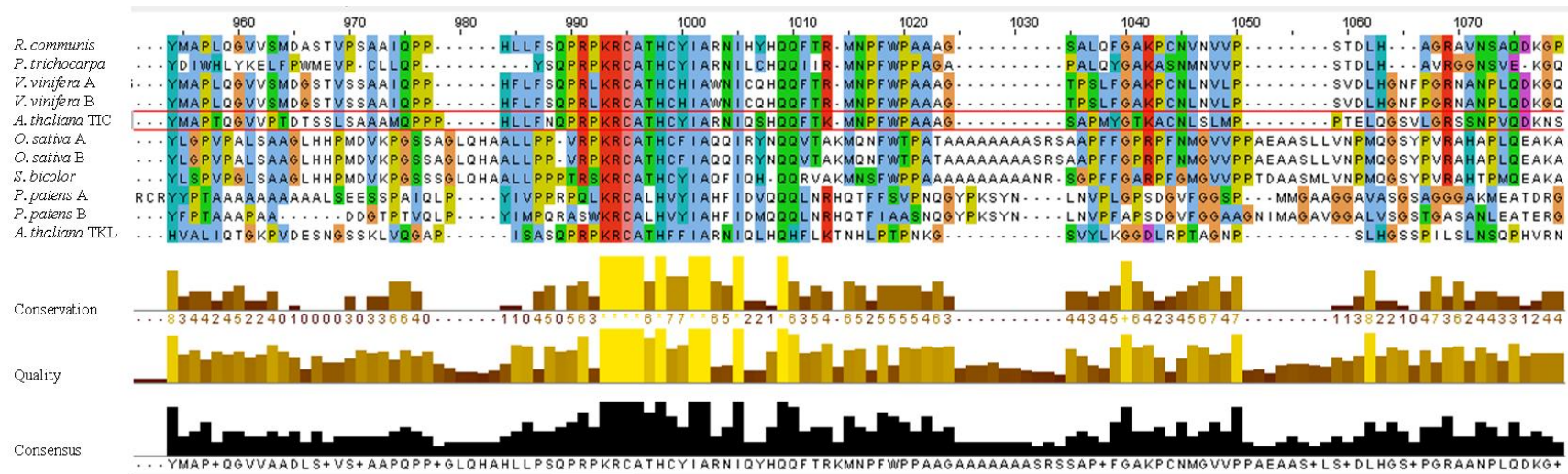
Figure III.17D. Alignment of *TIC* translated sequence and TIC related sequences (continuation).
A fragment of the sequences alignment between amino acids 955 and 1075 is shown.
TIC sequence is indicated with a red box. For legends and features below the alignment see figure III.17A.
Note that the sequences from the eudicotyledons do not posses small blocks present in the monocotyledons (965 to 984, 1024 to 1035 and 1052 to 1060).
Block E (see discussion).
Arabidopsis thaliana (thale cress) TIC and TKL, *Ricinus communis* (castor oil plant) putative ATP binding protein (XP_002516769.1), *Vitis vinifera* (grape) predicted and unnamed protein (XP_002277982.1 (A) and CBI26227.1 (B), respectively), *Populus trichocarpa* (black cottonwood or balsam poplar) predicted protein (XP_002311616.1), *Oryza sativa* (rice) hypotetical protein OsJ_24809 (A) and Os07g0571100 (B), *Sorghum bicolor* (sorghum) hypotetical protein 02g036890, *Physcomitrella patens* (common moss) predicted proteins XP_001760051.1 (A) and XP_001758408.1. (B).

sequence alignments tools resulted in similar alignments. Fragments of the alignment obtained from the EBI are displayed in figure III.17. Several interesting features were observed in this alignment. This included that *A. thaliana* TIC sequence was positioned between the sequences from eudicots and monocots and that TKL lay away from all the group of vascular plants. The degree of conservation between monocotyledoneans and dicotyledoneans was higher within their members than between these groups. Despite this clear divergence, the sequences shared blocks of amino acid residues highly conserved and some amino-acid identities (see discussion for further details). Furthermore the sequences of cereals presented stretches of residues exclusive to this group (figure III.17D). It was also noted that the sequences from the briophytes, represented by the common moss, were larger and therefore created gaps in the alignment.

The multiple sequence alignment was followed by the generation of a phylogenetic tree. This tree showed an evolutionary pattern that revealed the characteristics above described from the alignment. The first land plants, the mosses represented by *Psycomitrella patens*, exhibited a clear separation from the tracheophytes, within the later monocotyledons and dicotyledons demonstrated their expected divergence (figure III.18). The phylogenetic tree also revealed that TIC and TKL could share a common ancestor, but that since the duplication that originated the vascular plants, these proteins diverged. Furthermore all TIC-like sequences from the tracheophytes were found to be more similar to TIC than to TKL. Summarizing this bioinformatic analysis indicated that TIC and TKL could have acquired different functions in *A. thaliana* as they have diverged through evolution.

2) *TKL* does not have a role in the circadian clock.

TIC is essential to maintain circadian rhythms. As several components of the *A. thaliana* circadian clock share partially redundant activities, it was possible that *TIC* and *TKL* could share partially overlapping functions within the clock. To assess if *TKL* could have a role in the circadian clock, T-DNA insertion mutants from the SALK (SALK_028176; *tkl-1*) and SAIL (SAIL_714 A02; *tkl-2*) collections were acquired (figure III.19). Homozygous lines for *tkl-1* and *tkl-2* were obtained and analysed macroscopically and for their clock rhythms. The phenotype of both *tkl-1* and *tkl-2* single mutants was evaluated by growing them under short and long days. Under these conditions, both

Figure III.18. Phylogenetic tree of TIC related sequences.
The sequences were aligned using CLUSTALW2 from the website EMBL-EBI
(http://www.ebi.ac.uk/Tools/clustalw2/index.html). From the derived alignment results, a
phylogentic three was constructed.
The phylogram displayed the divergence observed in the alignment. Nodes separating
briophytes from tracheophytes and dicotyledons from monocotyledons are clearly
established. TKL sequence appeared as an outlier in this arrangement indicating early
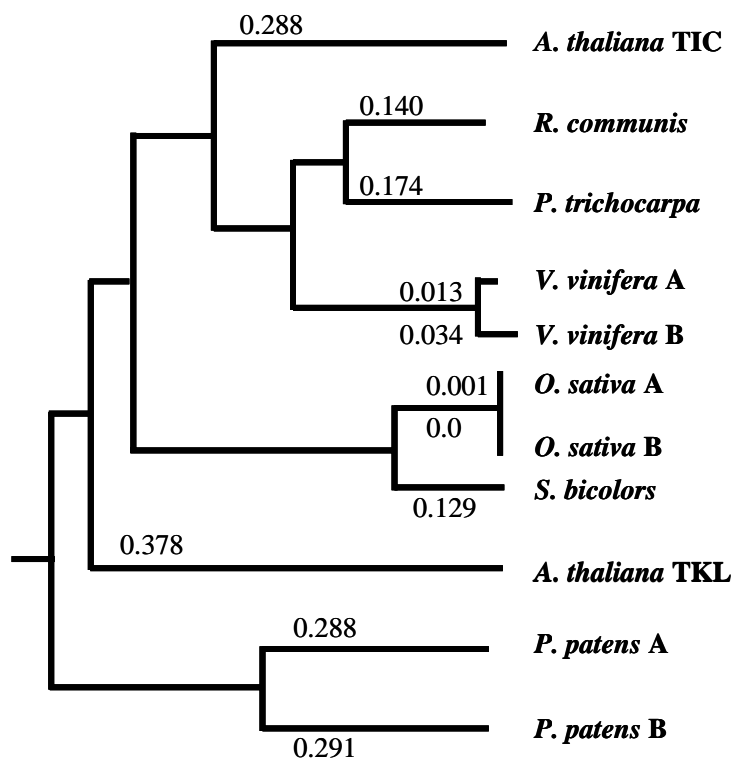divergence within the *A. thaliana* genome before the separation of tracheophytes.

Arabidopsis thaliana (thale cress) TIC and TKL, *Ricinus communis* (castor oil plant)
putative ATP binding protein (XP_002516769.1), *Vitis vinifera* (grape) predicted and
unnamed protein (XP_002277982.1 and CBI26227.1, respectively), *Populus trichocarpa*
(black cottonwood or balsam poplar) predicted protein (XP_002311616.1), *Oryza sativa*
(rice) hypotetical protein OsJ_24809 and Os07g0571100, *Sorghum bicolor* (sorghum)
hypotetical protein _02g036890, *Physcomitrella patens* (common moss) predicted proteins
XP_001760051.1 and XP_001758408.1.

The numbers indicate nucleotide substitution rate. The smaller is the value, the higher is the
similarity between the sequences within the branch.
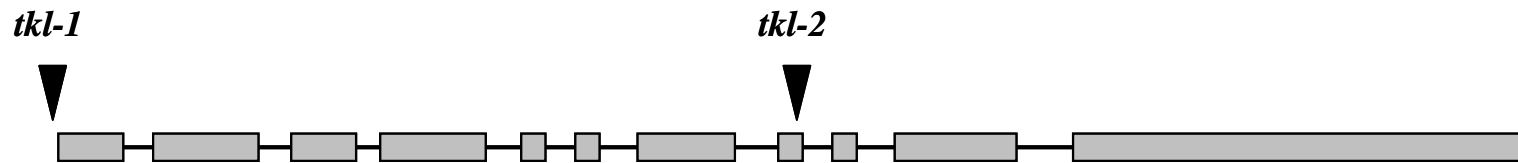
Figure III.19. *TKL* gene structure.
TKL sequence has a length of 3238 nucleotides divided in 11 exons. The encoded hypothethical protein has a length of 978 amino acids.
Two T-DNA insertion lines, SALK_028176 and SAIL_1285_H12, termed *tkl-1* and *tkl-2* were analyzed in this study. As seen in the diagram, the insertions are located between the promoter and first exon and between exons the 8th and the 9th exon for *tkl-1* and *tkl-2*, respectively.

mutants presented a phenotype as the wild-type plants. This indicated that *TKL* did not have a role in the developmental programme.

As neither *tkl-1* nor *tkl-2* showed developmental alterations, only *tkl-1*, which has an insertion between the promoter and the first exon (figure III.19), suggesting it is a stronger allele, was evaluated for its clock-driven luciferase expression. For this, the *tkl-1* lines were crossed to lines harbouring the luciferase gene under the promoter of clock controlled genes as *CAB* and *CCR2*. Circadian rhythms of established homozygous lines were studied by shifting the plants from cycling light/dark conditions to constant light or darkness. I found that *tkl-1* did not reveal any circadian defects. I observed that *tkl-1* did not exhibit an effect on period nor phase compared to wild type with both *CAB* and *CCR2* luciferase reporters, while *tic-2* showed the described low amplitude rhythm (figure III.20). This result suggested that *tkl-1* could be dispensable for the clock.

As *TKL* function could be partially redundant with *TIC*, but masked by the later, a double mutant between both genes was generated. This could uncover any subtle effects of *tkl* that would be rescued by a functional *TIC*, either in plant growth or within the clock. However I observed that under green house conditions, the double mutant *tic2/tkl-1* did not exhibit any visible phenotypic difference to *tic-2* single mutant (not shown). Consequently further analyses on *tkl* mutants were not further pursued, as all the gathered data suggested that TKL and TIC have no related functions within the circadian clock of *A. thaliana*.

A

B
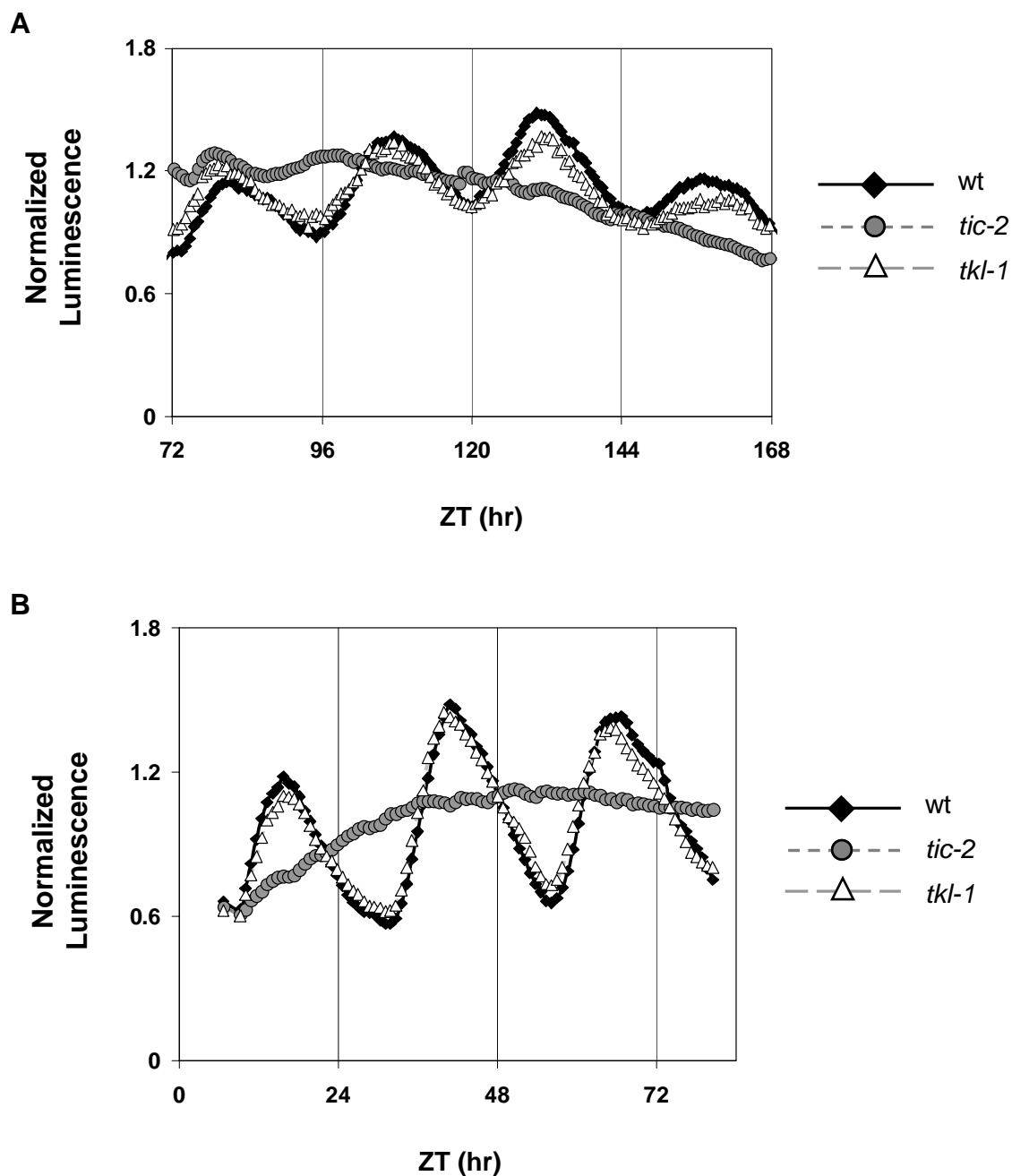
Figure III.20. TIC-like gene, *tickle* (*tkl*), was not found to have effects on the circadian rhythms of *CAB:LUC* and *CCR2:LUC* expression.
A) *CAB:LUC* luminescence rhythms of wild type (wt), *tic-2* and *tkl-1* under constant light after transferring seedlings to MS3 media.
B) *CCR2:LUC* luminescence rhythms of wild type, *tic-2* and *tkl-1* in constant darkness after transferring seedlings to MS3 media.
tkl-1 did not show any circadian defects either under constant light or darkness. *tkl-1* rhythm resembled that of wild type (compare white triangles with black diamonds).
The plotted data was either under constant light (A) or constant darkness (B) for at least 24 hr prior the recording of the shown data.

IV. Discussion

TIC was described as a nuclear component of the circadian clock that is necessary for maintaining clock-driven rhythms (Hall, 2003, Ding, 2007). In the absence of a functional *TIC*, circadian rhythms displayed shorter periods, a lower amplitude and an early phase of expression. Both the early phase of gene expression and the shorter period coincided with *tic* dysfunctional clock being reset late at night (Hall, 2003). The expression of the clock genes examined was advanced in *tic*, but without affecting their expression levels, with exception of *LHY*. The finding that *LHY* expression was constitutively low in *tic*, led to the conclusion that *TIC* participated in mediating differentially the expression of *CCA1* and *LHY* (Ding, 2007). Though the circadian defects shown by *tic* indicated that it should work close to the central oscillator, the mechanism by which *TIC* could confer its action within the oscillator remained obscure.

To expand on *TIC* function within the oscillator, I performed a transcriptomic analysis taking into account that *tic* clock stops just before dawn. Consequently the experimental design consisted in two sampling time-points: the dawn-anticipation assay in which seedlings were collected prior to the shift to the light period and the clock-resetting assay in which plants received a light pulse during the night causing a "jetlag" (figure II.1 I-A). Through the dawn-anticipation assay, I expected to find those genes affected by the clock arrest in *tic*. As light is the main environmental cue that entrains the clock, with the clock-resetting assay, I tested the effect of light in clock entrainment and its dependence on *TIC*. As the clock in *tic* would restart earlier than the wild type, the responses to light entrainment could be influenced by their respective physiological and transcriptional programme. Furthermore as *tic* presented a stress-like phenotype, the transcript profile allowed me to reveal the alteration of several metabolic processes probably associated with its phenotype. Through this work, I found that *tic* was hypersensitive to ROS and ABA, had altered starch metabolism, as well as defects in abiotic and biotic stress responses. Furthermore a plausible mechanism for *TIC* function was established by its interaction with the kinase AKIN10, as the activity of the later on the clock was dependent of *TIC*. This mechanism would involve the sensing of the cellular metabolic status by AKIN10, which would activate TIC, and consequently the later could exert its function in the clock entrainment to dawn.

Microarray expression profile

General overview

The microarray analysis included four separate array experiments, and consequently, the same number of pair-wise expression profiles examinations. From the four possible comparisons between the two experimental conditions and the two genotypes (figure II.1-II), the work that I present here mainly focused on the mutant *versus* wild-type comparisons under both physiological conditions: dawn anticipation and clock resetting. The microarray transcript profile analysis gave a general panorama of the behaviour of wild type and *tic-2* under the physiological conditions tested. The Principal Component Analysis (PCA) provided the first insight into the transcriptional changes that occurred between the genotypes and the conditions. At first glance, it seemed striking that the physiological conditions (resetting *versus* dawn) had a major effect, and therefore, importance in the transcriptome changes (figure III.1A). However the result was logical because the experimental conditions can be viewed as light *versus* dark, conditions that would lead to a drastic transcriptional switch. The gene expression changes would be a consequence of the direct light induction of gene expression, as well as of the controlled gene expression by the circadian clock after the later was reset. Thus not surprisingly, the number of genes that were found as differentially expressed by comparing a single genotype between both experimental conditions was higher than when comparing both genotypes in a single condition (figure III.1B).

I found that *tic-2* transcriptional profile was different from the wild type, regardless of the conditions. This was suggested from the distance between the genotypes in the component 2 of the PCA (figure III.1A). This result indicated that regardless of time and environmental conditions, *tic-2* had a gene expression pattern that differed from wild type. Nonetheless, the resetting of the clock caused a higher increase in the number of genes differentially expressed in *tic-2* than in the wild type. This was clearly seen in the PCA component 1, as a longer distance separated the light treated samples to those kept in the dark in the *tic-2* background (compare the distance between the white and black symbols in figure III.1A in both genotypes). This observation was reflected in the Venn diagrams as *tic-2* expression profile presented around ~3,000 genes differentially expressed, while the wild type displayed a change in only ~2,000 (figure III.1B right panel). The response of *tic-2* to the clock resetting suggested that the alteration of its clock did not impair clock

light entrainment nor light responses. However *tic*-2 response toward light was exacerbated as seen by the quantity of genes differentially expressed compared to wild type. This could be taken as an indication that *tic-2* required a major transcriptional reprogramming to cope with environmental changes. Thus *tic-2* seemed to be a hypersensitive mutant to a light environmental change.

Clock genes expression in *tic-2*.

As *tic* is a circadian clock mutant, I first analysed the gene expression profile of clock and clock related genes. Not surprisingly, many clock genes to date described were misregulated between *tic-2* and wild type (table III). Most of the genes, with exception of *LHY* and *FLC*, were upregulated in *tic-2* (table III, *tic-2 versus* wt comparisons). Evening genes such as *TOC1*, *GI*, *LUX*, *ELF3* and *CHE* were overexpressed in *tic-2*. This result was contradictory with previous analysis where Ding *et al.* (2007) described that the mean expression levels of evening genes as *TOC1*, *GI* and *ELF3* were not altered in *tic*. The difference between these results could be the time-points of both analyses, as I studied gene expression prior to dawn and Ding *et al.* (2007) made a time course. Then it is possible that the microarray profile studied here coincided with the peaks of gene expression in *tic* which has an early phase of gene expression (Ding, 2007). However the differences in gene expression before dawn reported by Ding *et al.* (2007) were subtle compared to the fold-change reported here (table III). Additionally it is also possible that the differences were a consequence of the ecotype, as in the published work Ws-2 (*tic-1* allele) was used and the profile that I examined was in Col-0 (*tic-2* allele).

Besides the overexpression of the evening genes described above, the comparison of gene expression between *tic-2* and wild type showed that *PRR9*, *PRR7* and *PRR3* were overexpressed in *tic-2* (table III). The arguments mentioned above about the microarray time-points coinciding with the peaks of expression or the background effects could also apply to the overexpression of the *PRR* gene family. However only the expression of *PRR9* was analysed previously, and it was found that *PRR9* expression in *tic-1* was identical to wild type (Ding, 2007). Another gene not previously analysed, which I found differentially expressed in *tic-2* was *LUX*, also known as *PHYTOCLOCK* (table III). This finding was interesting as *LUX* encodes for a Myb-like transcription factor related in sequence to *CCA1* and *LHY*, but whose expression is evening phased (Hazen, 2005). Though the sequences of DNA that LUX bind still are unknown, the overexpression of this gene could be partially

responsible for the clock gene misexpression in *tic-2*. Contrary to *tic-2* short hypocotyls and delayed flowering, it was reported that *lux* resulted in a long hypocotyls and early flowering (Hazen, 2005), therefore *tic* and *lux* display opposite phenotypes.

The transcript profiles from the clock-resetting *versus* dawn-anticipation comparisons showed that *GI*, *PPR9* and *PRR7* were induced by light (table III). These genes have been suggested as light-input elements to the clock as their expression is responsive to light (Locke, 2006). Finding that *GI*, *PPR9* and *PRR7* could be transcriptionally induced in both genotypes in the clock resetting-assay, suggested that clock light responsiveness was not altered in *tic-2*. Thus these genes might still work as light-integrating components to the circadian clock in *tic-2*. This clock-gene light responsiveness indicated that the clock in *tic-2* could be entrained, albeit with defects. Therefore *tic-2* defects in the clock do not impair its capacity to respond to a light environmental change.

In conclusion, most of the clock genes from the current clock model were misexpressed in *tic-2*. From these the vast majority was overexpressed in *tic-2* compared to the wild type. This could be due to an early phase of expression of *tic-2*.

Gene Ontology Overview

The enrichment of gene ontology (GO) categories derived from the differentially expressed genes provided a panorama of the altered transcript profile of *tic-2* (table IV). I found that *tic-2* had a different expression profile to stress responses and environmental cues. Based on the results, I decided to investigate *tic* physiology to characterize the mutant beyond its clock phenotypes. At the same time, this analysis provided an insight into the pervasiveness of the circadian clock in development and the stress-like phenotype of *tic*. This included a slow growth rate and leaf serration.

In the next sections I will discuss the results obtained through this characterization that demonstrated that *tic* mutation causes an array of pleiotropic phenotypes.

Nucleotide metabolism and transcription

Several GO categories related to DNA, transcription, and nucleic-acid metabolism were highlighted in *tic-2* profile (table IV). These GO terms correlated with the change of expression of multiple genes involved in these processes, as well as with the expression of transcription factors (table V). Among these genes, *PAB5* and *ZWILLE/AGO10* have been described in mRNA translation, processing and degradation (Belostotsky, 2003), and in

miRNA translational repression (Brodersen, 2008), respectively. Furthermore it was shown that an *ago10* mutant had higher levels of cupper superoxide dismutase (*CSD2*) mRNA (Brodersen, 2008). Interestingly *tic-2* transcription profile had high levels of *AGO10* mRNA, which in turn will partly explain the repression of the transcription of *CSD2* (table V). In the case of *PAB5*, its transcription has been shown to be limited to reproductive tissues and developing seeds (Belostotsky, 2003). Therefore it was striking to find it highly expressed in *tic-2*. It is tempting to speculate that *TIC* may be involved in the silencing or specific repression of *PAB5*. Besides these two particular genes, many ribosomal subunits, as well as RNA polymerases, in particular the sigma subunit of chloroplasts RNA polymerases, were misregulated (table V). Some of them were only differentially expressed in the dawn anticipation assay. This suggested that the clock arrest in *tic-2* could have consequences in setting global transcription at an appropriate time frame. Thus it is predictable that the circadian clock would influence the timing of general transcriptional events. However other genes within this category were either induced or repressed in both experimental conditions in *tic-2* (table V), suggesting that their misexpression is a result of the mutation. A mechanism of *TIC* in transcriptional control is still obscure, though probably the observed effects were due to the disruption of the circadian clock.

Finding GO terms in DNA and RNA processes as enriched was unexpected. Previously it was reported that these components were not circadian regulated (Harmer, 2000, Covington 2008). Covington *et al.* (2008) reported that categories related to DNA replication and chromatin structure, RNA processing, the cell cycle, as well as protein synthesis, secretion and degradation presented few transcripts with an oscillation pattern. However in the transcriptional profile reported here, these categories appeared as overrepresented (table IV). This suggests that the clock and nucleic-acid metabolism are linked. In the mammalian circadian clock, a link exists between the mentioned processes and the oscillator, as the clock component CLOCK is itself a histone acetylase (Doi, 2006, Grimaldi, 2009). Other reports have mentioned that DNA repair capacity is circadian regulated (Kang, 2009). Similarly in cyanobacteria, KaiC ATPase activity, but not its kinase activity correlated with the cell cycle and cellular division (Dong, 2010). Therefore it could be plausible that *TIC* has a role in nucleic acid metabolism and cell cycle or that these events are under a so far masked circadian control. Considering that transcription requires an open state of chromatin, transcriptional control by the circadian clock would have an effect on DNA chromatin structure and *vice versa*. So far, the only link established between the plant clock and DNA chromatin status has been the description of *TOC1*

expression by histone acetylation/deacetylation cycles (Perales, 2007). The transcriptional profile from *tic-2* suggested that timing DNA and RNA processes is influenced by the circadian clock. Establishing a relationship between chromatin structure and the circadian clock and the role of *TIC* in this regard will require further research into this area.

tic-2 phenotypic characterization.

The first developmental report of *tic* described it as a short hypocotyl mutant with chlorotic leaves and with a slight decrease in rosette size compared to the wild type (Hall, 2003). Because no further morphological and physiological description of *tic-1* was reported, I describe here *tic-2* morphology, development (on the Col-0 background) and physiology, guide all by the microarray transcript profile.

tic-2 presented a decrease growth rate compared to wild type that was photoperiod independent. The rosette size and number of leaves in *tic-2* were decreased relative to wild type. This caused a delay flowering time in *tic-2* as scored by the number of days after sawing (figure III.2). Though *tic-1* was described with chlorotic leaves as a seedling (Hall, 2003), in greenhouse conditions *tic-2* acquired a deep green coloration of its leaves, which also displayed a degree of serration at the edges. Both characteristics were more evident under a longer photoperiod (figure III.2). The dark green colour of *tic-2* leaves could be attributable to the higher expression of genes involved in chlorophyll synthesis as well as a higher content of iron (table V). Genes as *PORB* and *HEME1*, whose proteins participate in chlorophyllide and porphyrin synthesis, respectively, were overexpressed in *tic-2*, indicated that the mutant could synthesize more chlorophyll than wild type, and consequently, would acquire a dark green colour. As the ferritins, which bind iron in green tissues, were also overexpressed at the transcript level, a higher content of iron could lead to a darker pigmentation. In conclusion, *tic-2* plants displayed a striking different morphology attributable to a deregulation of several processes.

One of the pathways that appeared altered in *tic-2* was starch degradation (table IV). Because either a low rate of carbon fixation by photosynthesis during the light period or an inability to use the assimilated carbon could lead to a slower growth rate, I tested starch accumulation in *tic* plants. As seen in figure III.3, *tic-2* produced starch but was unable of degrading it during the night period. This resulted in *tic-2* displaying a starch excess phenotype. This phenotype resembled that of *gi*, which has been described as a mutant that causes a starch excess phenotype (Eimert, 1995). However, the cause for starch accumulation in *gi* is unknown, as it has not been involved directly in starch degradation.

Thus the mutation of genes not directly involved in starch catabolism can result in starch accumulation, as is the case for the clock mutants *tic-2* and *gi*.

The starch accumulation in *tic-2* did not match its transcript profile because several key genes involved in starch degradation were overexpressed in the mutant (table V). As a particular example, the glucan water dikinase (SEX1), which catalyses the first step in starch remobilization (Yu, 2001), was overexpressed in *tic-2*. This apparent contradiction suggests that the cause of starch accumulation may be due to altered enzymatic activities in starch catabolism. It has been demonstrated that starch synthesis and degradation are under circadian control (Smith, 2007). The genes involved in these processes presented a peak of expression that tracked dawn and dusk dependent on the photoperiod length (Smith, 2007, Zeeman 2007). Furthermore though the mRNA changes obeyed a circadian rhythm, the proteins involved in starch metabolism were shown not to cycle. Because the enzymes involved in starch synthesis and starch breakdown seem to require phosphorylation of the starch glucose residues for their action (Smith, 2007, Zeeman 2007), *tic-2* starch accumulation could be a consequence of altered phosphorylation events. On support of this hypothesis, I did not find transcriptional changes in glucose or triose transporters, which would also lead to starch accumulation (Walters, 2004, Niittlya, 2004). In summary, *tic-2* presented a starch excess phenotype that might be a result of defective phosphorylation events.

Regardless of the mechanism that led to starch accumulation in *tic* and *gi*, is clear that their role in carbohydrate metabolism is regulatory. Neither mutant has been associated with starch metabolism *per se*, nor has described hypothetical enzymatic activities within their encoded proteins. The consequences of the starch excess phenotype are striking, as demonstrated by the *gi* metabolite profile. Instead of having low oligosaccharide levels as would be expected from starch overaccumulation, *gi* showed higher amounts of the main primary carbohydrates as glucose, fructose, sucrose, mannose as well as TCA intermediates (Messerli, 2007). Recently Graf *et al.* (2010) proposed that plant fitness results from the proper timing of anticipation of dawn with the starch degradation during the night. These authors showed that the double mutant *cca1/lhy* had lower starch content than wild type and presented an early onset of starch degradation and induction of starvation response genes. Both processes were in accordance with the short period of the *cca1/lhy*. However it was found that *toc1* and *ztl* mutants did not affect starch consumption (Graf, 2010). Therefore not all clock mutants affect starch degradation. As *tic* is a short-period mutant with starch excess, the theory of arrested growth rate due to lack

of carbohydrates may not apply. Starch was slowly remobilized after an extension of the night in *tic* and *gi* (figure III.3). Therefore they would have available sucrose as the metabolite profile of *gi* previously indicated (Messerli, 2007). Therefore not all clock mutants affect starch degradation.

In conclusion *tic-2* affected developmental processes by an as yet unknown mechanism. *tic-2* altered starch metabolism that together with the data from other clock mutants indicated a complex interaction between the circadian clock and carbohydrate metabolism.

Iron homeostasis in *tic-2*.

Unexpectedly, cellular iron homeostasis appeared as an enriched GO term specific to *tic-2* (table IV). Within this category the genes that were differentially expressed with high transcript levels were the ferritins and some iron transporters (table V). Iron is an essential micronutrient which is a structural component of macromolecules involved in photosynthesis, respiration and metabolism between others (Buchanan, 2000; Briat 2007). I therefore decided to test the relationship between *tic* and iron homeostasis.

Ferritins are proteins found in all kingdoms that bind iron and thus serving as a cellular reservoir (Briat, 2009). In plants, ferritins transcripts are induced under iron excess conditions and serve as protection against ROS (Briat, 2009; Ravet, 2008 respectively). *A. thaliana* extracts iron from the soil by the so-called strategy I, which involves acidification of the rhizosphere by proton release from the roots, followed by the reduction of ferric iron by the Fe(III) chelate reductase (FRO2*)* and iron transport by the iron transporter 1 (IRT1) (Kim, 2007). This results in net import of iron into the plant. I found that *tic-2* had higher expression of ferritins, which suggested that the mutant is sensing an excess of iron. If that were so, the capability of the mutant to uptake iron from the rhizosphere should be increased compared to wild type. The acidification response of the rhizosphere (figure III.4) showed that *tic-2* had a diminished response to iron availability compared to wild type. Thus either the mutant did not perceive an excess of iron or the overexpression of the ferritins was a consequence of another signal.

The results from the root-acidification-response assay should be interpreted carefully, as I could not observed the expected responses toward iron availability (control), iron excess (FeSO$_4$) or iron deficiency (iron chelator: ferrozine), as described by Yi *et.al.* (1996). These authors reported that in a root-acidification-response assay, only plants grown under iron deficient conditions acidified their rhizosphere when shifted to a media

with basal iron supply, whereas those grown under iron sufficient conditions did not release protons when transferred to a media with basal iron content (Yi, 1996). The results from the test presented in figure III.4 showed that plants previously grown in media with basal or excessive iron content acidified more readily the media than those grown in media with chelated iron. Thus the results obtained are difficult to interpret coherently with the published data. Furthermore the observed change of pH could be a consequence of other physiological responses, as the MS1 control media has an excess of iron content (Ute Kraemer, personal communication).

During the course of this study, *TIC* was isolated in a screen for iron regulators of ferritin expression (Duc, 2009). The authors found that *tic* had a higher constitutive expression of ferritins. This result that correlates to the expression profile from the microarray described here (table V). Also Duc *et al.* (2009) showed that the iron content of soil grown plants was similar between the *tic* and the wild type. However when plants were grown *in vitro*, the mutant had less iron and was hypersensitive to an excess of iron in the media. Therefore *TIC* is involved in maintaining iron homeostasis. The mechanism through which *TIC* participates in iron regulation and transcriptional control of ferritins is still unknown.

tic-2 is hypersensitive to oxidative stress

Just as the GO terms corresponding to the circadian clock and iron homeostasis appeared as enriched in the microarray data with genes that were mainly induced, GO terms corresponding to responses to ROS, oxidative stress, oxidoreductase and peroxidase activities were enriched mainly by genes that were repressed in *tic-2* (table IV and V). Therefore I tested *tic-2* susceptibility to compounds that produce ROS, including methylviologen dichloride (MV) and hydrogen peroxide (H_2O_2). As demonstrated by the germination assays, I found that *tic-2* was hypersensitive to oxidative stress (figure III.5).

This physiological test confirmed what was expected from the transcript profile. The induced genes in *tic-2* were *CAT1*, *CAT3* and *SEN1*. These have all been described as markers of oxidative stress *in planta*, as they are induced upon these conditions (Gadjev, 2006). Furthermore the alternative oxidase (*AOX1a*), and some enzymes involved in photorespiration, were also overexpressed *tic-2* (table V). The former is induced under stress conditions and ameliorates ROS production by accepting electrons from ubiquinone without energy conservation. AOX1a is essential for plant development as its mutation led to higher ROS production and plant susceptibility to stress, whereas its overexpression

diminished ROS production (Maxwell, 1999; Giraud 2008). However *AOX1a* overexpression in *tic-2* was not sufficient to overcome the additional stress imposed by MV and H_2O_2. This suggested that the mutant proceeds through development under a permanent stress, and consequently cannot cope with an increase in ROS production. Induction of *AOX1a* in *tic-2* under normal conditions indicated that *tic-2* have a defect in its metabolism that leads to either higher ROS production or an impairment in ROS quenching mechanisms. Thus *tic*-2 responds to increased levels of ROS as a basal mechanism for survival.

Based on the transcript profile, *tic-2* could have a defect in mitochondria or chloroplast, either in structure or cellular crosstalk. However structural defects lead to a complex reprogramming (Noguchi, 2008)). It was reported that the loss of the respiratory complex I led to higher expression of ROS scavenging enzymes and their enzymatic activities resulting in a plant more resistant to ozone (Dutilleul, 2003). Interestingly a mutation in *AOX1a* provoked susceptibility to drought only under high light (Giraud, 2008). As another example, thylakoid and cytosolic ascorbate peroxidases single mutants had increased resistance to heat and susceptibility to oxidative stress, respectively, and had a different transcript profile and behaviour as a double mutant (Miller, 2007). These examples demonstrate the complexity of ROS signalling, which makes its mechanistic dissection difficult. Therefore unravelling what mechanism caused *tic* susceptibility to oxidative stress or what led to resistance in *gi* (Kurepa, 1998) would require further research.

I found that *tic-2* was hypersensitive to oxidative stress and its transcriptomic profile displayed misexpression of several genes involved in photosynthesis and respiration. As these two metabolic processes produce ROS, I hypothesized that clock entrainment by the light signal could be through either redox changes in proteins or changes in energy sources (ATP/AMP ratio, sucrose levels). As the main photoreceptors are not necessary for clock entrainment and resetting (Yanovsky, 2000), I decided to test the effect of ROS producing compounds on clock rhythms. Thus I could reveal if these compounds could affect the clock and in parallel asses the differences between the mutant and the wild-type strain.

The addition of H_2O_2 and MV caused changes in the circadian clock periodicity of wild type in a concentration-dependent fashion (figures III.9 and III.10). This result suggested that the clock has a compensation mechanism toward oxidative stress similar to that of temperature. This ROS compensation mechanism could derive from the plant ROS

scavenging system, which could deal with ROS without compromising cellular functions. Regardless of the mechanism, it was found that after a threshold was surpassed, clock period was lengthened. This observation was clearly visible by the oxidative stress infringed by MV (figure III.10). This period lengthening effect could be due to metabolism diversification on ROS quenching reactions, consequently slowing other metabolic processes.

The use of MV to determine periodicity revealed that *tic* responded in the same fashion as the wild type (figure III.10C). This result indicated that the clock in *tic* was responsive to oxidative stress by MV (figure III.10C), even though *tic* showed hypersensitivity to this compound in a germination test (figure III.5). Though the clock in *tic* was responsive to MV, it was not perturbed by H_2O_2 application (figure III.9). This result suggested that the peroxidase activity in *tic*, which was found transcriptionally repressed (table V) was compromised.

To test the effect of inhibiting enzymes involved in oxido-reduction activities, I used DPI. This compound was originally thought to bind flavins, but further testing showed that it inhibits NADH:ubiquinone oxidoreductase, NADPH oxidases, NADPH cytochrome P450 oxidoreductases, xanthine oxidase and is capable of reacting with heme B groups of NADPH oxidases (Riganti, 2004) while increasing ROS in a dose dependent manner. In the experiments reported here, DPI showed no effect on wild type under the conditions tested, while it caused a period lengthening in *tic* at high concentrations (figure III.11). Thus, *tic* was more susceptible than wild type to DPI. *tic* susceptibility may arise due to an increased amount of electron flow through membrane bound NADPH oxidases in mitochondria or either as a consequence of higher ROS production.

Finally because *tic* had a higher expression of *AOX1a*, I subjected plants to the AOX1a specific inhibitor SHAM (Nelson, 2000). It has been shown that AOX1a inhibition diminishes plant fitness and performance because the rate of photosynthesis decreases as photorespiration is blocked. If AOX1a is required under normal growth conditions, I expected that *tic* would be more susceptible to SHAM than wild type becasue *AOX1a* was transcriptionally induced in the mutant. Addition of SHAM did not affect the clock period with a constant pattern through the experiments in the wild type, whereas in *tic* at low SHAM concentrations, periodicity was decreased (figure III.12). Consequently *tic* was hypersensitive to AOX1a inhibition, probably because *tic* metabolism has a higher rate of photorespiration. Notably SHAM was the only compound tested that reduced free-running

period, though an explanation for this particular behaviour is beyond the interpretation of the collected data.

In conclusion, *tic* was hypersensitive to oxidative stress and ROS-generating compounds altered clock periodicity of wild type and *tic* in a dose and genotype dependent manner.

ABA related responses in *tic-2*.

As ABA hormone stimulus appeared as an overrepresented GO term in the microarray datasets (table IV) and circadian clock and ABA microarray data have been shown to overlap (Mizuno, 2008), I focused on this hormone and its related responses than on the other potentially interesting hormone pathways also misregulated in the microarray data.

One of the classical ABA assays that described mutants as hyper and hyposensitive to this hormone is a germination assay under increasing ABA concentrations (Rook, 2006). Consequently I tested the effect of ABA on *tic-2* to establish, if any, a relationship between the mutant transcript profile and the hormone. The germination assay indicated that *tic-2* had a hypersensitive phenotype to ABA (figure III.6). This result suggested that *tic-2* could have higher amounts ABA or that the ABA signalling pathways are sensitized to the hormone, and consequently, overreact to it. I did not measure cellular ABA levels in *tic-2*, but the microarray expression data did not indicated that the mutant would have higher amounts of this hormone. The only ABA biosynthetic gene misregulated in *tic-2* was *ABA2* (table V). Furthermore this gene appeared as repressed only in the dawn-anticipation assay, suggesting that its missexpression was not a constitutive trait of *tic-2*. Therefore it might be more likely that ABA signalling is altered in *tic-2*.

The *tic-2* sensitized ABA signalling hypothesis finds support on the transcript profile. This profile included the induction of an ABRE (ABA responsive element) binding transcription factor, as well the overexpression of the kinases *SNRK2.2* and *SNRK 2.3*. Previously it has been shown that these kinases together with *SNRK2.6/OST1* are essential for plant development and ABA-mediated stress-gene expression (Fujii, 2009). A triple mutant of these genes showed insensitivity to ABA in a germination assay as well as the lack of expression of ABA inducible genes as *RD22*, *COR15A* between others. The *snrk2.2 /snrk2.2/ snrk2.2* triple mutant phenotype is opposite to *tic-2*. The later was hypersensitive to ABA, *SNRK2.2* and *SNRK2.3* were overexpressed and *tic-2* expression profile displayed induction of several ABA inducible genes as *COR15A* and *RD22* (table V). Together this

data supported the idea of a constitutive or sensitized ABA signalling in the *tic-2* mutant. Interestingly effects of ABA on the clock were reported earlier. Hanano *et al.* (2006) found that ABA biosynthetic mutants had a short period, and that ABA application lengthened periodicity. As *tic* is a short period mutant (Hall, 2003), it is unlikely that the observed defects in ABA signalling in *tic-2* are related to its circadian defects.

This sensitized ABA signalling, was suggestive of a stressed mutant. ABA is a key hormone produced under several environmental stresses as drought, salinity and cold (Shinosaki, 1996). Therefore not surprisingly, many genes that are induced upon drought or cold stress were also induced by ABA (Shinozaki, 1996; Seki, 2007). Besides the overexpression of *COR15A* and *RD22* in *tic-2* expression profile, a plethora of drought and cold responsive genes and transcription factors such as *DREB2A*, *ERD7*, *ERD3 ERD4*, and *ERD10*, and *COR15B* were overexpressed (table V). *DREB2A* is s key transcription factor in controlling gene expression under drought (Liu, 1998), whereas the *ERD* genes are responsible for the tolerance to dehydration (Seki, 2007). The induction of these genes reinforced the idea of *tic-2* being a stressed mutant.

Based on the high expression of drought-resistance genes, I hypothesized that *tic-2* could display resistance to drought stress. In order to test this hypothesis, I subjected wild type and *tic-2* plants to mild and severe drought conditions during 3 weeks. I found that *tic-2* was tolerant to mild drought and to severe drought conditions at least within the duration of the experiment (figure III.7). *tic-2* leaves did not exhibited plasmolysis nor was the plant growth rate was compromised. Only under non-watered conditions, *tic-2* leaves displayed slight signs of stress. On the other hand, leaves of the wild-type plants were wilted and necrotic (figure III.7). The consequent effect was a detriment on growth and survival. Furthermore, the wild-type non-watered plants could not recover from drought after re-watering started, whereas *tic-2* did (not shown). As a conclusion, the overexpression of the drought/cold responsive set of genes in *tic-2* could be causal to provide the mutant with resistance to drought conditions.

tic-2 not only was drought tolerant, but also consumed less water during the 3 weeks of water arrest. The amount of water the mutant consumed, compared to the wild type during the same time lapse, was significantly less (figure III.7B). This could be explained by a lower rate of transpiration and consequently less water loss or alternatively that water usage is diminished due to the slower growth rate of the mutant. *tic-2* was genetically tolerant to drought as it displayed around a 40% less of water consumption than wild type.

Water is lost through transpiration by the stomata pores. The stomata opening is controlled by both light and ABA and the effect of both is gated by the circadian clock (Robertson, 2008). Therefore it was plausible that *tic-2* drought resistance derived from either ABA and clock effects on the stomatal aperture or to a morphological trait as a reduced number of stomata. To address this question I performed scanning electron microscopy (SEM) of *tic-2* and wild-type leaves. Preliminary results indicated that cell size and stomata number per leaf area were similar in both genotypes (figure IV.1). The only structural difference observed was the presence of some meristemoids in *tic-2*. Though I cannot rule out that the stomatal aperture was different, a more careful examination will be required to assess this issue. As the findings in this thesis indicated that *tic-2* was drought resistant and hypersensitive to ABA, and the later may be result of sensitized ABA signalling, it would not be a surprise to find that the mutant has a lower transpiration rate and that its stomata aperture is reduced compared to the wild type. This remains to be tested.

Biotic interaction between *tic-2* and *Psedomonas syringae*.

As *tic-2* mutant showed hypersensitivity to ABA and ROS, and more generally abiotic-stress responses, I wondered how *tic-2* would respond to a challenge of stressful biotic stimuli. To test this, I infected wild type and *tic-2* with *Psedomonas syringae*. To determine the role of the circadian clock and diurnal effects in the biotic interaction, the plants were infected either at dawn or at dusk, respectively.

From this experiment two interesting aspects emerged. First, the susceptibility of the wild type toward *P. syringae* was dependent on the time of the day, as the wild type presented a lower rate of infection in the evening than in the morning (figure III.8). This effect was not observed when using an avirulent bacterial strain. Second, the diurnal or clock-gated effect of susceptibility to infection was absent in *tic-2*. Furthermore *tic-2* was hypersensitive to *P. syringae*, as it had higher rates of bacterial growth under both conditions. These results suggested that *tic-2* was more readily infected either due to an intrinsic susceptibility to the bacteria or to a disrupted circadian clock.

During the introduction section, I mentioned that hormone levels fluctuate during the day and that the hormone effects on gene expression are controlled and gated by the circadian clock (Covington, 2008). Therefore the different bacterial growth rate in wild type could be a consequence of a different hormone profile leading to a higher susceptibility in the morning. Similarly the susceptibility could arise from the stomatal
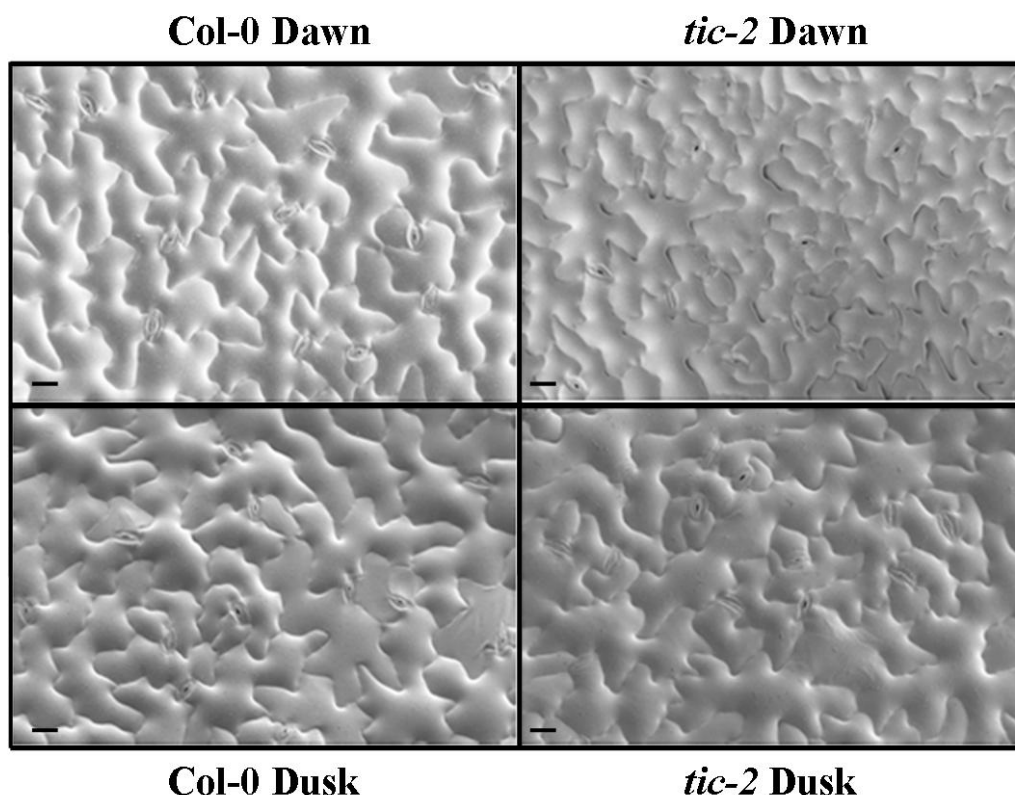
Figure IV.1. Scanning electromicroscopy revealed that a difference in stomata number between *tic-2* and wild type was not the reason for the diminished water loss observed in *tic-2*.

Wild type and *tic-2* plants were grown under short-day conditions (8:16) and leaves were detached at dawn or at dusk, respectively, for scanning electromicroscopy imaging.

Cell size and structure was not found drastically altered in *tic-2*, as it resembled wild-type structure. The number of stomata per area was similar between the genotypes, indicating that the stomatal index was not modified. In *tic-2* leaves, meristemoids were observed with a higher frequency than the wild type.

Preliminary examinations of stomatal aperture did not indicate a significant difference between *tic-2* and wild type. Around 10 to 14 stomata are present in each leaf area.

Black bars at the bottom of the photographs represent the scale and are equivalent to 10 μM. Photographs were taken with a Zeiss microscope at a 750 X magnification.

aperture, as stomata are opened before dawn and closed prior to dusk (Robertson, 2008). However the observed phenomena may not be so simple. It has been described that plants require light for establishing the hypersensitive response as well as the systemic acquired resistance (SAR) upon a biotic interaction. Also it was found that high light led to resistance against *P. syringae* infection (Roden, 2009). Similarly, roles for the phytochrome photoreceptors in establishing the salicylic acid mediated defence and the SAR (Griebel, 2008) and for the cryptochromes in the regulation of pathogen resistant genes have been reported (Wu, 2010). The results I obtained are contradictory with those from Griebel *et al.* (2008), as these authors found a higher infection rate during the dark period. However it must be noted that the conditions employed during infection were different. Griebel *et al.* (2008) directly inoculated the bacteria in the plant leaves. My infection assays mimicked a more natural infection as bacteria was topically sprayed.

The gated susceptibility effect to bacterial infection was lost in *tic-2*, as it presented the same rate of infection both at dawn and dusk. One possibility is that the clock timing that controls hormone signalling and effectiveness is disrupted and that this leads to a higher susceptibility. However to proof this hypothesis, one would need to observe the same behaviour in other clock mutants. The previous assays described in this thesis uncovered that *tic-2* was hypersensitive to ABA, raising the possibility that the mutant has exacerbated ABA signalling. This observation could explain the higher susceptibility to *P. syringae*, because though ABA participates in bacterial infections by triggering the closure of stomata, it also counteracts the effects of salicylic acid, jasmonic acid and ROS production, consequently promoting bacterial growth (Torres-Zabala, 2009, Ton, 2009). Furthermore based on *tic-2* hypersensitivity to ROS, bacterial growth could be a consequence of *tic-2* not triggering ROS production upon infection. Another alternative to direct ROS production and quenching could be the redox state of the plastoquinone pool in chloroplast. It has been observed that a reduced state of plastoquinone led to resistance while an oxidized state displayed the same susceptibility to bacterial infection as the control plants (Muhlenbock, 2008, Roden, 2009). In conclusion, *tic-2* was hypersensitive to bacterial infection and its susceptibility to *P. syringae* was independent of the time of day when the inoculation ocurred.

TIC biochemical function

TIC is one of the few circadian-clock regulators that is not under an apparent circadian control. Ding *et al.* (2007) previously showed that *TIC* mRNA and its protein levels did not cycle. Also TIC was found to be constitutively nuclear localised (Ding, 2007). However the *TIC* effect on the circadian clock is time specific as noted by a clock arrest before dawn (Hall, 2003). Consequently elucidating a mechanism by which TIC acquires a time-specific action on the circadian clock, in particular to clock entrainment, may lead to a better understating of TIC function. With this aim in mind, a biochemical approach was undertaken to start to understand TIC function.

TIC protein interacting partners

To search for proteins that could interact with TIC, a yeast two hybrid (Y2H) screen using the amino terminus of TIC sequence was performed. Through this screen, it was found that TIC could interact with several candidates, some of which are presented in table VI. Though most candidate interactors have not yet been confirmed by other means, associating the microarray expression profile with this selected list of candidate interactors could shed light into TIC function in the plant cell. Most of the interactors found were transcription factors or were involved in transcription. This correlated with the GO, which highlighted processes as transcription factor activity and regulation (table IV). Furthermore, the known transcriptional activity of some of these putative protein interactors correlates with the changes observed in the transcript profile of *tic-2*.

The interaction of TIC with MYC2 could explain, at least in part, the changes of gene expression of a vast quantity of transcription factors. This is because MYC2 controls the induction of several transcription factors. Furthermore MYC2 has been shown to regulate the gene expression of jasmonic acid, and induces flavonoid biosynthetic genes, as well as responses to oxidative stress (Dombrecht, 2007). This is contrasting with *tic-2*, as jasmonic acid related genes, the flavonoid biosynthetic pathway and oxidative stress quenching genes were repressed. Consequently *tic-2* displayed a transcriptional expression pattern similar to that of *myc2*. These gene expression patterns provide support of a TIC-MYC2 interaction that would be responsible of the gene expression of these pathways. In this sense, MYC2 transcription activity will require TIC as a partner in a hypothetical transcription complex.

Another TIC candidate interactor that had correlation with the microarray expression profile was the Cleavage Stimulation Factor 77 (CSTF77), which is a

homologue of a RNA 3' processing complex conserved in the eukaryotic kingdom (Yao, 2002). Recently it has been shown that *CSTF77* is involved in the repression of flowering locus C (*FLC*) mRNA. A *cstf77* mutant, carrying an in-frame mutation in this one copy gene, caused higher expression of *FLC* transcript (Schurger, 2010). Interestingly, *FLC* was the only clock-related gene that had constitutive repression in *tic-2* (table III). This could be explained by a mechanism in which TIC antagonizes the activity of its interactor. Then, CSTF77 will repress *FLC* expression, seen in *tic-2* expression profile, and TIC function will be to relieve this repression by targeting CSFT77 to degradation or impeding its action.

The locus At5g55070, corresponding to a putative dehydrogenase, was an interesting TIC interacting partner, as this locus has been implicated in oxidative stress responses (Sweetlove, 2002). It could be feasible that the interaction between TIC and this protein may be involved in oxidative stress regulation or signalling and consequently the disruption of this signal transduction participated in the oxidative stress hypersensitivity observed in *tic-2* (figure III.5). Exploring this idea awaits experimentation.

In conclusion it would be plausible to think that TIC could be an integral part of several protein complexes and its interaction with them could lead to either a stable complex promoting transcription as in the case of MYC2 or either impeding the action of other proteins (figure IV.2).

TIC-AKIN10 interaction in the circadian clock.

One of the main candidates from the Y2H screens, due to its physiological activity, was the protein kinase AKIN10 (table VI). This TIC protein interactor was interesting because it is involved in stress responses, in particular to carbohydrate availability and energy signalling in the dark to light transitions (Baena-González, 2007 and 2008). The interaction between TIC and AKIN10 was confirmed in yeast and notably this interaction showed higher specificity with AKIN10 than with AKIN11 (figure III.13). Furthermore it was found that TIC and AKIN10 could interact through an *in vitro* pull-down experiment and that AKIN10 was capable of trans-phosphorylating TIC protein in an *in vitro* phosphorylation assay (figure III.14). Both *in vitro* assays provided support to a hypothesis where TIC activity could be triggered upon phosphorylation by AKIN10 action.

Considering that AKIN10 interaction with TIC could have an effect on the later in its circadian activity, I assayed for effects on the circadian clock by the kinases AKIN10 and AKIN11. As effective T-DNA lines from these kinases were not available, I used

117
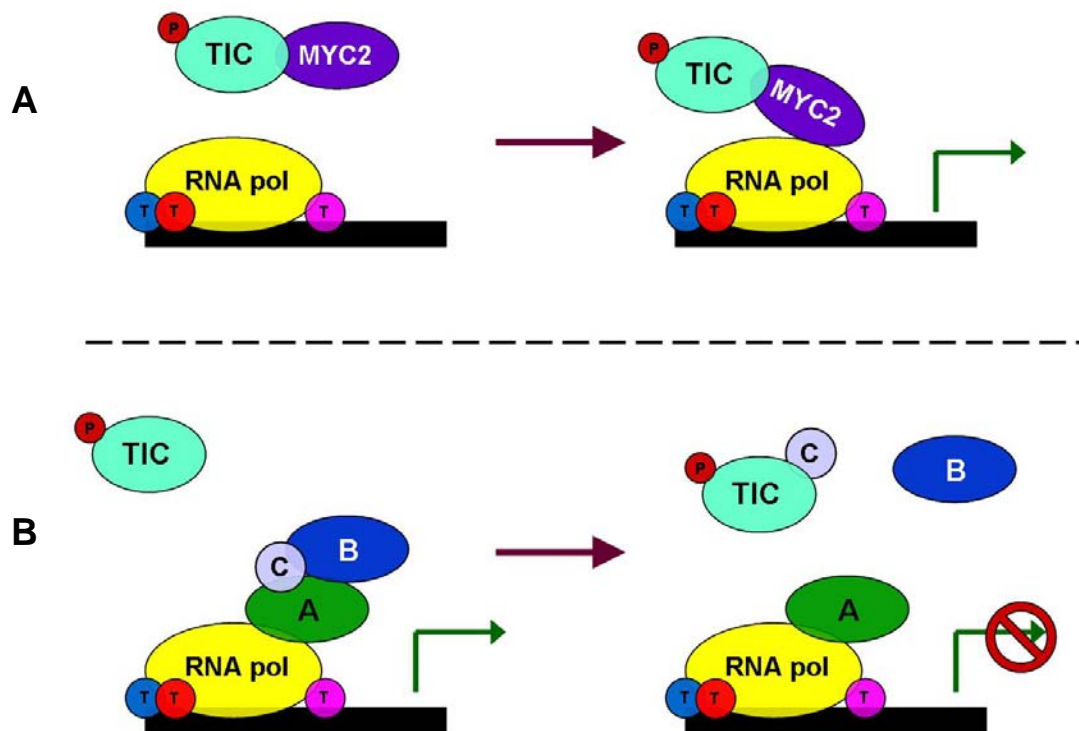
Figure IV.2 Possible scenarios for TIC transcriptional control.
TIC could participate in transcriptional control through interacting with other proteins associated to transcriptional processes. This hypothetical function could be time-specific, as for example by activation through phosphorylation, or TIC could be active through the day in non circadian roles, as for example iron homeostasis.

In one scenario (A), TIC interaction with transcription factors (MYC2 in the example), could be necessary for the transcriptional activity of the later. In a second scenario (B), TIC could disrupt transcriptional complexes through interacting with one or more of its components either once bound to DNA or prior to the transcriptional complex assembly.

Letters in the figures indicate hypothetical protein complexes or transcription factors. TIC is depicted in this scheme phosphorylated indicated by a red circle labeled with a P (phosphate). RNApol indicates RNA polymerase and the associated proteins with the RNApol are indicated with circles with a T (TATA binding proteins and other factors).

inducible lines. As seen in figure III.15, both kinases did not have an effect on clock rhythms as long as they were not transcriptionally induced. Interestingly upon transcriptional activation, only *AKIN10* had a lengthening effect on circadian periodicity (figure III.15). Therefore *AKIN10* activity could have a role in the circadian clock. However the period lengthening could be consequence of the kinase activity independent of TIC.

In order to test if *AKIN10* effect in the circadian clock depended on TIC, a *tic-2/AKIN10* line was evaluated on its effect on clock periodicity. I found that the *CCA1:LUC* driven rhythms were dependent of *TIC*, as in the *tic-2/AKIN10* construct the lengthening of period did not took place (figure III.16). Therefore the result indicated that *TIC* is epistatic to *AKIN10*, as the activity of the later only had an effect with a functional *TIC*. It cannot be discarded that the period lengthening could be masked due to the dampened rhythms observed in *tic-2*; however the evidence so far collected is compelling to a requirement of *TIC* for *AKIN10* activity toward the circadian clock.

I demonstrated that *tic-2* presented a starch excess phenotype (figure III.3). This result is consistent with an interaction between TIC and AKIN10 as RNA interference (RNAi) lines of *AKIN10/AKIN11* were unable to breakdown starch during the night (Baena-González, 2007). Thus it could be suggested that disruption of TIC-AKIN10 interaction could lead to an impairment of starch breakdown. However the epistasis observed between TIC and AKIN10 within the circadian clock may not apply to the starch excess phenotype of *tic-2* described in this thesis for and the starch accumulation reported for *AKIN10* silencing lines (Baena-González, 2007). Earlier findings demonstrated that SnRK1 kinases were required for starch synthesis in *Psycomitrella patens* and in plants (Thelander, 2004 ; Halford, 2009). Also the SnRK1 was indispensable for the induction of sucrose synthase expression and ADP glucose pyrophosphorylase redox activation (Tiessen, 2003, Halford, 2009), both enzymes participating in starch synthesis. Furthermore the moss knockout of the SnRK1 (SNF1a and SNF1b) displayed photoperiodic and metabolic defects (Thelander, 2004) similar to those of *tic* reported in this work. Therefore SnRK1 is essential for both starch synthesis and catabolism.

Baena-González (2007) reported that the transcriptional induction of the dark induced genes (*DIN*), which are activated upon stress and repressed by sugar and light, required AKIN10/AKIN11. The *tic-2* transcript profile showed that *DIN1/SEN1*, *DIN4*, *DIN6/ASN1* and *DIN10* were overexpressed. This result is consistent with *tic-2* constitutive stress responsive transcriptome and with a probable starvation response before dawn.

Similarly this profile suggests that TIC-AKIN10 interaction is specific to the oscillator and that AKIN10 do not require a functional TIC in order to perform other metabolic activities. Therefore the TIC-AKIN10 interaction in relation to carbohydrate metabolism may be complex and indirect.

Based on *tic* arrest of the circadian clock prior to dawn, the hypothesis that TIC activity should be triggered at a specific time of day was followed in this discussion. Nonetheless other mechanisms are plausible. As for example instead TIC could be active through the day and be inactivated in a time-specific manner prior to dawn. Similarly TIC activity could be modified through phosphorylation-dephosphorylaton cycles during the diurnal cycle. Considering that AKIN10 can interact with SKP1 (S-phase kinase associated protein 1) and consequently mediates its proteasomal binding of an ubiquitin ligase (Farrás, 2001), TIC specific activity could be determined by its degradation. Though TIC protein was shown to be constant through day and night, the protein monitored was driven by the cauliflower mosaic virus 35S promoter (Ding, 2007), which could have masked proteosomal degradation events.

In summary, TIC-AKIN10 interaction and its effect on clock periodicity suggested a mechanism through which TIC could exert its function, as well as it opened a possible link between metabolism and energy signalling in regard of the circadian-clock entrainment. Clarifying and establishing these mechanisms will require further research in the area.

TIC-like sequences: TKL.

Previously it was reported that within *A. thaliana* genome existed another sequence that when translated showed similarity to *TIC*, called *TICKLE* (*TKL*) (Ding, 2007). Both sequences were similar despite the differences in the length of their putative encoded proteins of 1550 and 978 amino acids for TIC and TKL, respectively. TKL conceptually could have a function within the circadian clock as many genes belonging to the same family tend to have redundant or partially redundant functions. Furthermore TIC-like sequences were restricted to the plant kingdom (figure III.17).

TIC sequence phylogeny showed that TIC sequence was present since the origin of land plants, as it was present in *Physcomitrella patens*. Interestingly besides the moss, two TIC-like sequences were also present in the genome of grape and rice. This result suggested that the putative genome duplication of TIC sequence would have taken place before the emergence of plants. Both TIC-like sequences would have been present as

plants divided in monocots and dicots, followed then by independent gene loss in some species as exemplified by *Sorghum bicolor* and *Populus trichocarpa*. However the possibility of a gene loss before the origin of tracheophytes followed by genome duplication cannot be discarded. Strikingly, TIC sequence was found to have higher similarity to TIC-like sequences within the dicots than to TKL. This would imply that TIC sequence was conserved as speciation took place, but that TKL sequence diverged. Another explanation could be that TIC and TKL diverged a long time ago as is suggested by the pylogenetic tree (figure III.18). Consequently each gene acquired a different function. Supporting this statement, multiple-sequence-alignment curator applications discarded TKL sequence before generating a final phylogenetic tree, as the sequence was considered to be a divergent outgroup. This finding could explain why I did not observe that TKL could have a role in the *A. thaliana* circadian clock, as I discuss below.

Interestingly the TIC-like sequences displayed blocks or hypothetical domains highly conserved. For example a domain rich in arginine and therefore highly polar is conserved in the proximal amino terminus (domain A, figure III.17A). A second block of residues positively charged with arginine and lysine surrounded by proline is conserved (domain D, figure III.17B). The presence of proline could suggest a folding within the protein that could either expose or cover the charged area. Between these charged areas, borders a conserved region with hydrophobic and negatively charged amino acids (domain B, figure III.17B). However the most interesting feature was block E which exhibited a polar region with two cysteines, two of them conserved with all the tracheophytes (except *TKL*) and one of them conserved in all the sequences (domain E, figure III.17). This could imply that TIC could be sensitive to redox modifications and therefore activity through cysteine bridges. However these structure speculations would require experimental confirmation.

TKL within the circadian clock.

To assess if *TKL* could have a function in the circadian clock, I searched for available T-DNA insertion lines and generated homozygous mutants harbouring luciferase as a reporter gene under the control of the clock promoters *CAB* or *CCR2*. The analyses of clock-driven rhythms, either under constant light or in constant darkness, were not perturbed in the *tkl-1* mutant (figure III.19). Thus this result indicated that *TKL* does not have a function in driven clock rhythms. Furthermore both *tkl-1* and *tkl-2* single mutants did not present any phenotypic alteration in rosette size or plant shape. Additionally their

flowering time was similar to the wild type. The flowering time as an output of the circadian clock suggested that at least the photoperiod pathway was not affected.

Considering that the function of *TKL* could be redundant to *TIC*, in a *TIC* wild-type background, a genetic role of *TKL* could be masked. To explore this idea, I generated double mutants between *tic-2* and *tkl-1*. The double mutant displayed a phenotype similar to the *tic-2* single mutant, suggesting that the absence of a phenotype in *tkl-1* single mutant was not due to redundancy with *TIC*.

The phylogenetic analysis performed here (figure III.17 and III.18), and the results obtained through *tkl* circadian clock and phenotypic characterization (Figure III.19), indicated that *TIC* and *TKL* sequences had diverged and therefore have different functions, at least with respect to circadian rhythms. In support of this conclusion, microarray expression profiles available through the Botany Array Resource (BAR) indicated that *TKL* is not circadian regulated. Furthermore the expression profiles of TKL and TIC were different toward abiotic stress, in particular to heat and cold (data not shown). Therefore it is plausible that both TIC and TKL have different functions within *A. thaliana*.

V. Conclusions

Microarray gene expression analysis of *tic-2* suggested that *TIC* is involved in several metabolic processes and abiotic-sensing responses.

TIC mutation resulted not only in a disrupted circadian clock gene expression, but also in a stress phenotype. *tic* developmental defects included a slower growth rate and serration of leaves, as well as accumulation of starch.

tic displayed hypersensitivity to ROS and ABA, as well as susceptibility to biotic stress by *P. syringae*, but *tic* was tolerant to drought conditions.

Circadian clock periodicity can be affected by ROS generating compounds. The extent of the effect of these chemicals depended on the genotype. Methylviologen lengthened the period of wild type and *tic*, whereas hydrogen peroxide and SHAM affected the period of wild type and *tic*, respectively.

TIC could interact with the kinase AKIN10 *in vitro* and served as a substrate for this kinase. *TIC* and *AKIN10* were epistatic on the circadian clock, as AKIN10 lengthening of period required functional TIC.

TKL was not found to be associated with the circadian clock, as its mutation displayed wild-type rhythms both under constant light and in darkness.

VI. Perspectives

The research work presented here unveiled *TIC* functions beyond its role in maintaining circadian rhythms. *tic-2* transcriptomic analysis helped unravel several stress associated phenotypes and responses that were not previously observed. Taken together, the constitutive stress behaviour of *tic-2* could explain its slower growth and altered development. If the mutant has to invest more of its energy sources in dealing with inappropriate ROS production, is unable of remobilize carbon stores, such as starch, and it mounts a drought tolerance response probably as an effect of diminished gas exchange, photosynthesis and homeostasis would be affected. Thus *tic-2* growth rate would be "slow down" as a strategy for survival.

One question that remained elusive through *tic-2* characterization was the relationship between its function within the circadian clock and the stress behaviour. As the circadian clock controls at least 30% of the transcriptome (Covington, 2008), it is no surprise that a disruption in the oscillator will lead to pleitropic phenotypes. However no other clock mutant to date described has shown such a extensive array of phenotypes as *tic-2*. Widespread metabolic alterations in *tic-2* are thus to date unique. Circadian clock mutants have been mainly described on their effects on rhythm generation and some clock outputs as flowering time (Imaizumi, 2010). Evidence of the selective advantage provided by a functional clock in phase with its environment demonstrated that, in the end, the circadian clock improved photosynthesis and general fitness (Dodd, 2005). Both short and long period mutants were outcompeted by the wild-type strain, regardless that the clock was entrained on a daily basis. This indicated that the phase of gene expression is crucial for an enhanced fitness. Though this may hold true, as seen for *tic-2*, it is unknown if clock mutants may have secondary effects on metabolism that in turn affect plant fitness. Recently Graf *et al.* (2010) argued that the fitness provided by the clock was not by improving photosynthesis, as Dodd *et al.* (2005) suggested, but that is due to correct timing of dawn with use of carbon supplies. However clarifying the role of carbon and clock would require investigating the behaviour of clock mutants with both short and long periods and analysing these clock mutants fitness respective to their starch accumulating phenotype. In this sense, exploring *tic* and *gi* mutants would be extremely helpful in establishing the role of starch degradation and the anticipation of dawn.

Recently the effects on metabolism and plant performance as a consequence of disrupted rhythms in circadian clock mutants have been reported (Legnaioli, 2009;

Fukushima, 2009). The central oscillator component *TOC1* have been implicated in plant responses to drought by controlling stomata aperture through the circadian and diurnal regulation of the H subunit of the magnesium-protoporphyrin IX chelatase, also known as *GENOME UNCOUPLED 5* (*ABAR/GUN5*) (Legnaioli, 2009). In a comprehensive work, Fukushima *et al.* (2009) demonstrated that the triple mutant *prr9/prr7/prr5* had several metabolic defects that were different to those as a consequence of *CCA1* overexpression. The authors found that the triple mutant had altered primary metabolism, in particular the tricarboxilic acid cycle (TCA), as well as biosynthethic pathways involved in chlorophyll, carotenoid, tocopherol and ABA. In this thesis, though the metabolite profile of *tic-2* was not analysed, the physiological tests and the transcriptome analysis revealed that a single mutation could have effects in these and more pathways than the *prr9/prr7/prr5*. From this, it can be concluded that *TIC* has greater role in linking metabolism and the circadian clock than previously studied clock genes. Also it is tempting to speculate that the circadian clock and primary metabolism associated with mitochondria respiration and photosynthesis are tightly linked. In support of this hypothesis, in this work, I found misexpression of genes related to mitochondria metabolism in *tic-2*. Furthermore, the *prr9/prr7/prr5* triple mutant was severely affected in the metabolism of the TCA (Fukushima, 2009). This would be linked to alterations in mitochondria respiration processes. Determining the extent of interaction between the clock and metabolism would require biochemical knowledge of the clock components beyond the circadian-clock interactions.

It is still unclear if the mutations in the clock genes are the cause or the consequence of the transcriptomic and metabolic reprogramming so far observed. One scenario would be that the clock components have other functions beyond the circadian clock. Another possibility, which I favour, is that the circadian clock is linked to primary metabolic functions. Therefore a continuous crosstalk through signalling between the clock and the organelles, and more generally, cellular metabolism could be responsible of providing a selective advantage upon a changing environment.

A prime example of an interconnection between transcriptomic and metabolic pathways is seen in the mutant *gigantea*. The *GI* locus, which encodes for a protein with uncharacterized domains, is involved in rosette development (Redei, 1962) and flowering time (Fowler, 1999), starch metabolism (Eimert, 1995; Messerli, 2007), circadian clock (Fowler, 1999; Park, 1999) and resistance to oxidative stress (Kurepa, 1998). In this sense, *TIC* may also be involved in a plethora of metabolic events as demonstrated through this work. How can single genes have a role in so many processes? Further research will be

needed to address this question, but it is plausible that TIC may interact with several proteins in different complexes affecting transcriptional reprogramming in a diverse fashion (figure IV.2).

Determining the extent of interaction between the clock and metabolism would require knowledge of the clock components beyond their effects in circadian clock so far described. Probably an understanding of this interconnection, would also require a shift of ideas in the area to expand research interests. Given the pervasiveness of the circadian clock, a more integrative view of the effects of the known clock mutants could clarify the extent of their roles in metabolic events and homeostasis.

So far, I have discussed the probable relationship between the circadian clock, metabolism and stress responses, and how they could be linked. One can ask how do the clock gene products exert their function? In the particular case and interest of this research, TIC association with AKIN10 provides a hypothetical mechanism by which the former could be specifically activated. *TIC* is involved in clock entrainment by the light signal at dawn and its time-specific function within the clock coincided with the dark to light transition and metabolic reprogramming by AKIN10. It is at the verge of dawn when a major transcriptomic and metabolic reprogramming occurs, as carbon stores reach their minimum levels, the ATP/AMP ratio is low and the onset of photosynthesis takes place. Therefore TIC phosphorylation by AKIN10 could be an entrainment signal to the circadian clock (figure IV.3). As the oscillator can still be entrained in a quadruple photoreceptor mutant (Yanovsky, 2000), it is not photo-transducing signals, but rather a metabolic signal derived from photosynthesis and general metabolism, integrated by AKIN10 and TIC, that entrains the clock. In this scenario, the clock would anticipate the dark to light transition, but as light increases the ATP/AMP ratio through photosynthesis, this signal would reset the clock.

Further experimentation would be required to test if the circadian clock can be entrained by a metabolic signal. If so it would be a difficult task to separate the internal metabolic stimuli from the environmental cue as both take place at the same time on a daily basis in the real world. Addressing this topic, though challenging, would be an exciting task, as it would provide an integrative view of the biology that underlies life every day with each new sunrise.
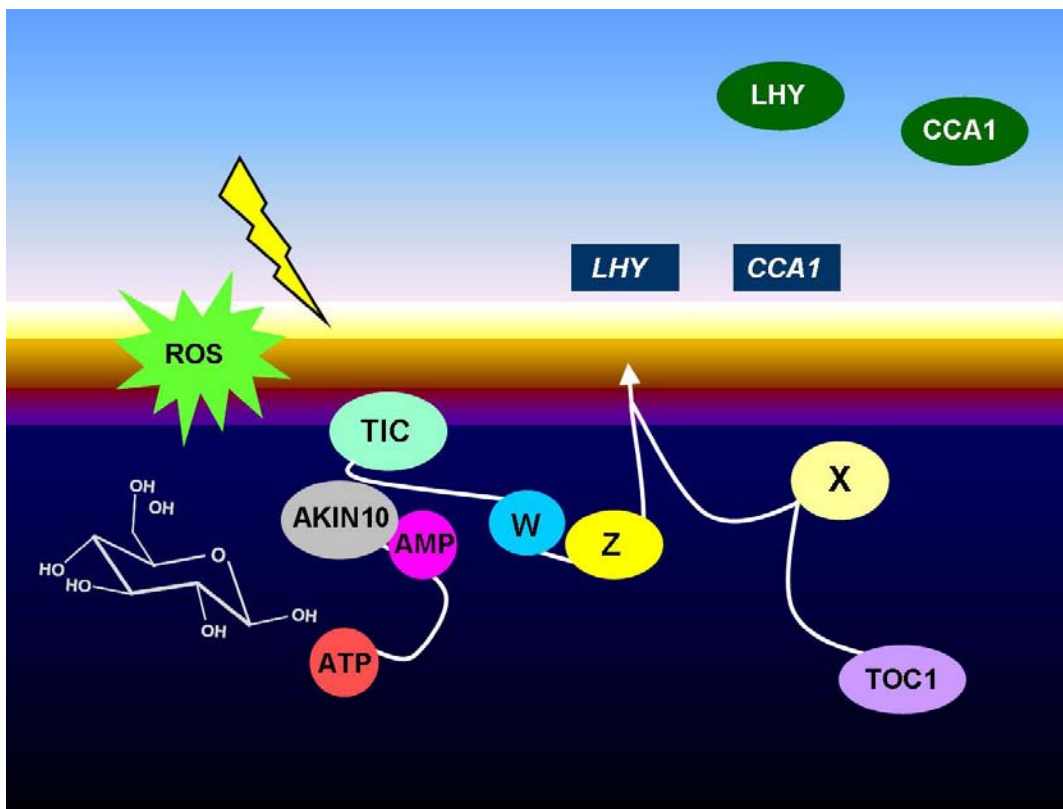
Figure IV. 3. Proposed model of TIC action within the circadian clock.
TIC may act as an integrator of metabolic derived signals at dawn to the circadian clock. TIC could participate in the anticipation of the dawn-light through either changes in the cellular redox status or a direct oxido-reduction of TIC protein. These changes could also be originated by light.
Similarly TIC action could be triggered upon phosphorylation by AKIN10. AKIN10 would sense changes in the carbohydrate availability (depicted with a glucose molecule) as changes in the AMP/ATP ratio and thus would phosphorylate TIC as one of its targets. Then activated TIC could interact with other proteins or protein complexes. These interactions could be with the transcription factors revealed during the YH2 or with undiscovered components (labeled as W and Z in the figure). TIC action within the clock for driving morning clock-gene expression could be by either directly interacting with the proposed X factor in the clock three loop model or indirectly through other proteins (labeled as W and Z in the figure). Thus TIC would participate in closing the loop between TOC1 and *CCA1*/*LHY* expression and entraining the circadian clock toward the oncoming day.

White lines and arrows indicate interactions between molecules and induction of transcription, respectively. Day and night are indicated by clear pale blue and dark blue respectively. Dawn and dusk are indicated by graded color changes representing the sunrise/sunset (left and right side respectively)

VII. References

Acevedo-Hernandez, G.J., Leon, P., and Herrera-Estrella, L.R. (2005). Sugar and ABA responsiveness of a minimal RBCS light-responsive unit is mediated by direct binding of ABI4. Plant J **43,** 506-519.

Alabadi, D., Oyama, T., Yanovsky, M.J., Harmon, F.G., Mas, P., and Kay, S.A. (2001). Reciprocal regulation between TOC1 and LHY/CCA1 within the Arabidopsis circadian clock. Science **293,** 880-883.

Allen, T., Koustenis, A., Theodorou, G., Somers, D.E., Kay, S.A., Whitelam, G.C., and Devlin, P.F. (2006). Arabidopsis FHY3 specifically gates phytochrome signaling to the circadian clock. Plant Cell **18,** 2506-2516.

Allison, D.B., Cui, X., Page, G.P., and Sabripour, M. (2006). Microarray data analysis: from disarray to consolidation and consensus. Nat Rev Genet **7,** 55-65.

Al-Shahrour, F., Minguez, P., Tarraga, J., Montaner, D., Alloza, E., Vaquerizas, J.M., Conde, L., Blaschke, C., Vera, J., and Dopazo, J. (2006). BABELOMICS: a systems biology perspective in the functional annotation of genome-scale experiments. Nucleic Acids Res **34,** W472-476.

Anderson, S.L., Somers, D.E., Millar, A.J., Hanson, K., Chory, J., and Kay, S.A. (1997). Attenuation of phytochrome A and B signaling pathways by the Arabidopsis circadian clock. Plant Cell **9,** 1727-1743.

Ashburner, M., Ball, C.A., Blake, J.A., Botstein, D., Butler1, H., Cherry, J.M., Davis, A.P., Dolinski, K., Dwight, S.S., Eppig, J.T., Harris, M.A., Hill, D.P., Issel-Tarver, L., Kasarskis, A., Lewis, S., Matese, J.C., Richardson, J.E., Ringwald, M., Rubin, G.M., and Sherlock, G. (2000) Gene Ontology: tool for the unification of biology. Nat Genet **25**, 25 – 29.

Baena-Gonzalez, E., Rolland, F., Thevelein, J.M., and Sheen, J. (2007). A central integrator of transcription networks in plant stress and energy signalling. Nature **448,** 938-942.

Baena-Gonzalez, E., and Sheen, J. (2008). Convergent energy and stress signaling. Trends Plant Sci **13,** 474-482.

Bartoli, C.G., Yu, J., Gomez, F., Fernandez, L., McIntosh, L., and Foyer, C.H. (2006). Inter-relationships between light and respiration in the control of ascorbic acid synthesis and accumulation in Arabidopsis thaliana leaves. J Exp Bot **57,** 1621-1631.

Baudry, A., Ito, S., Song, Y.H., Strait, A.A., Kiba, T., Lu, S., Henriques, R., Pruneda-Paz, J.L., Chua, N.H., Tobin, E.M., Kay, S.A., and Imaizumi, T. (2010). F-box proteins FKF1 and LKP2 act in concert with ZEITLUPE to control Arabidopsis clock progression. Plant Cell **22,** 606-622.

Becker, B., Holtgrefe, S., Jung, S., Wunrau, C., Kandlbinder, A., Baier, M., Dietz, K.J., Backhausen, J.E., and Scheibe, R. (2006). Influence of the photoperiod on redox regulation and stress responses in Arabidopsis thaliana L. (Heynh.) plants under long- and short-day conditions. Planta **224,** 380-393.

Bell-Pedersen, D., Cassone, V.M., Earnest, D.J., Golden, S.S., Hardin, P.E., Thomas, T.L., and Zoran, M.J. (2005). Circadian rhythms from multiple oscillators: lessons from diverse organisms. Nat Rev Genet **6,** 544-556.

Belostotsky, D.A. (2003). Unexpected complexity of poly(A)-binding protein gene families in flowering plants: three conserved lineages that are at least 200 million years old and possible auto- and cross-regulation. Genetics **163,** 311-319.

Berendzen, K. (2005). Functional Analysis of AMP-activated protein kinases in *Arabidopsis thaliana*. PhD doctoral thesis, Marburg, Germany.

Blasing, O.E., Gibon, Y., Gunther, M., Hohne, M., Morcuende, R., Osuna, D., Thimm, O., Usadel, B., Scheible, W.R., and Stitt, M. (2005). Sugars and circadian regulation make major contributions to the global regulation of diurnal gene expression in Arabidopsis. Plant Cell **17,** 3257-3281.

Blazejczyk, M., Miron, M., and Nadon, R. (2007). FlexArray: A statistical data analysis software for gene expression microarrays. Genome Quebec, Montreal, Canada, URL http://genomequebec.mcgill.ca/FlexArray

Briat, J.F., Duc, C., Ravet, K., and Gaymard, F. (2009). Ferritins and iron storage in plants. Biochim Biophys Acta.

Briat, J.F., Curie, C., and Gaymard, F. (2007). Iron utilization and metabolism in plants. Curr Opin Plant Biol **10**, 276-282.

Brodersen, P., Sakvarelidze-Achard, L., Bruun-Rasmussen, M., Dunoyer, P., Yamamoto, Y.Y., Sieburth, L., and Voinnet, O. (2008). Widespread translational inhibition by plant miRNAs and siRNAs. Science **320,** 1185-1190.

Brody, S., and Harris, S. (1973). Circadian rhythms in neurospora: spatial differences in pyridine nucleotide levels. Science **180,** 498-500.

Buchanan, B., Gruissem, W., and Jones, R. (2000). Biochemistry and Molecular Biology of Plants. American Society of Plant Biologists. Courier companies. Rockville, Maryland, USA.

Caspar, T., Lin, T.P., Kakefuda, G., Benbow, L., Preiss, J., and Somerville, C. (1991). Mutants of Arabidopsis with Altered Regulation of Starch Degradation. Plant Physiol **95,** 1181-1188.

Cordero, F., Botta, M., and Calogero, R.A. (2007). Microarray data analysis and mining approaches. Brief Funct Genomic Proteomic **6,** 265-281.

Covington, M.F., and Harmer, S.L. (2007). The circadian clock regulates auxin signaling and responses in Arabidopsis. PLoS Biol **5,** e222.

Covington, M.F., Maloof, J.N., Straume, M., Kay, S.A., and Harmer, S.L. (2008). Global transcriptome analysis reveals circadian regulation of key pathways in plant growth and development. Genome Biol **9,** R130.

Daniel, X., Sugano, S., and Tobin, E.M. (2004). CK2 phosphorylation of CCA1 is necessary for its circadian oscillator function in Arabidopsis. Proc Natl Acad Sci U S A **101,** 3292-3297.

De Block, M., Verduyn, C., De Brouwer, D., and Cornelissen, M. (2005). Poly(ADP-ribose) polymerase in plants affects energy homeostasis, cell death and stress tolerance. Plant J **41,** 95-106.

Ding, Z., Millar, A.J., Davis, A.M., and Davis, S.J. (2007a). TIME FOR COFFEE encodes a nuclear regulator in the Arabidopsis thaliana circadian clock. Plant Cell **19,** 1522-1536.

Ding, Z., Doyle, M.R., Amasino, R.M., and Davis, S.J. (2007b). A complex genetic interaction between Arabidopsis thaliana TOC1 and CCA1/LHY in driving the circadian clock and in output regulation. Genetics **176,** 1501-1510.

Dodd, A.N., Salathia, N., Hall, A., Kevei, E., Toth, R., Nagy, F., Hibberd, J.M., Millar, A.J., and Webb, A.A. (2005). Plant circadian clocks increase photosynthesis, growth, survival, and competitive advantage. Science **309,** 630-633.

Dodd, A.N., Gardner, M.J., Hotta, C.T., Hubbard, K.E., Dalchau, N., Love, J., Assie, J.M., Robertson, F.C., Jakobsen, M.K., Goncalves, J., Sanders, D., and Webb, A.A. (2007). The Arabidopsis circadian clock incorporates a cADPR-based feedback loop. Science **318,** 1789-1792.

Doi, M., Hirayama, J., and Sassone-Corsi, P. (2006). Circadian regulator CLOCK is a histone acetyltransferase. Cell **125,** 497-508.

Dombrecht, B., Xue, G.P., Sprague, S.J., Kirkegaard, J.A., Ross, J.J., Reid, J.B., Fitt, G.P., Sewelam, N., Schenk, P.M., Manners, J.M., and Kazan, K. (2007). MYC2 differentially modulates diverse jasmonate-dependent functions in Arabidopsis. Plant Cell **19,** 2225-2245.

Dong, G., Yang, Q., Wang, Q., Kim, Y.I., Wood, T.L., Osteryoung, K.W., van Oudenaarden, A., and Golden, S.S. (2010). Elevated ATPase activity of KaiC applies a circadian checkpoint on cell division in Synechococcus elongatus. Cell **140,** 529-539.

Duc, C., Cellier, F., Lobreaux, S., Briat, J.F., and Gaymard, F. (2009). Regulation of iron homeostasis in Arabidopsis thaliana by the clock regulator time for coffee. J Biol Chem **284,** 36271-36281.

Dunlap, J.C., Loros, J.J., DeCoursey, P.J. (2003). Chronobiology. Biological Timekeeping. Sinauer Associates. Maryland, USA.

Dutilleul, C., Garmier, M., Noctor, G., Mathieu, C., Chetrit, P., Foyer, C.H., and de Paepe, R. (2003). Leaf mitochondria modulate whole cell redox homeostasis, set antioxidant capacity, and determine stress resistance through altered signaling and diurnal regulation. Plant Cell **15,** 1212-1226.

Eckel-Mahan, K., and Sassone-Corsi, P. (2009). Metabolism control by the circadian clock and vice versa. Nat Struct Mol Biol **16,** 462-467.

Eimert, K., Wang, S.M., Lue, W.I., and Chen, J. (1995). Monogenic Recessive Mutations Causing Both Late Floral Initiation and Excess Starch Accumulation in Arabidopsis. Plant Cell **7,** 1703-1712.

Engelke, D.R., Krikos, A., and Ginsburg, D. (1990).Purification of Thermus aquaticus DNA polymerase expressed in Escherichia coli. Anal Biochem **191**, 396-400.

Fankhauser, C., and Staiger, D. (2002). Photoreceptors in Arabidopsis thaliana: light perception, signal transduction and entrainment of the endogenous clock. Planta **216,** 1-16.

Farrás R, Ferrando A, Jásik J, Kleinow T, Okrész L, Tiburcio A, Salchert K, del Pozo C, Schell J, Koncz C. (2001). SKP1-SnRK protein kinase interactions mediate proteasomal binding of a plant SCF ubiquitin ligase. EMBO J. **20**, 2742-56.

Fowler, S.G., Cook, D., and Thomashow, M.F. (2005). Low temperature induction of Arabidopsis CBF1, 2, and 3 is gated by the circadian clock. Plant Physiol **137,** 961-968.

Fowler S, Lee K, Onouchi H, Samach A, Richardson K, Morris B, Coupland G, Putterill J. (1999). GIGANTEA: a circadian clock-controlled gene that regulates photoperiodic flowering in Arabidopsis and encodes a protein with several possible membrane-spanning domains. EMBO J. 1999. **18**, 4679-88.

Franklin, K.A., and Whitelam, G.C. (2007). Light-quality regulation of freezing tolerance in Arabidopsis thaliana. Nat Genet **39,** 1410-1413.

Fujii, H., and Zhu, J.K. (2009). Arabidopsis mutant deficient in 3 abscisic acid-activated protein kinases reveals critical roles in growth, reproduction, and stress. Proc Natl Acad Sci U S A **106,** 8380-8385.

Fukushima, A., Kusano, M., Nakamichi, N., Kobayashi, M., Hayashi, N., Sakakibara, H., Mizuno, T., and Saito, K. (2009). Impact of clock-associated Arabidopsis pseudo-response regulators in metabolic coordination. Proc Natl Acad Sci U S A **106,** 7251-7256.

Gadjev, I., Vanderauwera, S., Gechev, T.S., Laloi, C., Minkov, I.N., Shulaev, V., Apel, K., Inze, D., Mittler, R., and Van Breusegem, F. (2006). Transcriptomic footprints disclose specificity of reactive oxygen species signaling in Arabidopsis. Plant Physiol **141,** 436-445.

Gallego, M., and Virshup, D.M. (2007). Post-translational modifications regulate the ticking of the circadian clock. Nat Rev Mol Cell Biol **8,** 139-148.

Giraud, E., Ho, L.H., Clifton, R., Carroll, A., Estavillo, G., Tan, Y.F., Howell, K.A., Ivanova, A., Pogson, B.J., Millar, A.H., and Whelan, J. (2008). The absence of ALTERNATIVE OXIDASE1a in Arabidopsis results in acute sensitivity to combined light and drought stress. Plant Physiol **147,** 595-610.

Graf, A., Schlereth, A., Stitt, M., and Smith, A.M. (2010). Circadian control of carbohydrate availability for growth in Arabidopsis plants at night. Proc Natl Acad Sci U S A.

Grant, G.R., Manduchi, E., and Stoeckert, C.J., Jr. (2007). Analysis and management of microarray gene expression data. Curr Protoc Mol Biol **Chapter 19,** Unit 19 16.

Griebel, T., and Zeier, J. (2008). Light regulation and daytime dependency of inducible plant defenses in Arabidopsis: phytochrome signaling controls systemic acquired resistance rather than local defense. Plant Physiol **147,** 790-801.

Grimaldi, B., Nakahata, Y., Kaluzova, M., Masubuchi, S., and Sassone-Corsi, P. (2009). Chromatin remodeling, metabolism and circadian clocks: the interplay of CLOCK and SIRT1. Int J Biochem Cell Biol **41,** 81-86.

Grimm, E., and Arbuthnot, P. (1995). Rapid Purification of Taq DNA polymerase by freezing and high temperature thawing of bacterial expression cultures. Nucleic Acids Res **23**, 4518-4519.

Halford, N.G., and Hey, S.J. (2009). Snf1-related protein kinases (SnRKs) act within an intricate network that links metabolic and stress signalling in plants. Biochem J **419,** 247-259.

Hall, A., Bastow, R.M., Davis, S.J., Hanano, S., McWatters, H.G., Hibberd, V., Doyle, M.R., Sung, S., Halliday, K.J., Amasino, R.M., and Millar, A.J. (2003). The TIME FOR COFFEE gene maintains the amplitude and timing of Arabidopsis circadian clocks. Plant Cell **15,** 2719-2729.

Hanano, S., Domagalska, M.A., Nagy, F., and Davis, S.J. (2006). Multiple phytohormones influence distinct parameters of the plant circadian clock. Genes Cells **11,** 1381-1392.

Harmer, S.L., Hogenesch, J.B., Straume, M., Chang, H.S., Han, B., Zhu, T., Wang, X., Kreps, J.A., and Kay, S.A. (2000). Orchestrated transcription of key pathways in Arabidopsis by the circadian clock. Science **290,** 2110-2113.

Harmer, S.L. (2009). The circadian system in higher plants. Annu Rev Plant Biol **60,** 357-377.

Hashida, S.N., Takahashi, H., and Uchimiya, H. (2009). The role of NAD biosynthesis in plant development and stress responses. Ann Bot **103,** 819-824.

Hazen, S.P., Schultz, T.F., Pruneda-Paz, J.L., Borevitz, J.O., Ecker, J.R., and Kay, S.A. (2005). LUX ARRHYTHMO encodes a Myb domain protein essential for circadian rhythms. Proc Natl Acad Sci U S A **102,** 10387-10392.

Hicks, K.A., Millar, A.J., Carre, I.A., Somers, D.E., Straume, M., Meeks-Wagner, D.R., and Kay, S.A. (1996). Conditional circadian dysfunction of the Arabidopsis early-flowering 3 mutant. Science **274,** 790-792.

Hinsch, M., and Staskawicz, B. (1996). Identification of a new Arabidopsis disease resistance locus, RPs4, and cloning of the corresponding avirulence gene, avrRps4, from Pseudomonas syringae pv. pisi. Mol Plant Microbe Interact **9,** 55-61.

Hirota, T., Lewis, W.G., Liu, A.C., Lee, J.W., Schultz, P.G., and Kay, S.A. (2008). A chemical biology approach reveals period shortening of the mammalian circadian clock by specific inhibition of GSK-3beta. Proc Natl Acad Sci U S A **105,** 20746-20751.

Hotta, C.T., Gardner, M.J., Hubbard, K.E., Baek, S.J., Dalchau, N., Suhita, D., Dodd, A.N., and Webb, A.A. (2007). Modulation of environmental responses of plants by circadian clocks. Plant Cell Environ **30,** 333-349.

Hubbard, K.E., Robertson, F.C., Dalchau, N., and Webb, A.A. (2009). Systems analyses of circadian networks. Mol Biosyst **5,** 1502-1511.

Imaizumi, T. (2010). Arabidopsis circadian clock and photoperiodism: time to think about location. Curr Opin Plant Biol **13,** 83-89.

Irizarry, R.A., Bolstad, B.M., Collin, F., Cope, L.M., Hobbs, B., and Speed, T.P. (2003). Summaries of Affymetrix GeneChip probe level data. Nucleic Acids Res **31,** e15.

Ishikawa, K., Ogawa, T., Hirosue, E., Nakayama, Y., Harada, K., Fukusaki, E., Yoshimura, K., and Shigeoka, S. (2009). Modulation of the poly(ADP-ribosyl)ation reaction via the Arabidopsis ADP-ribose/NADH pyrophosphohydrolase, AtNUDX7, is involved in the response to oxidative stress. Plant Physiol **151,** 741-754.

James, P., Halladay, J., and Craig, E.A. (1996). Genomic libraries and a host strain designed for highly efficient yeast two hybrid selection in yeast. Genetics **144,**1425-1436.

Jossier, M., Bouly, J.P., Meimoun, P., Arjmand, A., Lessard, P., Hawley, S., Grahame Hardie, D., and Thomas, M. (2009). SnRK1 (SNF1-related kinase 1) has a central role in sugar and ABA signalling in Arabidopsis thaliana. Plant J **59,** 316-328.

Kang, T.H., Reardon, J.T., Kemp, M., and Sancar, A. (2009). Circadian oscillation of nucleotide excision repair in mammalian brain. Proc Natl Acad Sci U S A **106,** 2864-2867.

Kevei, E., Gyula, P., Feher, B., Toth, R., Viczian, A., Kircher, S., Rea, D., Dorjgotov, D., Schafer, E., Millar, A.J., Kozma-Bognar, L., and Nagy, F. (2007). Arabidopsis thaliana circadian clock is regulated by the small GTPase LIP1. Curr Biol **17,** 1456-1464.

Kim, W.Y., Fujiwara, S., Suh, S.S., Kim, J., Kim, Y., Han, L., David, K., Putterill, J., Nam, H.G., and Somers, D.E. (2007). ZEITLUPE is a circadian photoreceptor stabilized by GIGANTEA in blue light. Nature **449,** 356-360.

Kim, S.A., and Guerinot, M.L. (2007). Mining iron: iron uptake and transport in plants. FEBS Lett **581,** 2273-2280.

Kohsaka, A., and Bass, J. (2007). A sense of time: how molecular clocks organize metabolism. Trends Endocrinol Metab **18,** 4-11.

Kurepa, J., Smalle, J., Van Montagu, M., and Inze, D. (1998). Oxidative stress tolerance and longevity in Arabidopsis: the late-flowering mutant gigantea is tolerant to paraquat. Plant J **14,** 759-764.

Laemmli, U.K. (1970). Cleavage of structural proteins during the assembly of the head of bacteriophage T4. Nature **227,** 680-685.

Lamia, K.A., Sachdeva, U.M., DiTacchio, L., Williams, E.C., Alvarez, J.G., Egan, D.F., Vasquez, D.S., Juguilon, H., Panda, S., Shaw, R.J., Thompson, C.B., and Evans, R.M. (2009). AMPK regulates the circadian clock by cryptochrome phosphorylation and degradation. Science **326,** 437-440.

Le Guen, L., Thomas, M., Bianchi, M., Halford, N.G., and Kreis, M. (1992). Structure and expression of a gene from Arabidopsis thaliana encoding a protein related to SNF1 protein kinase. Gene **120,** 249-254.

Lee, H.C. (1997). Mechanisms of calcium signaling by cyclic ADP-ribose and NAADP. Physiol Rev **77,** 1133-1164.

Legnaioli, T., Cuevas, J., and Mas, P. (2009). TOC1 functions as a molecular switch connecting the circadian clock with plant responses to drought. EMBO J **28,** 3745-3757.

Li, S., Lauri, A., Ziemann, M., Busch, A., Bhave, M., and Zachgo, S. (2009). Nuclear activity of ROXY1, a glutaredoxin interacting with TGA factors, is required for petal development in Arabidopsis thaliana. Plant Cell **21,** 429-441.

Liu, Q., Kasuga, M., Sakuma, Y., Abe, H., Miura, S., Yamaguchi-Shinozaki, K., and Shinozaki, K. (1998). Two transcription factors, DREB1 and DREB2, with an EREBP/AP2 DNA binding domain separate two cellular signal transduction pathways in drought- and low-temperature-responsive gene expression, respectively, in Arabidopsis. Plant Cell **10,** 1391-1406.

Liu, F., Marquardt, S., Lister, C., Swiezewski, S., and Dean, C. (2010). Targeted 3' processing of antisense transcripts triggers Arabidopsis FLC chromatin silencing. Science **327,** 94-97.

Locke, J.C., Southern, M.M., Kozma-Bognar, L., Hibberd, V., Brown, P.E., Turner, M.S., and Millar, A.J. (2005). Extension of a genetic network model by iterative experimentation and mathematical analysis. Mol Syst Biol **1,** 2005 0013.

Locke, J.C., Kozma-Bognar, L., Gould, P.D., Feher, B., Kevei, E., Nagy, F., Turner, M.S., Hall, A., and Millar, A.J. (2006). Experimental validation of a predicted feedback loop in the multi-oscillator clock of Arabidopsis thaliana. Mol Syst Biol **2,** 59.

Makino, S., Matsushika, A., Kojima, M., Yamashino, T., and Mizuno, T. (2002). The APRR1/TOC1 quintet implicated in circadian rhythms of Arabidopsis thaliana: I. Characterization with APRR1-overexpressing plants. Plant Cell Physiol **43,** 58-69.

Martin-Tryon, E.L., and Harmer, S.L. (2008). XAP5 CIRCADIAN TIMEKEEPER coordinates light signals for proper timing of photomorphogenesis and the circadian clock in Arabidopsis. Plant Cell **20,** 1244-1259.

Mas, P., Kim, W.Y., Somers, D.E., and Kay, S.A. (2003). Targeted degradation of TOC1 by ZTL modulates circadian function in Arabidopsis thaliana. Nature **426,** 567-570.

Mas, P. (2008). Circadian clock function in Arabidopsis thaliana: time beyond transcription. Trends Cell Biol **18,** 273-281.

Matsui, A., Ishida, J., Morosawa, T., Mochizuki, Y., Kaminuma, E., Endo, T.A., Okamoto, M., Nambara, E., Nakajima, M., Kawashima, M., Satou, M., Kim, J.M., Kobayashi, N., Toyoda, T., Shinozaki, K., and Seki, M. (2008). Arabidopsis transcriptome analysis under drought, cold, high-salinity and ABA treatment conditions using a tiling array. Plant Cell Physiol **49,** 1135-1149.

Matsushika, A., Makino, S., Kojima, M., and Mizuno, T. (2000). Circadian waves of expression of the APRR1/TOC1 family of pseudo-response regulators in Arabidopsis thaliana: insight into the plant circadian clock. Plant Cell Physiol **41,** 1002-1012.

Maxwell, D.P., Wang, Y., and McIntosh, L. (1999). The alternative oxidase lowers mitochondrial reactive oxygen production in plant cells. Proc Natl Acad Sci U S A **96,** 8271-8276.

McClung, C.R. (2006). Plant circadian rhythms. Plant Cell **18,** 792-803.

McWatters, H.G., Bastow, R.M., Hall, A., and Millar, A.J. (2000). The ELF3 zeitnehmer regulates light signalling to the circadian clock. Nature **408,** 716-720.

McWatters, H.G., Kolmos, E., Hall, A., Doyle, M.R., Amasino, R.M., Gyula, P., Nagy, F., Millar, A.J., and Davis, S.J. (2007). ELF4 is required for oscillatory properties of the circadian clock. Plant Physiol **144,** 391-401.

Merrow, M., Mazzotta, G., Chen, Z., and Roenneberg, T. (2006). The right place at the right time: regulation of daily timing by phosphorylation. Genes Dev **20,** 2629-2623.

Messerli, G., Partovi Nia, V., Trevisan, M., Kolbe, A., Schauer, N., Geigenberger, P., Chen, J., Davison, A.C., Fernie, A.R., and Zeeman, S.C. (2007). Rapid classification of phenotypic mutants of Arabidopsis via metabolite fingerprinting. Plant Physiol **143,** 1484-1492.

Michael, T.P., Mockler, T.C., Breton, G., McEntee, C., Byer, A., Trout, J.D., Hazen, S.P., Shen, R., Priest, H.D., Sullivan, C.M., Givan, S.A., Yanovsky, M., Hong, F., Kay, S.A., and Chory, J. (2008). Network discovery pipeline elucidates conserved time-of-day-specific cis-regulatory modules. PLoS Genet **4,** e14.

Millar, A.J., and Kay, S.A. (1991). Circadian Control of cab Gene Transcription and mRNA Accumulation in Arabidopsis. Plant Cell **3,** 541-550.

Millar, A.J., Carre, I.A., Strayer, C.A., Chua, N.H., and Kay, S.A. (1995a). Circadian clock mutants in Arabidopsis identified by luciferase imaging. Science **267,** 1161-1163.

Millar, A.J., Straume, M., Chory, J., Chua, N.H., and Kay, S.A. (1995b). The regulation of circadian period by phototransduction pathways in Arabidopsis. Science **267,** 1163-1166.

Miller, G., Suzuki, N., Rizhsky, L., Hegie, A., Koussevitzky, S., and Mittler, R. (2007). Double mutants deficient in cytosolic and thylakoid ascorbate peroxidase reveal a complex mode of interaction between reactive oxygen species, plant development, and response to abiotic stresses. Plant Physiol **144,** 1777-1785.

Mizoguchi, T., Wheatley, K., Hanzawa, Y., Wright, L., Mizoguchi, M., Song, H.R., Carre, I.A., and Coupland, G. (2002). LHY and CCA1 are partially redundant genes required to maintain circadian rhythms in Arabidopsis. Dev Cell **2,** 629-641.

Mizuno, T., and Yamashino, T. (2008). Comparative transcriptome of diurnally oscillating genes and hormone-responsive genes in Arabidopsis thaliana: insight into circadian clock-controlled daily responses to common ambient stresses in plants. Plant Cell Physiol **49,** 481-487.

Muhlenbock, P., Szechynska-Hebda, M., Plaszczyca, M., Baudo, M., Mateo, A., Mullineaux, P.M., Parker, J.E., Karpinska, B., and Karpinski, S. (2008). Chloroplast signaling and LESION SIMULATING DISEASE1 regulate crosstalk between light acclimation and immunity in Arabidopsis. Plant Cell **20,** 2339-2356.

Nakahata, Y., Kaluzova, M., Grimaldi, B., Sahar, S., Hirayama, J., Chen, D., Guarente, L.P., and Sassone-Corsi, P. (2008). The NAD+-dependent deacetylase SIRT1 modulates CLOCK-mediated chromatin remodeling and circadian control. Cell **134,** 329-340.

Nakahata, Y., Sahar, S., Astarita, G., Kaluzova, M., and Sassone-Corsi, P. (2009). Circadian control of the NAD+ salvage pathway by CLOCK-SIRT1. Science **324,** 654-657.

Nakamichi, N., Kiba, T., Henriques, R., Mizuno, T., Chua, N.H., and Sakakibara, H. (2010). PSEUDO-RESPONSE REGULATORS 9, 7, and 5 are transcriptional repressors in the Arabidopsis circadian clock. Plant Cell **22,** 594-605.

Nelson, D., and Cox, M. (2000) Lehninger Principles of Biochemistry. 3rd ed. Worth Publishers. NY USA

Niittyla, T., Messerli, G., Trevisan, M., Chen, J., Smith, A.M., and Zeeman, S.C. (2004). A previously unknown maltose transporter essential for starch degradation in leaves. Science **303,** 87-89.

Nogales-Cadenas, R., Carmona-Saez, P., Vazquez, M., Vicente, C., Yang, X., Tirado, F., Carazo, J.M., and Pascual-Montano, A. (2009). GeneCodis: interpreting gene lists through enrichment analysis and integration of diverse biological information. Nucleic Acids Res **37,** W317-322.

Noguchi, K., and Yoshida, K. (2008). Interaction between photosynthesis and respiration in illuminated leaves. Mitochondrion **8,** 87-99.

Nozue, K., Covington, M.F., Duek, P.D., Lorrain, S., Fankhauser, C., Harmer, S.L., and Maloof, J.N. (2007). Rhythmic growth explained by coincidence between internal and external cues. Nature **448,** 358-361.

Oelze, M.L., Kandlbinder, A., and Dietz, K.J. (2008). Redox regulation and overreduction control in the photosynthesizing cell: complexity in redox regulatory networks. Biochim Biophys Acta **1780,** 1261-1272.

Ouyang, Y., Andersson, C.R., Kondo, T., Golden, S.S., and Johnson, C.H. (1998). Resonating circadian clocks enhance fitness in cyanobacteria. Proc Natl Acad Sci U S A **95,** 8660-8664.

Panda, S., Poirier, G.G., and Kay, S.A. (2002). tej defines a role for poly(ADP-ribosyl)ation in establishing period length of the arabidopsis circadian oscillator. Dev Cell **3,** 51-61.

Para, A., Farre, E.M., Imaizumi, T., Pruneda-Paz, J.L., Harmon, F.G., and Kay, S.A. (2007). PRR3 Is a vascular regulator of TOC1 stability in the Arabidopsis circadian clock. Plant Cell **19,** 3462-3473.

Park DH, Somers DE, Kim YS, Choy YH, Lim HK, Soh MS, Kim HJ, Kay SA, Nam HG. (1999). Control of circadian rhythms and photoperiodic flowering by the Arabidopsis GIGANTEA gene. Science. 1999 **285,** 1579-82.

Perales, M., and Mas, P. (2007). A functional link between rhythmic changes in chromatin structure and the Arabidopsis biological clock. Plant Cell **19,** 2111-2123.

Piechulla, B., and Gruissem, W. (1987). Diurnal mRNA fluctuations of nuclear and plastid genes in developing tomato fruits. EMBO J **6,** 3593-3599.

Plautz, J.D., Straume, M., Stanewsky, R., Jamison, C.F., Brandes, C., Dowse, H.B., Hall, J.C., and Kay, S.A. (1997). Quantitative analysis of Drosophila period gene transcription in living animals. J Biol Rhythms **12,** 204-217.

Polge, C., and Thomas, M. (2007). SNF1/AMPK/SnRK1 kinases, global regulators at the heart of energy control? Trends Plant Sci **12,** 20-28.

Pruneda-Paz, J.L., Breton, G., Para, A., and Kay, S.A. (2009). A functional genomics approach reveals CHE as a component of the Arabidopsis circadian clock. Science **323,** 1481-1485.

Qin, X.J., Hudson, L.G., Liu, W., Timmins, G.S., and Liu, K.J. (2008). Low concentration of arsenite exacerbates UVR-induced DNA strand breaks by inhibiting PARP-1 activity. Toxicol Appl Pharmacol **232,** 41-50.

Ramsey, K.M., Yoshino, J., Brace, C.S., Abrassart, D., Kobayashi, Y., Marcheva, B., Hong, H.K., Chong, J.L., Buhr, E.D., Lee, C., Takahashi, J.S., Imai, S., and Bass, J. (2009). Circadian clock feedback cycle through NAMPT-mediated NAD+ biosynthesis. Science **324,** 651-654.

Ravet, K., Touraine, B., Boucherez, J., Briat, J.F., Gaymard, F., and Cellier, F. (2009). Ferritins control interaction between iron homeostasis and oxidative stress in Arabidopsis. Plant J **57,** 400-412.

Rawat, R., Schwartz, J., Jones, M.A., Sairanen, I., Cheng, Y., Andersson, C.R., Zhao, Y., Ljung, K., and Harmer, S.L. (2009). REVEILLE1, a Myb-like transcription factor, integrates the circadian clock and auxin pathways. Proc Natl Acad Sci U S A **106,** 16883-16888.

Rhoads, D.M., and Subbaiah, C.C. (2007). Mitochondrial retrograde regulation in plants. Mitochondrion **7,** 177-194.

Riganti, C., Gazzano, E., Polimeni, M., Costamagna, C., Bosia, A., and Ghigo, D. (2004). Diphenyleneiodonium inhibits the cell redox metabolism and induces oxidative stress. J Biol Chem **279,** 47726-47731.

Robertson, F.C., Skeffington, A.W., Gardner, M.J., and Webb, A.A. (2009). Interactions between circadian and hormonal signalling in plants. Plant Mol Biol **69,** 419-427.

Roden, L.C., and Ingle, R.A. (2009). Lights, rhythms, infection: the role of light and the circadian clock in determining the outcome of plant-pathogen interactions. Plant Cell **21,** 2546-2552.

Rook, F., Hadingham, S.A., Li, Y., and Bevan, M.W. (2006). Sugar and ABA response pathways and the control of gene expression. Plant Cell Environ **29,** 426-434.

Sambrook, J., and Russell, D.W. (2001). Molecular Cloning a laboratoty manual. NY, USA. 3rd ed Cold Spring Harbor Laboratory Press.

Sanchez, J.P., Duque, P., and Chua, N.H. (2004). ABA activates ADPR cyclase and cADPR induces a subset of ABA-responsive genes in Arabidopsis. Plant J **38,** 381-395.

Schaffer, R., Ramsay, N., Samach, A., Corden, S., Putterill, J., Carre, I.A., and Coupland, G. (1998). The late elongated hypocotyl mutation of Arabidopsis disrupts circadian rhythms and the photoperiodic control of flowering. Cell **93,** 1219-1229.

Seki, M., Umezawa, T., Urano, K., and Shinozaki, K. (2007). Regulatory metabolic networks in drought stress responses. Curr Opin Plant Biol **10,** 296-302.

Shinozaki, K., and Yamaguchi-Shinozaki, K. (1996). Molecular responses to drought and cold stress. Curr Opin Biotechnol **7,** 161-167.

Smith, A.M., and Stitt, M. (2007). Coordination of carbon supply and plant growth. Plant Cell Environ **30,** 1126-1149.

Somers, D.E., Devlin, P.F., and Kay, S.A. (1998). Phytochromes and cryptochromes in the entrainment of the Arabidopsis circadian clock. Science **282,** 1488-1490.

Somers, D.E., Schultz, T.F., Milnamow, M., and Kay, S.A. (2000). ZEITLUPE encodes a novel clock-associated PAS protein from Arabidopsis. Cell **101,** 319-329.

Song, H.R., and Carre, I.A. (2005). DET1 regulates the proteasomal degradation of LHY, a component of the Arabidopsis circadian clock. Plant Mol Biol **57,** 761-771.

Souther, M.M, and Millar, A. (2005). Circadian genetics in the model higher plant, Arabidopsis thaliana. Methods Enzymol **393**, 23-35.

Staiger, D., Allenbach, L., Salathia, N., Fiechter, V., Davis, S.J., Millar, A.J., Chory, J., and Fankhauser, C. (2003). The Arabidopsis SRR1 gene mediates phyB signaling and is required for normal circadian clock function. Genes Dev **17,** 256-268.

Sweetlove LJ, Heazlewood JL, Herald V, Holtzapffel R, Day DA, Leaver CJ, Millar AH. (2002). The impact of oxidative stress on Arabidopsis mitochondria. Plant J. **32**, 891-904.

Sugano, S., Andronis, C., Ong, M.S., Green, R.M., and Tobin, E.M. (1999). The protein kinase CK2 is involved in regulation of circadian rhythms in Arabidopsis. Proc Natl Acad Sci U S A **96,** 12362-12366.

Thelander, M., Olsson, T., and Ronne, H. (2004). Snf1-related protein kinase 1 is needed for growth in a normal day-night light cycle. EMBO J **23,** 1900-1910.

Thimm, O., Blasing, O., Gibon, Y., Nagel, A., Meyer, S., Kruger, P., Selbig, J., Muller, L.A., Rhee, S.Y., and Stitt, M. (2004). MAPMAN: a user-driven tool to display genomics data sets onto diagrams of metabolic pathways and other biological processes. Plant J **37,** 914-939.

Tiessen, A., Prescha, K., Branscheid, A., Palacios, N., McKibbin, R., Halford, N.G., and Geigenberger, P. (2003). Evidence that SNF1-related kinase and hexokinase are involved in separate sugar-signalling pathways modulating post-translational redox activation of ADP-glucose pyrophosphorylase in potato tubers. Plant J **35,** 490-500.

Ton, J., Flors, V., and Mauch-Mani, B. (2009). The multifaceted role of ABA in disease resistance. Trends Plant Sci **14,** 310-317.

Tornero, P., and Dangl, J.L. (2001). A high-throughput method for quantifying growth of phytopathogenic bacteria in Arabidopsis thaliana. Plant J **28,** 475-481.

Torres Zabala, M., Bennett, M.H., Truman, W.H., and Grant, M.R. (2009). Antagonism between salicylic and abscisic acid reflects early host-pathogen conflict and moulds plant defence responses. Plant J **59,** 375-386.

Toth, R., Kevei, E., Hall, A., Millar, A.J., Nagy, F., and Kozma-Bognar, L. (2001). Circadian clock-regulated expression of phytochrome and cryptochrome genes in Arabidopsis. Plant Physiol **127,** 1607-1616.

Tsesmetzis, N., Couchman, M., Higgins, J., Smith, A., Doonan, J.H., Seifert, G.J., Schmidt, E.E., Vastrik, I., Birney, E., Wu, G., D'Eustachio, P., Stein, L.D., Morris, R.J., Bevan, M.W., and Walsh, S.V. (2008). Arabidopsis reactome: a foundation knowledgebase for plant systems biology. Plant Cell **20,** 1426-1436.

Urano, K., Kurihara, Y., Seki, M., and Shinozaki, K. (2010). 'Omics' analyses of regulatory networks in plant abiotic stress responses. Curr Opin Plant Biol **13,** 132-138.

van der Horst, M.A., and Hellingwerf, K.J. (2004). Photoreceptor proteins, "star actors of modern times": a review of the functional dynamics in the structure of representative members of six different photoreceptor families. Acc Chem Res **37,** 13-20.

Walters, R.G., Ibrahim, D.G., Horton, P., and Kruger, N.J. (2004). A mutant of Arabidopsis lacking the triose-phosphate/phosphate translocator reveals metabolic regulation of starch breakdown in the light. Plant Physiol **135,** 891-906.

Wang, Z.Y., and Tobin, E.M. (1998). Constitutive expression of the CIRCADIAN CLOCK ASSOCIATED 1 (CCA1) gene disrupts circadian rhythms and suppresses its own expression. Cell **93,** 1207-1217.

Wijnen, H., and Young, M.W. (2006). Interplay of circadian clocks and metabolic rhythms. Annu Rev Genet **40,** 409-448.

Wormuth, D., Heiber, I., Shaikali, J., Kandlbinder, A., Baier, M., and Dietz, K.J. (2007). Redox regulation and antioxidative defence in Arabidopsis leaves viewed from a systems biology perspective. J Biotechnol **129,** 229-248.

Wu, Y., Kuzma, J., Marechal, E., Graeff, R., Lee, H.C., Foster, R., and Chua, N.H. (1997). Abscisic acid signaling through cyclic ADP-ribose in plants. Science **278,** 2126-2130.

Wu, L., and Yang, H.Q. (2010). CRYPTOCHROME 1 Is Implicated in Promoting R Protein-Mediated Plant Resistance to Pseudomonas syringae in Arabidopsis. Mol Plant.

Yanovsky, M.J., Mazzella, M.A., and Casal, J.J. (2000). A quadruple photoreceptor mutant still keeps track of time. Curr Biol **10,** 1013-1015.

Yao, Y., Song, L., Katz, Y., and Galili, G. (2002). Cloning and characterization of Arabidopsis homologues of the animal CstF complex that regulates 3' mRNA cleavage and polyadenylation. J Exp Bot **53,** 2277-2278.

Yi, Y., and Guerinot, M.L. (1996). Genetic evidence that induction of root Fe(III) chelate reductase activity is necessary for iron uptake under iron deficiency. Plant J **10,** 835-844.

Yin, L., Wang, J., Klein, P.S., and Lazar, M.A. (2006). Nuclear receptor Rev-erbalpha is a critical lithium-sensitive component of the circadian clock. Science **311,** 1002-1005.

Yin, L., Wu, N., Curtin, J.C., Qatanani, M., Szwergold, N.R., Reid, R.A., Waitt, G.M., Parks, D.J., Pearce, K.H., Wisely, G.B., and Lazar, M.A. (2007). Rev-erbalpha, a heme sensor that coordinates metabolic and circadian pathways. Science **318,** 1786-1789.

Yu, T.S., Kofler, H., Hausler, R.E., Hille, D., Flugge, U.I., Zeeman, S.C., Smith, A.M., Kossmann, J., Lloyd, J., Ritte, G., Steup, M., Lue, W.L., Chen, J., and Weber, A. (2001). The Arabidopsis sex1 mutant is defective in the R1 protein, a general regulator of starch degradation in plants, and not in the chloroplast hexose transporter. Plant Cell **13,** 1907-1918.

Zeeman, S.C., Smith, S.M., and Smith, A.M. (2007). The diurnal metabolism of leaf starch. Biochem J **401,** 13-28.

Zeilinger, M.N., Farre, E.M., Taylor, S.R., Kay, S.A., and Doyle, F.J., 3rd. (2006). A novel computational model of the circadian clock in Arabidopsis that incorporates PRR7 and PRR9. Mol Syst Biol **2,** 58.

Zeller, G., Henz, S.R., Widmer, C.K., Sachsenberg, T., Ratsch, G., Weigel, D., and Laubinger, S. (2009). Stress-induced changes in the Arabidopsis thaliana transcriptome analyzed using whole-genome tiling arrays. Plant J **58,** 1068-1082.

Zipfel, C., Robatzek, S., Navarro, L., Oakeley, E.J., Jones, J.D., Felix, G., and Boller, T. (2004). Bacterial disease resistance in Arabidopsis through flagellin perception. Nature **428,** 764-767.

Zuo, J., Niu, Q.W., and Chua, N.H. (2000). Technical advance: An estrogen receptor-based transactivator XVE mediates highly inducible gene expression in transgenic plants. Plant J **24,** 265-273.

VIII. Appendix

Table V. Genes differentially expressed relevant to this study

Genes that were found to be differentially expressed (see methods) are listed with their corresponding ATG code and their fold change value (log2). Fold change values derived from *tic-2 versus* wild-type comparisons and therefore reflect induction or repression respective to the mutant. Negative fold-change values are noted with a minus sign. Dashed lines indicate that the gene was not found as differentially expressed.

The genes were listed in categories based on their known or putative function and/or cellular localization relative to the topics studied in this work. A brief description of the genes product, activity or process is provided. Further particular details are found thorough the text in results and discussion sections.

ATG code	Gene name	Function/process	Dawn	Reset
Photosynthesis and chloroplast integrity				
At4g27440	*PORB*	Chlorophyllide synthesis	3.91	3.41
At5g54190	*PORA*	Chlorophyllide synthesis	1.63	---
At3g14930	*HEME1*	Porphyrin biosynthesis	1.00	1.50
At1g58290	*HEMA1*	Glutamyl-tRNA reductase catalyzing the NADPH-dependent reduction of Glu-tRNA to glutamate 1-semialdehyde (GSA) with. Involved in the early steps of chlorophyll biosynthesis.	0.91	0.99
At3g47470	*CAB4*	Photosynthesis/Light harvesting complex	0.88	---
At1g08550	*NPQ1 (AVDE1)*	Violaxanthin de-epoxidase	0.82	1.50
At5g54270	*CAB3*	Photosynthesis/Light harvesting complex	0.51	---
At3g16250	Ferredoxin	Photosynthesis	-1.02	---
At1g42550	*PMI1*	chloroplast movement	-1.05	-0.62
At4g24930	thylakoid lumenal 17.9 kDa protein	Photosynthesis	-1.06	---
Iron metabolic process				
At5g01600	*FER1*	Iron homeostasis	3.24	2.10
At2g40300	*FER4*	Iron homeostasis	3.06	3.33
At5g56080	*NAS2*	Iron transport	2.81	2.75
At3g56090	*FER3*	Iron homeostasis	---	2.36
At4g19690	*IRT1*	Iron transport	2.39	---
At1g80830	*NRAMP* metal ion transporter 1	Metal transporter	0.93	---

ATG code	Gene name	Function/process	Dawn	Reset
ABA and ABA related responses: drought, cold, water and salt stresses				
At5g05410	*DREB2A*	Transcription factor for drought/cold gene expression	2.49	1.97
At2g17840	*ERD7* early response dehydration	Drought/cold/salt stress	1.99	1.54
At2g42540	*COR15A*	Cold	1.65	1.95
At1g49720	ABRE binding factor	ABA responsive	1.56	1.00
At4g19120	*ERD3*	Drought/cold/salt stress	1.32	1.42
At1g30360	*EDR4*	Drought/cold/salt stress	1.23	0.60
At4g26080	*ABI1*	Negative regulator of ABA promotion of stomatal closure.	1.21	---
At1g20450	*ERD10*	Drought/cold/salt stress	1.15	---
At5g66880	*SNRK2.3*	ABA kinase	1.09	---
At5g25610	*RD22* Response to dessication	Drought/ABA responsive	0.87	---
At3g50500	*SNRK2.2*	ABA kinase	0.81	1.09
At2g42530	*COR15B*	Cold	0.73	3.23
At1g52340	*ABA2*	Conversion of xanthoxin to ABA-aldehyde during ABA biosynthesis	-0.96	---
Starch and carbohydrate metabolism				
At1g69830	*AMY3*	Starch degradation	3.61	3.74
At3g52180	*SEX4*	Phosphatase. Interacts with SnRK AKIN11. Binds starch.	1.64	1.94
At5g55700	*BAM4* β-amylase	Starch degradation	1.17	0.85
At1g10760	*SEX1* glucan water dikinase	Starch degradation	1.03	1.40
At1g28330	*DRM1*	Response to sucrose	1.99	-0.62
At1g71880	*SUC1*	Sucrose transport/ sucrose-proton symporter	-1.08	-0.72
At3g13450	*DIN4*	Light and sucrose stimulus responsive	1.50	0.67
At5g20250	*DIN10* Dark induced gene	Induced by dark treatment/ senescence/photosynthesis chemical inhibition and level of sugar in the cell.	0.85	---

ATG code	Gene name	Function/process	Dawn	Reset
DNA and RNA processes and Cell cycle				
At1g71770	*PAB5*	PolyA binding protein	2.53	2.80
At5g02820	DNA topoisomerase VIA (*SPO11*)	Replication	1.41	0.74
At5g43810	*ZWILLE/AGO10*	Elongation initiation factor 2c (Argonaute class). Required to establish the central-peripheral organization of the embryo apex and of central zone and peripheral zone cells in meristems.	1.28	0.87
At5g13730	RNA polymerase sigma subunit SigD (sigD) / sigma-like factor (SIG4)	Regulation of chloroplast transcription	1.12	0.89
At3g12610	*DRT100*	DNA damage/repair/toleration	1.06	1.30
At5g02470	*DP-2* transcription factor Cell cycle	Cell cycle core gene	0.83	0.97
At2g22490	*CYCD2* D-type cyclin	Cell cycle. Transcription regulated by sucrose but not phytohormones or nitrate	-0.63	---
At4g31210	DNA topoisomerase	Replication	-0.72	0.60
At3g46030	histone H2B	Nucleosome assembly	-0.87	---
At1g26910	60S ribosomal protein L10	60S structural protein. Translation	-0.87	---
At3g55280	60S ribosomal protein L23A	60S structural protein. Translation	-0.87	---
At3g03600	Ribosomal protein S2, mitochondrial	Mitochondrial ribosome small subunit	-0.87	-0.59
At1g07070	60S ribosomal protein L35a	Translation. Ribosome biogenesis	-0.87	---
At2g45710	40S ribosomal protein S27	40S structural protein. Translation.	-0.97	---
At1g07370	Proliferating cell nuclear antigen 1 (*PCNA1*)	Replication and cell cycle regulation	-0.97	0.77
At4g34730	Ribosome binding factor A	RNA binding and processing	-1.22	---

ATG code	Gene name	Function/process	Dawn	Reset
DNA and RNA processes and Cell cycle				
At5g24120	RNA polymerase sigma subunit SigE (SIG5)	Transcription of plastid genes in response to blue light	-1.38	-0.79
At1g08540	RNA polymerase sigma subunit SigB (sigB) / sigma factor 2 (SIG2)	Subunit chloroplast RNA polymerase. Induced by red and blue light	-0.74	---
At5g59180	DNA-directed RNA polymerase II	Transcription	-0.52	0.53
At5g41010	DNA-directed RNA polymerases I, II, and III 7 kDa subunit	Transcription. Non catalytic subunits.	-0.54	---
At1g68990	DNA-directed RNA polymerase, mitochondrial (RPOMT)	Transcription	-0.63	---
At2g24120	DNA-directed RNA polymerase, chloroplast (RPOPT)	Transcription	-0.80	---
At3g49000	DNA-directed RNA polymerase III RPC4	Transcription	---	-0.54
At1g59990	DEAD/DEAH box helicase (RH22)	Helicase	-1.44	-0.75
At2g32765	Small ubiquitin-like modifier 5 (SUMO)	SUMOlyation	-1.44	-0.86
Light perception and signalling				
At2g43010	*PIF4*	Transcription factor	4.63	1.38
At1g09570	*PHYA*	Red light photoreceptor	1.84	0.96
At5g64330	*NHP3*	Blue light signalling	1.76	2.26
At3g45780	*NHP1/PHOT1*	Blue light receptor	1.71	1.50

ATG code	Gene name	Function/process	Dawn	Reset
Redox homeostasis/Mitochondrial integrity/defense				
At5g02540	SDR Short chain dehydrogenase	Oxidoreductase activity	2.77	2.06
At1g20630	*CAT1*	Redox/catalase	2.51	1.51
At1g20620	*CAT3/SEN2*	Redox/catalase	1.43	1.70
At4g35770	*SEN1/DIN1*	Oxidative stress/aging/phosphate starvation	1.37	0.87
At3g22370	*AOX1A*	Electron transfer from the ubiquinone to oxygen without energy conservation. A marker for mitochondrial retrograde response.	1.28	0.97
At4g26670	Mitochondrial import inner membrane translocase subunit Tim17/Tim22/Tim23	Transport	2.11	2.91
At2g38400	Alanine glyoxylate aminotransferase	Photorespiration	2.02	---
At1g79440	succinate-semialdehyde dehydrogenase (*SSADH1*)	Mitochondrial NAD dependent catabolism reaction of succinic semialdehyde to succinate in the citric acid cycle.	1.93	1.08
At4g39660	Alanine--glyoxylate aminotransferase	Photorespiration	0.82	---
At1g06570	p-hydroxyphenyl pyruvate dioxygenase (HPPDase)/ *PSD1*	Catalyzes the first step in the synthesis of both plastoquinone and tocopherols in plants	0.68	---
At5g58270	Mitochondrial half-ABC transporter (*STA1*)	Responses to heavy metals	-0.73	---
At5g28840	GDP-D-mannose 3',5'-epimerase activity	Ascorbate biosynthesis	-0.86	---
At5g47910	Respiratory burst oxidase protein D (*RbohD*) / NADPH oxidase	Reactive oxygen species process. Defense	-0.89	---

ATG code	Gene name	Function/process	Dawn	Reset
Redox homeostasis/Mitochondrial integrity/defense				
At5g51060	Respiratory burst oxidase protein C (*RbohC*) / NADPH oxidase	ATP dependent NADPH oxidase	---	-1.81
At2g23420	Nicotinate phosphoribosyl transferase *NAPRT*	Nicotinate (NAD) salvage pathway	-0.94	---
At2g35380	*PER20*	Peroxidase activity	-0.96	-1.16
At2g29450	Glutathione S-transferase (103-1A)	Oxidative stress responses	-1.11	---
At3g29200	Chorismate mutase, chloroplast	L-ascorbate peroxidase. Redox	-1.17	---
At2g43510	Defensin-like (DEFL) family	Trypsin inhibitor, putative	-1.26	-1.57
At4g28390	ADP, ATP carrier protein, mitochondrial	Transport	-1.39	-1.94
At1g49380	Cytochrome c biogenesis protein family	Cytochrome complex assembly	-1.43	-0.69
At2g28190	Cu-Zn superoxide dismutase (*CSD2*)	Responses to oxidative stress, cupper and iron, and light	-1.63	-0.74
At5g67400	*PER73*	Redox/peroxidase	-1.72	-2.69
At4g31870	Gluthathione peroxidase	Redox	-3.40	-1.14
At5g58260	Expressed protein	NADH dehydrogenase complex (plastoquinone) assembly	-1.45	-0.56
At5g14760	L aspartate oxidase	NAD biosynthesis	-2.77	---

ATG code	Gene name	Function/process	Dawn	Reset
Primary amino acid metabolism				
At3g25900	Homocysteine S-methyl transferase 1 (*HMT-1*)	Methionine biosynthesis	1.45	---
At1g03090	3-methycrotonyl-CoA carboxylase 1 (*MCCA*)	Leucine degradation. Nuclear encoded and the active enzyme located in the mitochondria.	1.44	-0.65
At4g35830	*ACO* aconitate hydratase, cytoplasmic / aconitase	Interconversion of isocitrate and citrate via a cis-aconitate intermediate in both the TCA and glyoxylate cycles. Energy balance and iron post-trasncriptional regulation	0.81	0.84
At3g47340	ASN1 asparagine synthetase 1 (glutamine dependent)/ *DIN6*	Induced within 3 hours of dark treatment, in senescing leaves with exogenous photosynthesis inhibitors. Expression pattern is responding to the level of sugar in the cell.	1.94	---
Secondary metabolism and lipid metabolism				
At5g53120	*SPDS3* spermidine synthase,	Polyamine biosynthesis	-0.60	---
At4g34710	arginine decarboxylase 2 (*SPE2*)	Catalyzes the rate limiting first step of polyamine biosynthesis. Responses to cold and oxidative stress	-0.78	-0.62
At2g16500	arginine decarboxylase 1 (*SPE1*)/(*ADC1*)	Catalyzes the rate limiting first step of polyamine biosynthesis. Responses to cold and oxidative stress	-2.18	-0.94
At3g61530	ketopantoate hydroxymethyl transferase	Vitamin B5 synthesis	-0.81	---
At5g08640	flavonol synthase 1 (*FLS1*)	Flavonoids biosynthesis	-1.36	-0.97
At5g13930	naringenin-chalcone synthase (*CHS*)	Flavonoids and anthocyanins biosynthesis.	-2.67	-1.30
At5g24150	squalene monooxygenase 1,1 (*SQP1,1*)	Sterol biosynthesis	-4.16	-0.88

ATG code	Gene name	Function/process	Dawn	Reset
Secondary metabolism and lipid metabolism				
At5g24160	squalene monooxygenase 1,2 (*SQP1,2*)	Sterol biosynthesis. FAD binding	-0.68	---
At4g35790	Phospholipase D delta / PLD delta	Apoptosis	1.32	0.54
At3g45140	*LOX2*	Wounding/ jasmonic acid	-1.02	---
At1g55020	*LOX1*	Defense/wounding/ jasmonic acid biosynthesis	-1.63	-1.17

To the IMPRS 2006 recruitment and evaluation team. That is where this story began. Without their vote, all this adventure would have never had happen.

To Seth Davis, for giving me opportunity of joining his lab. Above all, for the freedom and support in taking the project to what I felt was the path follow.

To my PhD evaluation committee, for taking their time in reading this manuscript and accepting to be part of my PhD defence. Special thanks to George Coupland for his comments during the time of my PhD.

To the IMPRS class 2006 and programme, it was nice to part of a class; I guess for the last time in our lives. Similarly to the IMPRS 2007, that somehow adopted and included me within their class.

To the clock-lab. and the departmental members, who in one way or another contributed to my PhD.

To my friends and colleagues, with whom I shared parts of my life during these years in Cologne. You became the nearest and dearest ones in this part of the world. My life would have been extremely lonely without you.

To my family and friends in México, for their support and love even though we had an ocean in between us.

ERKLÄRUNG

„Ich versichere, dass ich die von mir vorgelegte Dissertation selbständig angefertigt, die benutzten Quellen und Hilfsmittel vollständig angegeben und die Stellen der Arbeit –einschließlich Tabellen, Karten und Abbildungen –, die anderen Werken im Wortlaut oder dem Sinn nach entnommen sind, in jedem Einzelfall als Entlehnung kenntlich gemacht habe; dass diese Dissertation noch keiner anderen Fakultät oder Universität zur Prüfung vorgelegen hat; dass sie – abgesehen von unten angegebenen Teil-publikationen – noch nicht veröffentlicht worden ist sowie, dass ich eine solche Veröffentlichung vor Abschluss des Promotionsverfahrens nicht vornehmen werde. Die Bestimmungen dieser Promotionsordnung sind mir bekannt. Die von mir vorgelegte Dissertation ist von Prof. Dr. George Coupland betreut worden."

Max-Planck-Institut für Züchtungsforschung,
Köln, 17 Mai, 2010,

Alfredo Sánchez Villarreal

TAGUNGEN

Poster Präsentationen:

Sánchez Villarreal, Alfredo and Davis, Seth J.

TIME FOR COFFEE sets the circadian clock at dawn by integrating metabolic signals

20th International Conference in Arabidopsis Research, Edinburgh, Scotland, United Kingdom. 30th June - 4th July 2009